Supplementary Material (ESI) for Chemical Science
This journal is (c) The Royal Society of Chemistry 2018

Supporting Information

XBphos-Rh: A Halogen-Bond Assembled Supramolecular Catalyst

Lucas Carreras,[a] Marta Serrano-Torné,[a] Piet W. N. M. van Leeuwen[b]*
and Anton Vidal-Ferran[a,c]*

[a]Institute of Chemical Research of Catalonia (ICIQ) & The Barcelona Institute of Science and Technology, Av. Països Catalans 16, 43007 Tarragona, Spain.

[b]LPCNO, INSA, 135 Avenue de Rangueil, F-31077 Toulouse, France.

[c]ICREA, Pg. Lluís Companys 23, 08010 Barcelona, Spain.

Supporting Information

Table of Contents

1. General Considerations:

All syntheses were carried out using chemicals as purchased from commercial sources unless otherwise stated. Air- and moisture-sensitive manipulations or reactions were performed under inert atmosphere, either in a glove box or with standard Schlenk techniques. Glassware was dried *in vacuo* before use with a hot air gun. All solvents were dried and deoxygenated by using a solvent purification system (SPS). Silica gel 60 (230−400 mesh) was used for column chromatography. NMR spectra were recorded in 400 MHz or 500 MHz spectrometers in $CDCl_3$ or CD_2Cl_2 unless otherwise cited. ^{1}H and ^{13}C NMR chemical shifts are quoted in ppm relative to residual solvent peaks. $^{11}B\{^{1}H\}$ NMR chemical shifts are quoted in ppm relative to $BF_3{\cdot}(CH_3)_2O$ in $CDCl_3$. $^{19}F\{^{1}H\}$ NMR chemical shifts are quoted in ppm relative to $CFCl_3$ in $CDCl_3$. $^{31}P\{^{1}H\}$ NMR chemical shifts are quoted in ppm relative to 85% phosphoric acid in water. HRMS spectra were recorded using ESI ionization method in positive mode. GC-MS analyses were performed using EI as ionization method. GC analyses were performed with a flame ionization detector. IR spectra were recorded using Attenuated Total Reflection (ATR) technique unless otherwise cited.

2. General Structural Comments on X-ray Crystals:

Determination of single crystal X-ray diffraction structure. Crystals suitable for X-ray measurement for complex **4** (**XBphos-Rh**) and complex **5** were obtained by solvent diffusion in the gas phase, using CH_2Cl_2 and *n*-pentane at –20 ºC under inert atmosphere. The measured crystals were prepared under inert conditions immersed in perfluoropolyether as protecting oil for manipulation.

Crystal structure determination for compounds **4** and **5** were carried out using a diffractometer equipped with an area detector and MoK_α radiation at –173 ˚C. Full-sphere data collection was used with ω and φ scans. Programs used: Data collection CrystalClear,[1] data reduction with CrysAlisPro[2] V/.60A and absorption correction with Scale3 Abspack scaling algorithm.[3]

Structure Solution and Refinement: Crystal structure solution was achieved using the computer program SHELXT.[4] Visualization was performed with the program SHELXle.[5] Missing atoms were subsequently located from difference Fourier synthesis and added to the atom list. Least-squares refinement on F^2 using all measured intensities was carried out using the program SHELXL 2015.[6] All non hydrogen atoms were refined including anisotropic displacement parameters.

Comments to **4** (**XBphos-Rh**): The asymmetric unit contains one cationic rhodium metal complex molecule, one BArF anion and 1.17 molecules of dichloromethane. The cationic metal complex is partially disordered in two orientations (ratio 77:33) showing always the iodine and the CO-group in anti-position. The main part of the CF_3-groups in the BArF anion is showing rotational disorder. The dichloromethane molecules are involved in the disorder of the cationic metal complex and are showing occupations of 0.40 and 0.77.

Comments to **5**: The asymmetric unit contains one molecule of the metal complex, one BArF anion and a half pentane molecule. The coordination complex is disordered in three orientations maintaining the rhodium atom always in the same position. The occupancy of this disorder is of 75:15:10. In the BArF anion most of the CF_3-groups are

[1] Data collection with CrystalClear-SM Expert 2.1 b29 (Rigaku, 2013).
[2] Data reduction with CrysAlisPro 1.171.38.37f (Rigaku OD, 2015).
[3] Empirical absorption correction using spherical harmonics implemented in Scale3 Abspack scaling algorithm, CrysAlisPro 1.171.38.37f (Rigaku OD, 2015).
[4] SHELXT; G. M. Sheldrick, *Acta Cryst.*, 2015, **A71**, 3-8.
[5] SHELXle; C. B. Huebschle, G. M. Sheldrick and B. Dittrich, *J. Appl. Cryst.*, 2011, **44**, 1281-1284.
[6] SHELXL; G. M. Sheldrick, *Acta Cryst.*, 2015, **C71**, 3-8.

showing rotational disorder. The structure refines as a two-component crystal with a ratio of 84:16.

3. Syntheses of Ligands 1, 2 and 3:

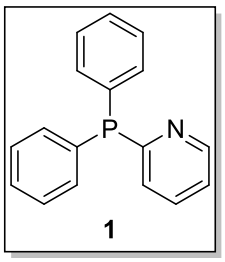

2-pyridyldiphenylphosphine (**1**): Ligand **1** was prepared according to a known procedure,[7] with the following modifications: 1.2 g (52 mmol, 2.25 equiv.) of metal Na and 6 g (46 mmol, 2.00 equiv.) of naphthalene in 75 mL of dry THF were sonicated in an ultrasounds bath for 30 minutes. This solution was cannulated to an effectively stirred solution of 6 g of triphenylphosphine (23 mmol, 1.00 equiv.) in 75 mL of dry THF under an argon atmosphere. This mixture was stirred for 12 h at 60 ºC and then the temperature was decreased to room temperature. From this point, the described protocol was followed.[7] Subsequently, 2.6 g of 2-chloropyridine (23 mmol, 1.00 equiv.) were added. The mixture obtained was worked up by distillation of THF at reflux and atmospheric pressure, vacuum drying, addition of 50 mL of 3 M aqueous ammonium chloride solution and 50 mL of dichloromethane, phase separation, washing, filtration of the combined organic phases, vacuum concentration, and recrystallization from boiling *n*-hexane. After cooling to ambient temperature 5 g of white crystalline 2-diphenylphosphino pyridine (82.0% yield) were collected by filtration. ^{1}H NMR, ^{13}C{^{1}H} NMR and ^{31}P{^{1}H} NMR data were in agreement with those previously reported.[8] ^{1}H NMR (400 MHz, $CDCl_3$) δ: 8.63 (dm, J = 4.8 Hz, 1 H), 7.45 (tt, J = 7.7, 2.4 Hz, 1 H), 7.35-7.20 (m, 10 H), 7.07 (ddm, J = 7.6, 4.8 Hz, 1 H), 6.99 (dm, J = 7.8 Hz, 1 H) ppm. ^{13}C{^{1}H} NMR (100 MHz, $CDCl_3$) δ: 164.1 (d, $J_{C–P}$ = 4.2 Hz), 150.4 (d, $J_{C–P}$ = 12.6 Hz), 136.3 (d, $J_{C–P}$ = 10.7 Hz), 135.8 (d, $J_{C–P}$ = 2.1 Hz), 134.3 (d, $J_{C–P}$ = 19.8 Hz), 129.2, 128.7 (d, $J_{C–P}$ = 7.1 Hz), 127.9 (d, $J_{C–P}$ = 15.5 Hz), 122.3 ppm. ^{31}P{^{1}H} NMR (162 MHz, $CDCl_3$) δ: –0.8 ppm. ESI-MS: $[M+H]^+$, 264.2.

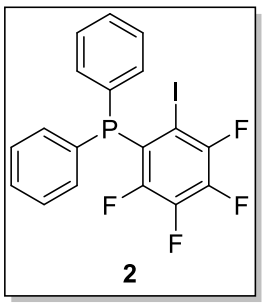

2-iodo-3,4,5,6-tetrafluorophenyldiphenylphosphine (**2**): Ligand **2** was prepared adapting the procedure from Meek *et al.* for the preparation of 2-bromo-3,4,5,6-tetrafluorophenyldiphenylphosphine.[9] A solution of 2.3 g (5.74 mmol, 1.50 equiv.) of 1,2-diiodotetrafluorobenzene in 20 mL of

[7] P. A. A. Klusener, J. C. L. Suykerbuyk and P. A. Verbrugge (Shell Internationale Research Maatschappij B. V.), EP499328A2, 1992.
[8] M. Mehta, I. García de la Arada, M. Pérez, D. Porwal, M. Oestreich and D. W. Stephan, *Organometallics*, 2016, **35**, 1030-1035.
[9] P. G. Eller and D. W. Meek, *J. Organometal. Chem.*, 1970, **22**, 631-636.

anhydrous tetrahydrofuran was cooled to −78 °C by immersion of the Schlenk flask in an acetone bath chilled with a cryocooler. To the cold, stirred solution was added dropwise 1.53 mL (3.83 mmol, 1.00 equiv.) of a 2.5 M solution of *n*-buthyllithium in *n*-hexane. After stirring the reaction mixture for 30 minutes, 0.72 mL (3.83 mmol, 1.00 equiv.) of diphenylchlorophosphine were added slowly. The pale yellow solution was stirred for an additional 45 minutes and then removed from the low temperature bath and allowed to warm to room temperature. After stirring for 1 h at room temperature, the reaction mixture was quenched with 10 mL of deionised water. The aqueous phase was extracted with dichloromethane (3 x 25 mL) and then the organic phases were combined, dried over $MgSO_4$ and the volatiles were removed. The residue was purified by column chromatography (SiO_2, *n*-hexane) to give the (2-iodo-3,4,5,6-tetrafluorophenyl)-diphenylphosphine as a thick yellow oil (1.23 g, 69.7% yield) that after some time evolved to a colourless solid. ^{1}H NMR (400 MHz, $CDCl_3$) δ: 7.43-7.34 (m, 10 H) ppm. $^{13}C\{^{1}H\}$ NMR (126 MHz, $CDCl_3$) δ: 148.9 (ddm, $J_{C–F}$ = 252.7 Hz; $J_{C–P}$ = 9.8 Hz), 147.6 (dtd, $J_{C–F}$ = 245.1 Hz; $J_{C–P}$ = 10.3 Hz; J = 0.3 Hz), 141.0 (dm, $J_{C–F}$ = 259.4 Hz), 134.3 (dd, $J_{C–P}$ = 12.0 Hz; J = 3.5 Hz), 132.9 (dd, $J_{C–P}$ = 20.9 Hz; J = 1.3 Hz), 131.7 (tm, $J_{C–P}$ = 9.4 Hz), 129.4, 128.9 (d, $J_{C–P}$ = 6.6 Hz), 125.4 (m), 90.0 (ddt, $J_{C–F}$ = 52.0 Hz; $J_{C–P}$ = 22.7 Hz; J = 3.9 Hz) ppm. $^{19}F\{^{1}H\}$ NMR (376 MHz, $CDCl_3$) δ: −110.3 (m, 1 F), −118.9 (m, 1 F), −148.9 (m, 1 F); −152.0 (m, 1 F) ppm. $^{31}P\{^{1}H\}$ NMR (162 MHz, $CDCl_3$) δ: 20.1 (ddd, $J_{P–F}$ = 24.3, 10.5, 3.9 Hz) ppm. IR (neat): 3066, 3011, 2923, 1612, 1597, 1582, 1487, 1429, 1363, 1330, 1297, 1275, 1261, 1244, 1183, 1158, 1100, 1024, 835, 778, 744, 709, 692, 641, 606, 493 cm^{-1}. HRMS ESI-MS (m/z): $[M+H]^+$ calcd. for $C_{18}H_{11}F_4IP^+$ 460.9574, found 460.9578. Melting point: 67 °C.

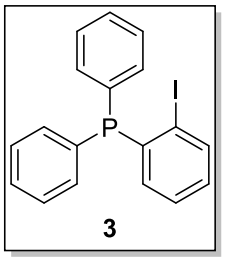

3

2-iodophenyldiphenylphosphine (**3**): A solution of diphenylphosphine (0.96 g, 5.05 mmol, 1 equiv.) in 20 mL of anhydrous tetrahydrofuran was cooled to −78 ºC by immersion of the Schlenk flask in an acetone bath chilled with a cryocooler. To the cold, stirred solution was added dropwise 2 mL (5.05 mmol, 1 equiv.) of a 2.5 M solution of *n*-buthyllithium in *n*-hexane, using a syringe pump, acquiring the solution an intense orange colour. After the reaction mixture was stirred for 30 minutes, 2.5 g (7.58 mmol, 1.5 equiv.) of 1,2-diiodobenzene dissolved in 10 mL of anhydrous THF were added slowly for 30 minutes. The resulting brownish solution

was stirred for an additional 45 minutes at −78 ºC and then warmed up to room temperature. After 60 minutes at room temperature, 10 mL of water were added to quench the mixture. The organic phase was extracted thrice with CH_2Cl_2 (25 mL), and then the organic fraction was evaporated. The crude mixture was purified by column chromatography using SiO_2 and cyclohexane as the eluent, to afford the 2-iodophenyldiphenylphosphine as a white solid (0.23 g, 11.5% yield). ^{1}H NMR, ^{13}C{^{1}H} NMR and ^{31}P{^{1}H} NMR data were in agreement with those previously reported.[10] ^{1}H NMR (400 MHz, $CDCl_3$) δ: 7.80 (ddd, *J* = 7.8, 3.1, 1.7 Hz, 1 H), 7.30-7.10 (m, 11 H), 6.90 (td, *J* = 7.6, 3.4 Hz, 1 H), 6.70 (dt, *J* = 7.6, 2.0 Hz, 1 H) ppm. ^{13}C{^{1}H} NMR (100 MHz, $CDCl_3$) δ: 142.4 (d, $J_{C–P}$ = 9.4 Hz), 139.9 (d, $J_{C–P}$ = 3.7 Hz), 136.4 (d, $J_{C–P}$ = 11.0 Hz), 134.5, 134.1 (d, $J_{C–P}$ = 20.4 Hz), 130.2, 129.1, 128.8 (d, $J_{C–P}$ = 7.2 Hz), 128.4, 107.2 (d, $J_{C–P}$ = 40.0 Hz) ppm. ^{31}P{^{1}H} NMR (162 MHz, $CDCl_3$) δ: 11.2 ppm. EI-MS: [M], 387.0.

[10] J. Bayardon, H. Laureano, V. Diemer, M. Dutartre, U. Das, Y. Rousselin, J.-C. Henry, F. Colobert, F. R. Leroux and S. Jugé, *J. Org. Chem.*, 2012, **77**, 5759-5769.

4. Syntheses of Complexes 4, 5, 6, 11 and 12:

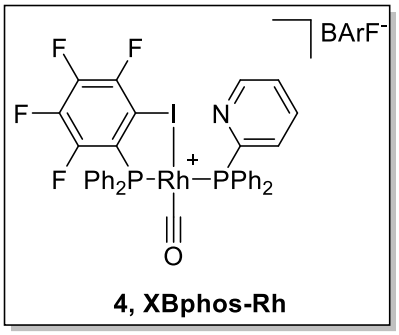

4, XBphos-Rh

XBphos-Rh, (**4**): In a glovebox filled with N_2, 58.0 mg (0.15 mmol, 0.5 equiv.) of $[Rh(Cl)(CO)_2]_2$ dimer were weighted in an amberised glass vial provided with a magnetic stirrer and were dissolved with 1 mL of CH_2Cl_2. Then, 274.0 mg of NaBArF (0.30 mmol, 1 equiv.) were added to the rhodium solution along with 1 mL of dichloromethane and the mixture was stirred for 1 hour at room temperature. In parallel, a solution of 2-$PyPPh_2$, **1** (78.6 mg, 0.30 mmol, 1 equiv.) and (2-iodo-3,4,5,6-tetrafluorobenzene)diphenylphosphine, **2** (137.0 mg, 0.30 mmol, 1 equiv.) in 2 mL of dichloromethane was prepared in a vial provided with a magnetic stirrer and was stirred for 1 hour at room temperature. At due time, the ligands' solution was added dropwise to the rhodium solution, observing some bubbling. This mixture was stirred for 1 hour at room temperature and then filtered with a nylon filter to remove the NaCl precipitate. The resulting red solution was partially evaporated (to *ca*. 1 mL volume), and then mixed with 5 mL of *n*-pentane, observing the formation of a precipitate. This precipitate was washed with cold diethyl ether (3 x 1 mL) and *n*-pentane (3 x 2 mL) and dried under vacuum to afford 380.3 mg of **4**, **XBphos-Rh** as a pale yellow solid in 74.2% yield. ^{1}H NMR (500 MHz, CD_2Cl_2) δ: 8.88 (dm, J = 5.0 Hz, 1 H), 7.91 (tm, J = 7.8 Hz, 1 H), 7.75-7.40 (m, 33 H), 7.34 (ddm, J = 7.8, 3.0 Hz, 1 H) ppm. ^{13}C{^{1}H} NMR (126 MHz, CD_2Cl_2) δ:[11] 185.1 (br s, C_{CO}), 162.2 (q, J_{C-B} = 49.8 Hz, C_{BArF}), 152.0 (dd, J_{C-P} = 67.0 Hz, J_{C-Rh} = 4.2 Hz, C_{Py}), 150.9 (ddm, J_{C-F} = 258.1 Hz, J = 11.4 Hz, C_I), 149.5 (d, J_{C-P} = 19.1 Hz, C_{Py}), 147.7 (dm, J_{C-F} = 250.5 Hz, C_I), 143.2 (dm, J_{C-F} = 267.5 Hz, C_I), 142.5 (dm, J_{C-F} = 263.7 Hz, C_I), 139.0 (d, J_{C-P} = 4.8 Hz, C_{Py}), 135.2 (C_{BArF}), 134.0 (d, J_{C-P} = 12.6 Hz, C_{Ph}), 133.0 (dd, J_{C-P} = 27.1 Hz, J_{C-Rh} = 2.2 Hz, C_{Ph}), 132.9 (d, J_{C-P} = 13.7 Hz, C_{Ph}), 130.1 (dd, J_{C-P} = 11.3 Hz, J_{C-Rh} = 1.7 Hz, C_{Ph}), 129.5 (C_{Py}), 127.3 (d, J_{C-P} = 1.5 Hz, C_{Py}), 129.3 (qm, J_{C-F} = 31.5 Hz, C_{BArF}), 125.0 (q, J_{C-F} = 272.4 Hz, C_{BArF}), 117.8 (m, C_{BArF}) ppm. ^{11}B{^{1}H} NMR (CD_2Cl_2, 128 MHz) δ: –6.8 ppm. ^{19}F{^{1}H} NMR (470 MHz, CD_2Cl_2) δ: –62.9 (s, 24 F),

[11] A heavily overlapped ^{13}C{^{1}H} NMR spectrum was observed due to multiple couplings of the carbons with other NMR active heteronuclei present in the molecule. Whenever possible the carbons where assigned with the help of other NMR experiments as it follows: C_{CO} (carbonyl carbon), C_{BArF} (BArF anion carbons), C_{Ph} (phenyl ring carbons), C_{Py} (pyridyl ring carbons), C_I (iodine-containing ring carbons). This also applies for complexes **5**, **6**, **11** and **12**.

–116.9 (m, 1F), –117.8 (m, 1F), –142.7 (m, 1F); –147.6 (m, 1F) ppm. $^{31}P\{^{1}H\}$ NMR (202 MHz, CD_2Cl_2) δ: 79.4 (ddd, $J_{P–P}$ = 276.0 Hz, $J_{P–Rh}$ = 110.9 Hz, $J_{P–F}$ = 14.2 Hz), 50.4 (dd, $J_{P–P}$ = 275.6 Hz, $J_{P–Rh}$ = 115.9 Hz) ppm. IR (neat): 2039 (CO), 1613, 1576, 1500, 1440, 1353, 1308, 1274, 1155, 1120, 1029, 999, 926, 886, 839, 767, 743, 713, 692, 681, 669, 547, 534, 510, 495, 467 cm^{-1}. HRMS ESI-MS (m/z): $[M–BArF]^+$ calcd. for $C_{36}H_{24}F_4INOP_2Rh^+$ 853.9363, found 853.9348.

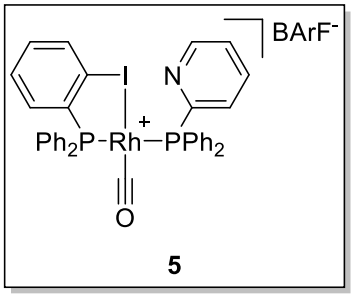

5

Complex **5**: Complex **5** was prepared identically to **XBphos-Rh**, but using 2-iodophenyldiphenylphosphine (**3**) as a ligand instead of **2**. Complex **5** was obtained as a yellow solid in 57.3% yield (113.1 mg, 0.07 mmol). ^{1}H NMR (400 MHz, CD_2Cl_2) δ: 8.77 (d, J = 4.6 Hz, 1 H), 7.95 (d, J = 7.7 Hz, 1 H), 7.81 (tm, J = 7.8 Hz, 1 H), 7.73 (br s, 8 H), 7.65-7.40 (27 H), 7.29 (qd, J = 7.5, 1.4 Hz, 2 H) ppm. $^{13}C\{^{1}H\}$ NMR (126 MHz, CD_2Cl_2) δ:[11] 186.1 (br s, C_{CO}), 162.2 (q, $J_{C–B}$ = 49.8 Hz, C_{BArF}), 153.7 (dd, $J_{C–P}$ = 68.2 Hz, $J_{C–Rh}$ = 3.5 Hz, C_{Py}), 149.9 (d, $J_{C–P}$ = 19.4 Hz, C_{Py}), 138.3 (d, $J_{C–P}$ = 5.1 Hz, C_{Py}), 136.6 (s, C_I), 135.5 (d, $J_{C–P}$ = 13.9 Hz, C_I), 135.2 (s, C_{BArF}), 134.6 (s, C_I), 134.2 (d, $J_{C–P}$ = 13.5 Hz, C_{Ph}), 133.5 (d, $J_{C–P}$ = 12.6 Hz, C_{Ph}), 132.5 (t, $J_{C–P}$ = 2.5 Hz, C_{Ph}), 130.8 (s, C_I), 130.4 (d, $J_{C–P}$ = 10.8 Hz, C_I), 129.9 (dd, $J_{C–P}$ = 10.8 Hz, $J_{C–Rh}$ = 6.9 Hz, C_{Ph}), 129.3 (qm, $J_{C–F}$ = 31.2 Hz, C_{BArF}), 126.6 (d, $J_{C–P}$ = 1.2 Hz, C_{Py}), 125.0 (q, $J_{C–F}$ = 272.4 Hz, C_{BArF}), 117.9 (m, C_{BArF}), 110.3 (dd, $J_{C–P}$ = 34.9 Hz, $J_{C–Rh}$ = 4.0 Hz, C_I) ppm. $^{11}B\{^{1}H\}$ NMR (CD_2Cl_2, 128 MHz) δ: –6.7 ppm. $^{19}F\{^{1}H\}$ NMR (376 MHz, CD_2Cl_2) δ: –62.9 (s, 24F) ppm. $^{31}P\{^{1}H\}$ NMR (162 MHz, CD_2Cl_2) δ: 72.2 (dd, $J_{P–P}$ = 270.7 Hz, $J_{P–Rh}$ = 108.4 Hz), 45.5 (dd, $J_{P–P}$ = 270.7 Hz, $J_{P–Rh}$ = 118.7 Hz) ppm. IR (neat): 2029 (CO), 1352, 1274, 1118, 886, 838, 743, 713, 681, 544, 514 cm^{-1}. HRMS ESI-MS (m/z): $[M–BArF]^+$ calcd. for $C_{36}H_{28}INOP_2Rh^+$ 781.9740, found 781.9703.

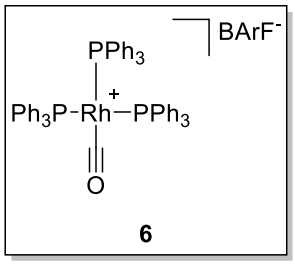

Tris-triphenylphosphine carbonyl rhodium (I) tetrakis[3,5-bis(trifluoromethyl)phenyl]borate, [Rh(CO)(PPh_3)$_3$]BArF (**6**): Compound **6** was synthesised by slightly modifying the synthesis reported by Hope *et al.*[12] A 25 mL Schlenk tube was filled with 54.8 mg of carbonylhydrido-tris(triphenylphosphine)rhodium(I) (0.06 mmol, 1 equiv.) and 5 mL of dichloromethane. Then, a solution of 60.3 mg of HBArF·2Et_2O[13] (0.06 mmol, 1.00 equiv.) in 1 mL of dichloromethane was added slowly to the solution, observing some bubbling due to the release of H_2. The reaction mixture was stirred at room temperature for 2 h before the volatile materials were removed under vacuum. The residue was washed with *n*-pentane (3 x 2 mL) and dried under vacuum to afford 67.2 mg of **6** (0.04 mmol) as a yellow solid in 63.4% yield. The $^{31}P\{^1H\}$ NMR data was identical with those reported by Hope.[12] ^1H NMR (500 MHz, CD_2Cl_2) δ: 7.74 (br s, 8 H), 7.56 (br s, 4 H), 7.50-7.35 (m, 17 H), 7.33-7.20 (m, 13 H), 7.10-6.90 (m, 15 H) ppm. $^{13}C\{^1H\}$ NMR (126 MHz, CD_2Cl_2) δ:[11] 187.1 (br m, C_{CO}), 162.2 (q, J_{C-B} = 49.8 Hz, C_{BArF}), 135.2 (s, C_{BArF}), 134.7 (d, J_{C-P} = 12.2 Hz, C_{Ph}), 134.3 (t, J_{C-P} = 6.2 Hz, C_{Ph}), 131.6 (s, C_{Ph}), 131.3 (d, J_{C-P} = 2.0 Hz, C_{Ph}), 129.3 (qm, J_{C-F} = 31.2 Hz, C_{BArF}), 129.2 (t, J_{C-P} = 5.1 Hz, C_{Ph}), 128.7 (d, J_{C-P} = 10.2 Hz, C_{Ph}), 125.0 (q, J_{C-F} = 272.4 Hz, C_{BArF}), 117.9 (m, C_{BArF}) ppm. $^{11}B\{^1H\}$ NMR (CD_2Cl_2, 128 MHz) δ: –6.6 ppm. $^{19}F\{^1H\}$ NMR (376 MHz, CD_2Cl_2) δ: –62.9 (s, 24 F) ppm. $^{31}P\{^1H\}$ NMR (162 MHz, CD_2Cl_2) δ: 31.0-28.0 (m) ppm.[14] IR (neat): 3064, 2036 (CO), 1611, 1481, 1437, 1353, 1274, 1119, 1000, 885, 838, 742, 692, 681, 668, 542, 509 cm^{-1}. HRMS ESI-MS (m/z): $[M–BArF]^+$ calcd. for $C_{55}H_{45}OP_3Rh^+$ 917.1733, found 917.1709.

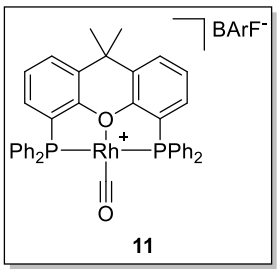

9,9-dimethyl-4,5-bis(diphenylphosphino)xanthene carbonyl rhodium (I) tetrakis[3,5-bis(trifluoromethyl)phenyl]borate, [Rh(CO)(Xantphos)]BArF (**11**): Compound **11** was prepared identically to complexes **4** and **5**, but using 1 equiv. of 9,9-dimethyl-4,5-bis(diphenylphosphino)xanthene as the ligand.

[12] H. C. S. Clark, K. S. Coleman, J. Fawcett, J. H. Holloway, E. G. Hope, J. Langer and I. M. Smith, *J. Fluorine Chem.*, 1998, **91**, 207-211.
[13] M. Brookhart, B. Grant and A. F. Volpe, Jr., *Organometallics*, 1992, **11**, 3920-3922.
[14] The $^{31}P\{^1H\}$ NMR spectrum of **6** is in agreement with the similar compound prepared by Hope *et al.* (see ref. 12 and Figure SI 64).

Complex **11** was obtained as a yellow solid in 69.2% yield (293.0 mg, 0.19 mmol). The $^{31}P\{^{1}H\}$ NMR data was in agreement with related [Rh(CO)(Xantphos)]BF_4 reported by van Leeuwen *et al.*[15] ^{1}H NMR (400 MHz, CD_2Cl_2) δ: 7.80 (dd, J = 7.6, 1.6 Hz, 2 H), 7.76-7.44 (m, 36 H), 1.75 (s, 6 H) ppm. $^{13}C\{^{1}H\}$ NMR (126 MHz, CD_2Cl_2) δ:[11] 188.5 (br m, C_{CO}), 162.2 (q, J_{C-B} = 49.8 Hz, C_{BArF}), 154.7 (t, J_{C-P} = 9.2 Hz, C_{Ph}), 135.2 (s, C_{BArF}), 134.7 (s, C_{Ph}), 133.8 (t, J_{C-P} = 7.4 Hz, C_{Ph}), 133.3 (s, C_{Ph}), 132.8 (s, C_{Ph}), 132.3 (t, J_{C-P} = 3.4 Hz, C_{Ph}), 130.1 (t, J_{C-P} = 5.6 Hz, C_{Ph}), 129.3 (qm, J_{C-F} = 31.3 Hz, C_{BArF}), 129.2 (t, J_{C-P} = 27.7 Hz, C_{Ph}), 128.2 (t, J_{C-P} = 3.7 Hz, C_{Ph}), 125.0 (q, J_{C-F} = 272.3 Hz, C_{BArF}), 119.5 (t, J_{C-P} = 18.5 Hz, C_{Ph}), 117.9 (m, C_{BArF}), 34.8, 33.9 ppm. $^{11}B\{^{1}H\}$ NMR (CD_2Cl_2, 128 MHz) δ: –6.6 ppm. $^{19}F\{^{1}H\}$ NMR (376 MHz, CD_2Cl_2) δ: –62.6 (s, 24 F) ppm. $^{31}P\{^{1}H\}$ NMR (162 MHz, CD_2Cl_2) δ: 39.9 (d, J_{P-Rh} = 122.4 Hz) ppm. IR (neat): 2012 (CO), 1611, 1438, 1401, 1353, 1273, 1116, 886, 839, 738, 712, 681, 600, 559, 517, 469 cm^{-1}. HRMS ESI-MS (m/z): $[M–BArF]^+$ calcd. for $C_{40}H_{32}O_2P_2Rh^+$ 709.0927, found 709.0943.

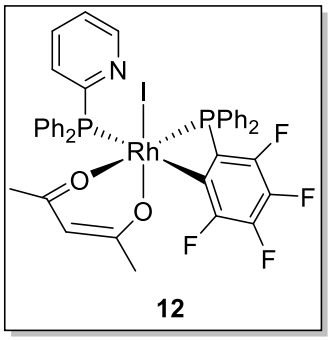

12

Complex (**12**): In a glovebox filled with N_2, 23.5 mg (0.07 mmol, 1 equiv.) of [Rh(acac)(cod)] were weighted in an vial provided with a magnetic stirrer and were dissolved with 1 mL of diethyl ether. Then, a solution of 1 mL of (2-iodo-3,4,5,6-tetrafluorobenzene)diphenylphosphine, **2** (34.2 mg, 0.07 mmol, 1 equiv.) and 2-$PyPPh_2$, **1** (19.5 mg, 0.07 mmol, 1 equiv.) in diethyl ether was stirred for five minutes and then was dropwise added to the rhodium precursor solution. During the addition, it was observed a change from yellow to a deep orange colour. The solution was stirred at reflux for 1 hour and an orange precipitate was formed. After decantation, the solid was washed with diethyl ether (3 x 1 mL) and *n*-pentane (3 x 2 mL) and dried under vacuum to afford 42.3 mg of **12** as an orange solid in 61.6% yield. ^{1}H NMR (500 MHz, CD_2Cl_2) δ: 8.40 (d, J = 4.8 Hz, 1 H), 7.85 (t, J = 8.3 Hz, 2 H), 7.56-7.14 (m, 21 H), 5.04 (s, 1 H), 1.90 (s, 3 H), 1.16 (s, 3 H) ppm. $^{13}C\{^{1}H\}$ NMR (126 MHz, CD_2Cl_2) δ:[11] 188.4 (d, J = 3.4 Hz, C_{CO}), 185.0 (s, C_{CO}), 159.0 (d, J = 58.2 Hz), 149.8 (d, J = 15.1 Hz), 136.5 (d, J = 9.4 Hz), 135.7 (d, J = 6.2 Hz), 135.4 (d, J = 9.8 Hz), 135.2 (d, J = 9.9 Hz), 134.6 (d, J

[15] A. J. Sandee, J. N. H. Reek, P. C. J. Kamer and P. W. N. M. van Leeuwen, *J. Am. Chem. Soc.*, 2001, **123**, 8468-8476.

= 11.0 Hz), 132.9 (d, *J* = 9.9 Hz), 132.0-130.0 (m), 129.0-127.0 (m), 126.8, 124.1, 123.7 (d, *J* = 1.4 Hz), 99.4, 99.1, 27.3, 26.4 ppm. $^{19}F\{^{1}H\}$ NMR (376 MHz, CD_2Cl_2) δ: –133.9 (t, $J_{F–P}$ = 20.7 Hz, 1 F), –134.7 (m, 1 F), –149.8 (m, 1 F), –162.6 (t, $J_{F–P}$ = 19.3 Hz, 1 F) ppm. $^{31}P\{^{1}H\}$ NMR (203 MHz, CD_2Cl_2) δ: 15.6 (d, $J_{P–Rh}$ = 81.9 Hz), –36.8 (d, $J_{P–Rh}$ = 101.6 Hz) ppm. IR (neat): 3054, 1576, 1513, 1466, 1434, 1094, 1015, 740, 689, 512 cm^{-1}. HRMS ESI-MS (m/z): $[M+Na]^+$ calcd. for $C_{40}H_{31}F_4INO_2P_2RhNa^+$ 947.9758, found 947.9763.

5. General Procedure for the Rh-mediated Hydroboration of Alkynes:

5.1. Hydroboration reaction optimization. Optimization table based on the results presented in the main manuscript (Table 3) is given below (Table SI 1):

Table SI 1. Optimization for the Rh-mediated hydroboration of alkynes.[a]

Entry	7a (equiv.)	HBpin (equiv.)	4 (mol%)	Solvent	8+9+10 yield%	Ratio 8:9:10
1	1.0	1.2	1	THF-d8	21.1	77:10:13
2	1.0	1.2	1	C_6D_6	14.3	77:13:10
3	1.0	1.2	1	CD_2Cl_2	29.2	61:10:29
4	1.0	1.2	5	CD_2Cl_2	68.1	78:4:18
5	**1.0**	**2.0**	**5**	**CD_2Cl_2**	**87.6**	**78:2:20**
6[b]	1.0	2.0	5	CD_2Cl_2	64.3	83:2:15

[a] Reactions were performed in deuterated solvent (0.5M) in a N_2-filled glovebox. Yields were determined by ^1H NMR using 1,2,4,5-tetramethylbenzene as the internal standard. HBpin = pinacolborane. [b] Experiment performed at 40 °C.

5.2. General procedure for Rh-mediated hydroboration. In a N_2-filled glove box, to a 10 mL screw cap tube provided with a stirrer were added the catalyst (**4**, **5**, **6** or **11**; 5 mol%), a known amount (from 0.1 to 0.5 equiv., 5 to 20 mg) of the internal standard (1,2,4,5-tetramethylbenzene), along with 600 µL of CD_2Cl_2. Then 0.3 mmol, (1 equiv.) of the alkyne were added and, finally, 0.4 mmol (1.2 equiv.) of borane were added. The mixture was stirred at 25 ºC for 24 h and then analysed by quantitative NMR and GC-FID (Scheme SI 1).

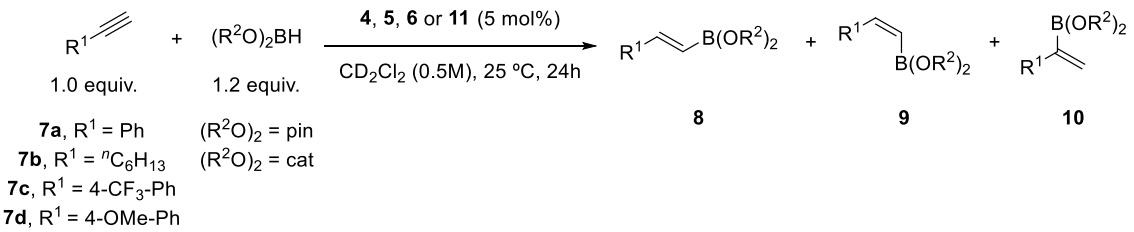

Scheme SI 1. General procedure for the hydroboration of alkynes; *pin*: pinacol, *cat*: catechol.

5.3. NMR and GC-FID analyses for the Rh-catalysed hydroboration reactions. The yield towards hydroboration products was calculated using ^{1}H qNMR, employing 1,2,4,5-tetramethylbenzene as internal standard (Sigma-Aldrich TraceCERT®). The different hydroboration major isomers (*E* and branched) were identified by previous reports in the literature and additionally by isolating them from the reaction mixture by flash chromatography (see section 5.4 in the SI). The minor *Z* isomer was directly assigned from the reaction mixture in agreement with previous reports in the literature.[16] Finally, the catecholborane derivatives were not isolated and directly assigned from the reaction mixture in agreement with previous reports in the literature.[17]

The reactions were also analysed by GC-FID analysis (5% phenyl methyl siloxane; 30 m x 320 µm x 0.25 µm). Carrier gas: He; pressure: 7.5 psi; split ratio: 50:1; injector temperature: 280 °C; detector temperature: 250 °C; flow rate: 1.5 mL/min; temperature program: 50 °C, 20 °C/min to 325 °C (5 min).[18]

[16] *Z* isomers were formed in low amounts, which made isolation not possible. Thus, *Z* isomers were identified according to previous reports in the literature. See: (a) T. Ohmura, Y. Yamamoto and N. Miyaura, *J. Am. Chem. Soc.*, 2000, **122**, 4990-4991. (b) J. Cid, J. J. Carbó and E. Fernández, *Chem. -Eur. J.*, 2012, **18**, 1512-1521.

[17] Catecholborane is sensitive to air and decomposes in the presence of transition metal complexes, phosphines, and other nucleophiles. It also applies to catecholborane derivatives. See: K. Burgess, W. A. Van der Donk, S. A. Westcott, T. B. Marder, R. T. Baker and J. C. Calabrese, *J. Am. Chem. Soc.*, 1992, **114**, 9350-9359. For this reason, catechol vinyl boronates could not be isolated and were identified according to previous reports in the literature. See: (a) H. C. Brown and S. K. Gupta, *J. Am. Chem. Soc.*, 1975, **97**, 5249-5255. (b) A. Y. Khalimon, P. M. Farha and G. I. Nikonov, *Dalton Trans.*, 2015, **44**, 18945-18956.

[18] The reactions employing catecholborane were not analysed by GC-FID.

5.3.1. Catalytic hydroboration of 7a with HBpin using complex 4:

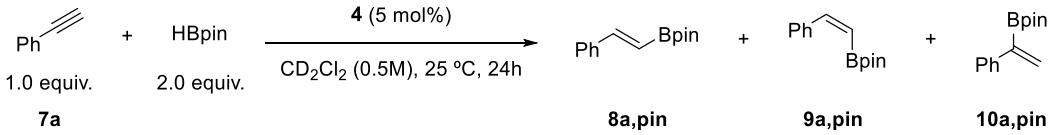

Scheme SI 2. Catalytic hydroboration of **7a** with pinacolborane (HBpin, 2 equiv.) using complex **4**.

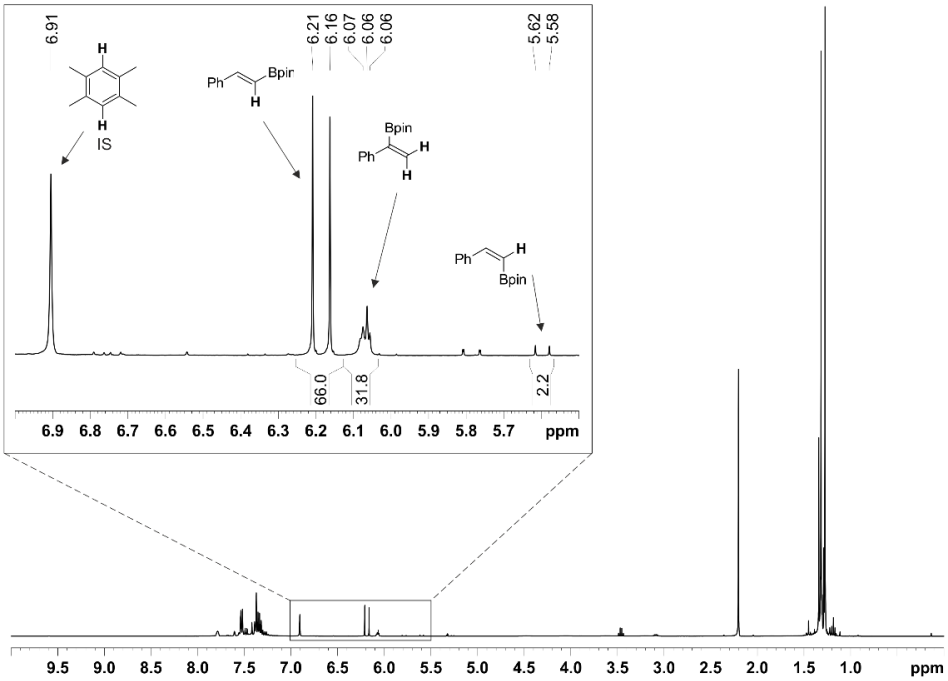

Figure SI 1. Reaction mixture ^{1}H NMR (400 MHz, CD_2Cl_2) of the catalytic hydroboration of **7a** and HBpin using complex **4**.

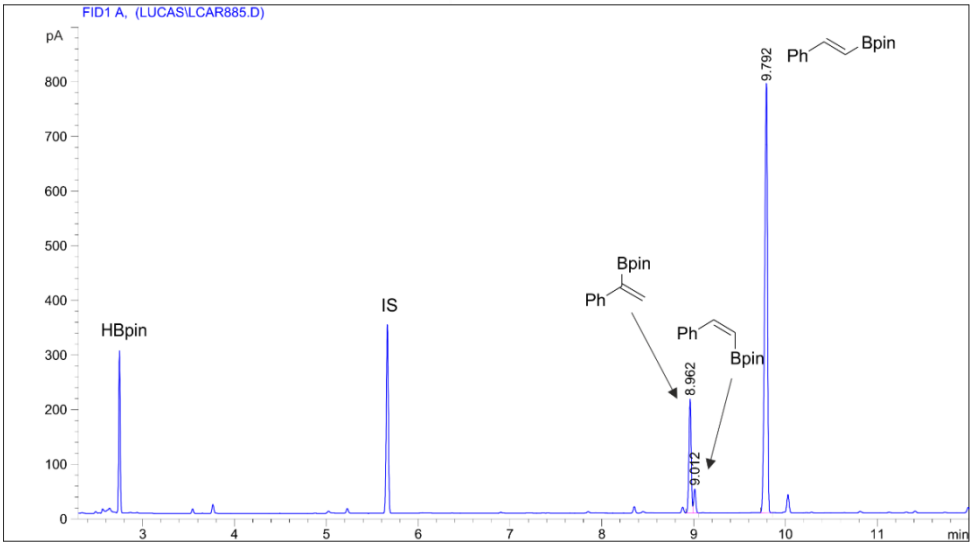

Figure SI 2. Reaction mixture GC-FID of the catalytic hydroboration of **7a** and HBpin using complex **4**. Peak 1 (rt = 8.962): Area%: 16.9. Peak 2 (rt = 9.012): Area%: 3.3. Peak 3 (rt = 9.792): Area%: 79.8.

5.3.2. Catalytic hydroboration of 7c with HBpin using complex 4:

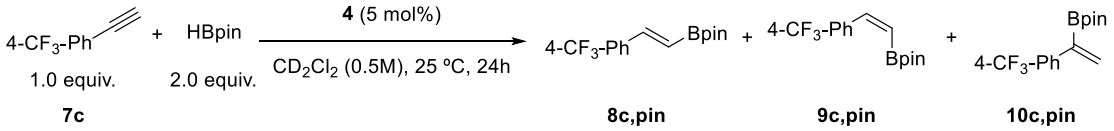

Scheme SI 3. Catalytic hydroboration of **7c** with pinacolborane (HBpin, 2 equiv.) using complex **4**.

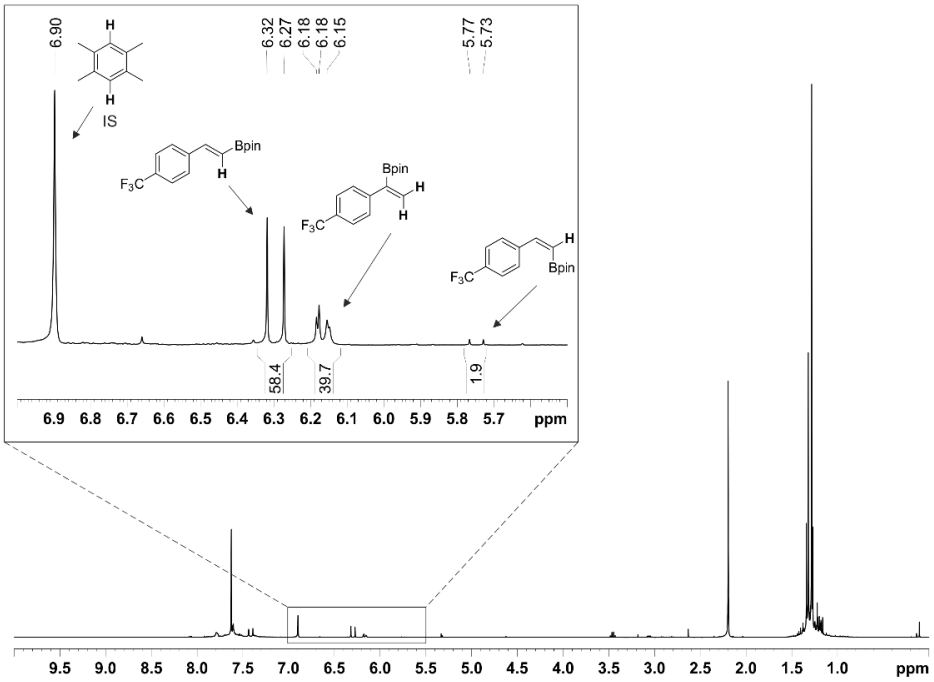

Figure SI 3. Reaction mixture ^{1}H NMR (400 MHz, CD_2Cl_2) of the catalytic hydroboration of **7c** and HBpin using complex **4**.

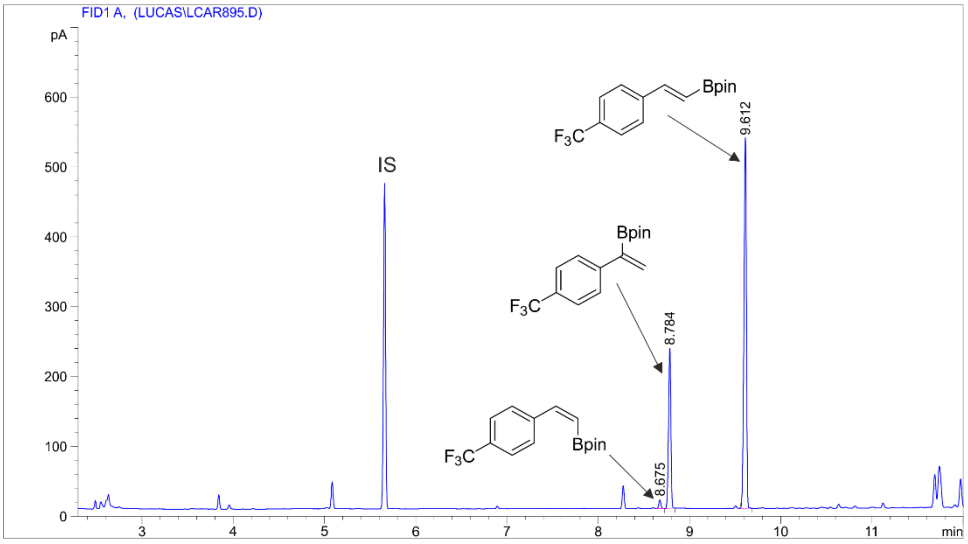

Figure SI 4. Reaction mixture GC-FID of the catalytic hydroboration of **7c** and HBpin using complex **4**. Peak 1 (rt = 8.675): Area%: 1.4. Peak 2 (rt = 8.784): Area%: 28.3. Peak 3 (rt = 9.612): Area%: 70.3.

5.3.3. Catalytic hydroboration of 7d with HBpin using complex 4:

Scheme SI 4. Catalytic hydroboration of **7d** with pinacolborane (HBpin, 2 equiv.) using complex **4**.

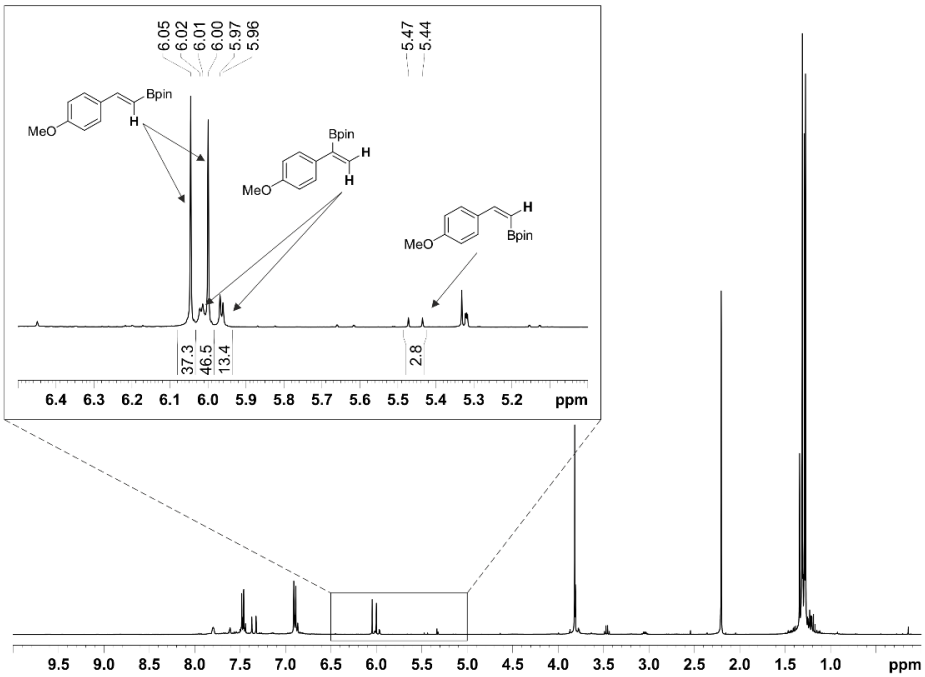

Figure SI 5. Reaction mixture ^{1}H NMR (400 MHz, CD_2Cl_2) of the catalytic hydroboration of **7d** and HBpin using complex **4**.

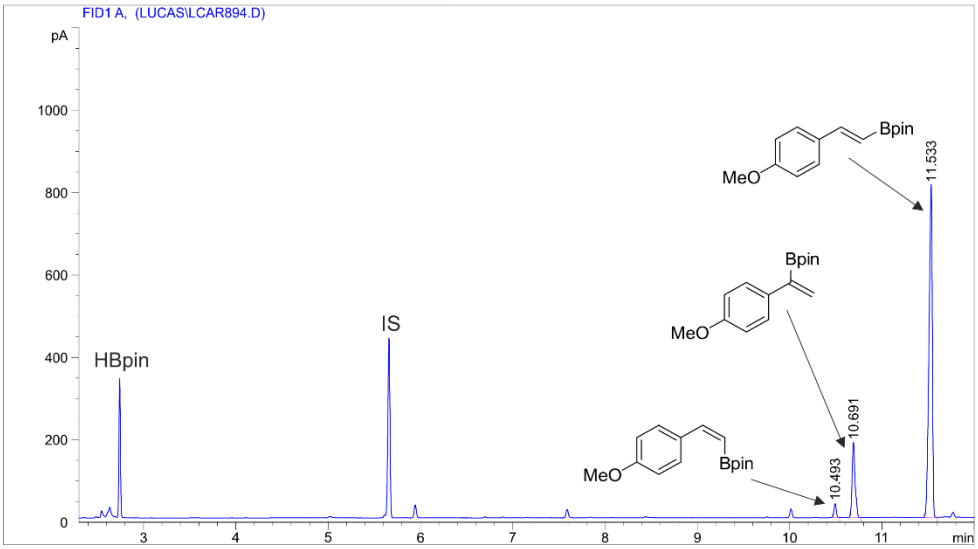

Figure SI 6. Reaction mixture GC-FID of the catalytic hydroboration of **7d** and HBpin using complex **4**. Peak 1 (rt = 10.493): Area%: 2.3. Peak 2 (rt = 10.691): Area%: 16.5. Peak 3 (rt = 11.533): Area%: 81.2.

5.3.4. Catalytic hydroboration of 7a with HBpin using complex 4:

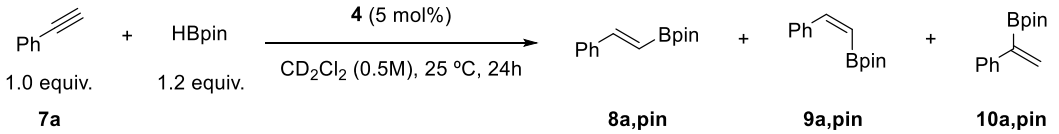

Scheme SI 5. Catalytic hydroboration of **7a** with pinacolborane (HBpin, 1.2 equiv.) using complex **4**.

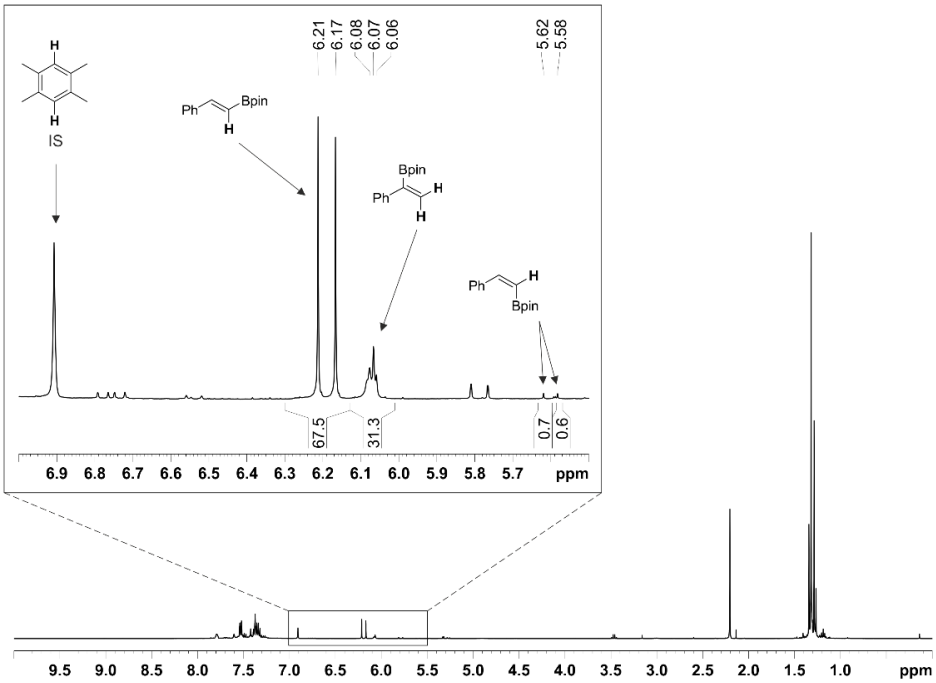

Figure SI 7. Reaction mixture ^{1}H NMR (400 MHz, CD_2Cl_2) of the catalytic hydroboration of **7a** and HBpin using complex **4**.

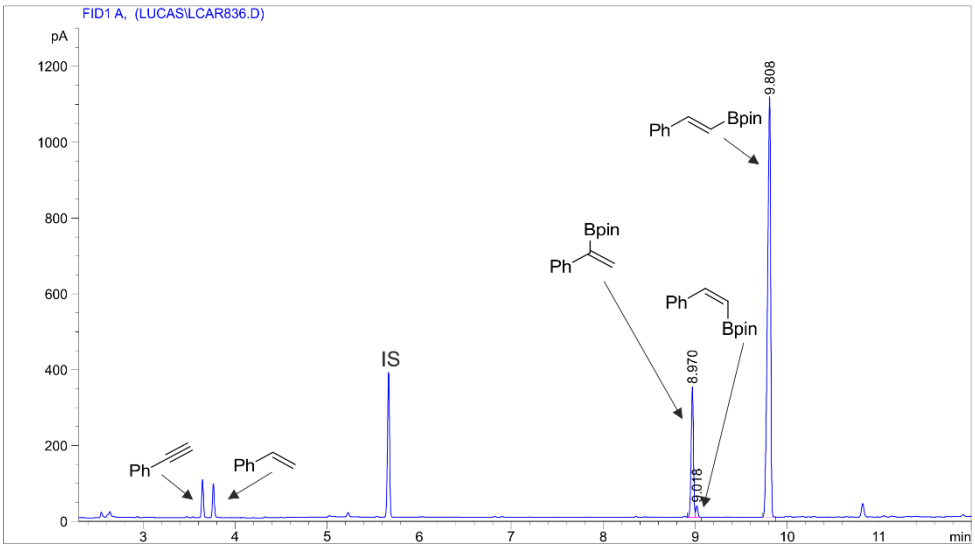

Figure SI 8. Reaction mixture GC-FID of the catalytic hydroboration of **7a** and HBpin using complex **4**. Peak 1 (rt = 8.970): Area%: 18.1. Peak 2 (rt = 9.018): Area%: 1.4. Peak 3 (rt = 9.808): Area%: 80.5.

5.3.5. Catalytic hydroboration of 7a with HBpin using complex 5:

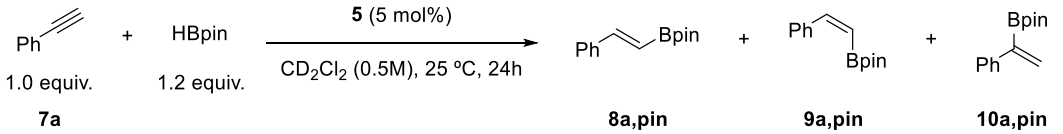

Scheme SI 6. Catalytic hydroboration of **7a** with pinacolborane (HBpin. 1.2 equiv.) using complex **5**.

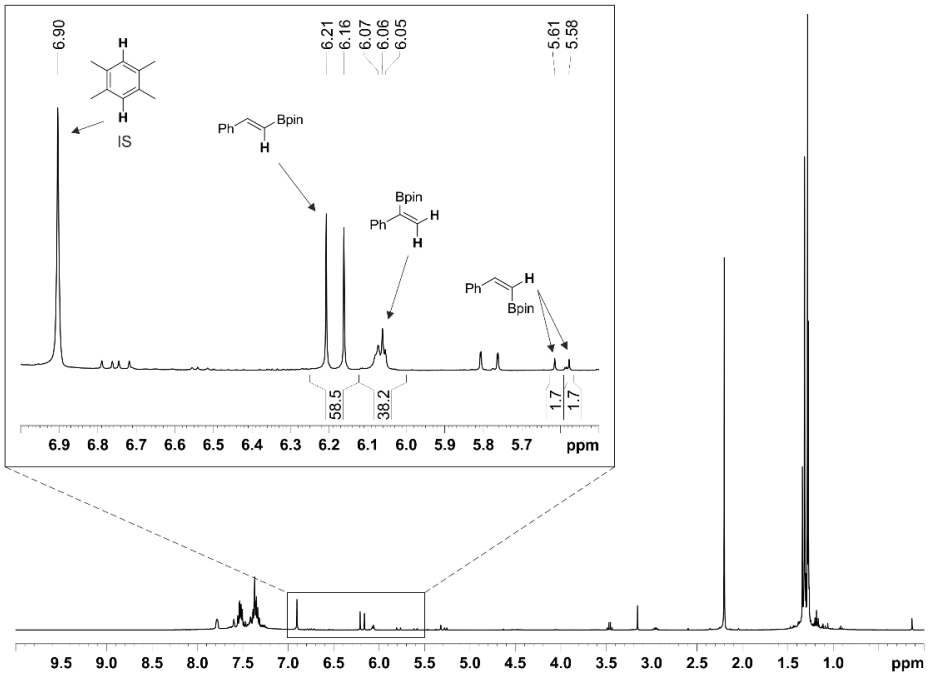

Figure SI 9. Reaction mixture ^{1}H NMR (400 MHz, CD_2Cl_2) of the catalytic hydroboration of **7a** and HBpin using complex **5**.

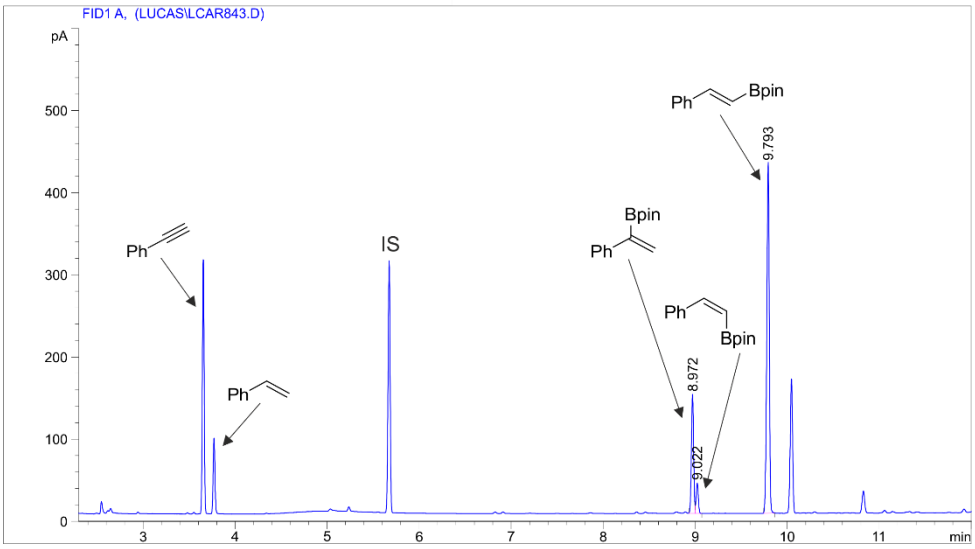

Figure SI 10. Reaction mixture GC-FID of the catalytic hydroboration of **7a** and HBpin using complex **5**. Peak 1 (rt = 8.972): Area%: 21.7. Peak 2 (rt = 9.022): Area%: 5.5. Peak 3 (rt = 9.793): Area%: 72.8.

5.3.6. Catalytic hydroboration of 7a with HBpin using complex 6:

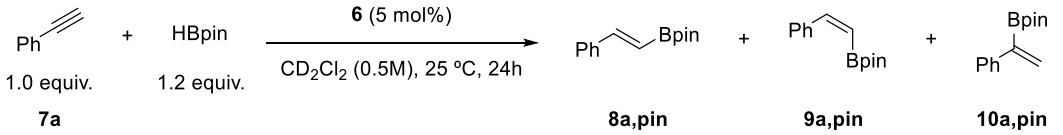

Scheme SI 7. Catalytic hydroboration of **7a** with pinacolborane (HBpin, 1.2 equiv.) using complex **6**.

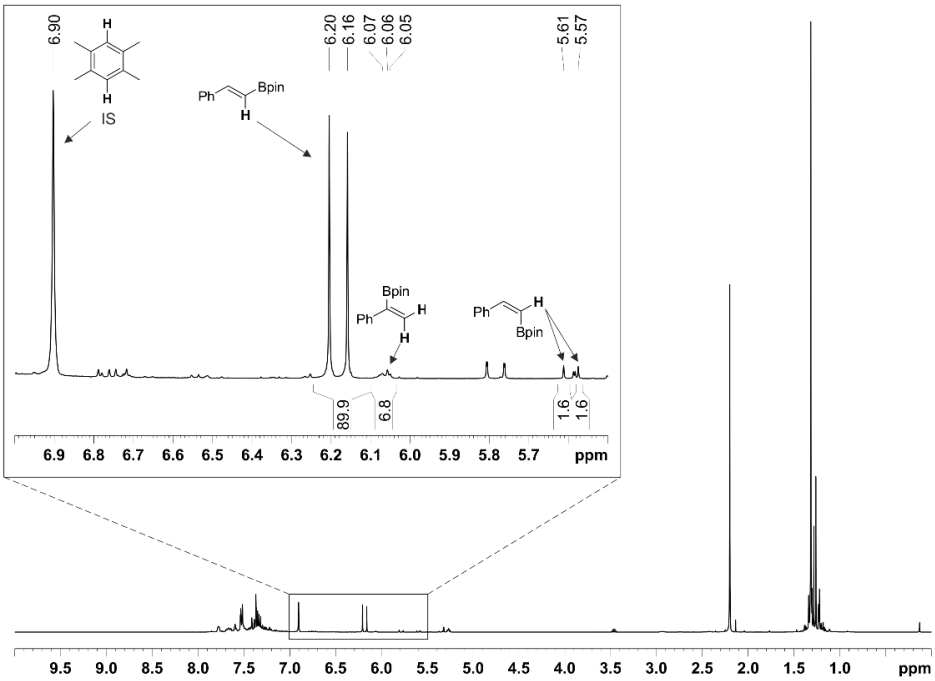

Figure SI 11. Reaction mixture ^{1}H NMR (400 MHz, CD_2Cl_2) of the catalytic hydroboration of **7a** and HBpin using complex **6**.

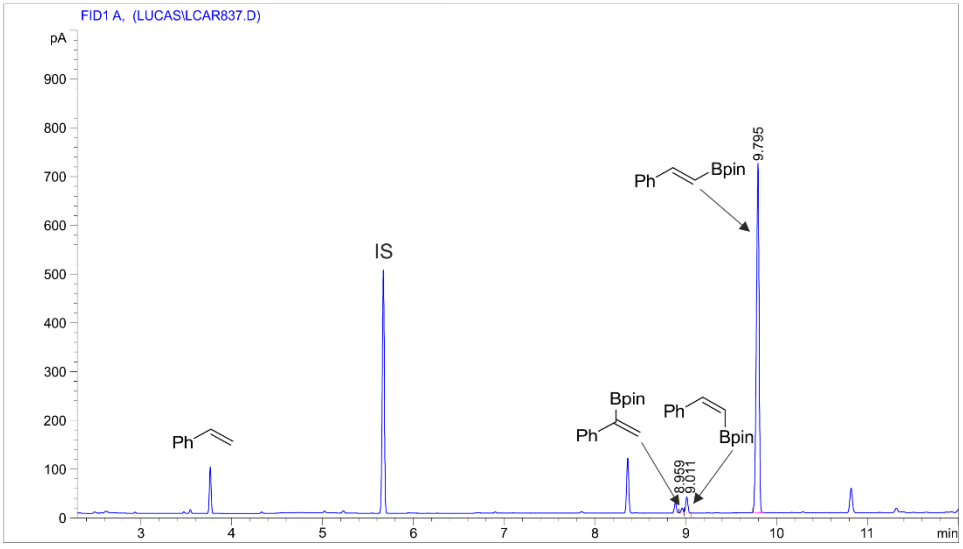

Figure SI 12. Reaction mixture GC-FID of the catalytic hydroboration of **7a** and HBpin using complex **6**. Peak 1 (rt = 8.959): Area%: 1.1. Peak 2 (rt = 9.011): Area%: 3.5. Peak 3 (rt = 9.795): Area%: 95.4.

5.3.7. Catalytic hydroboration of 7b with HBpin using complex 4:

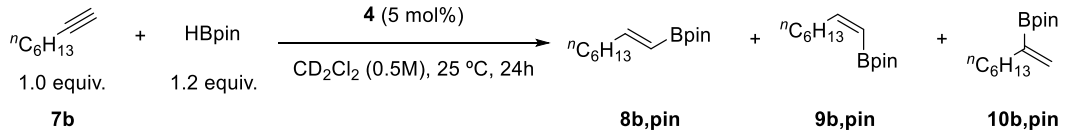

Scheme SI 8. Catalytic hydroboration of **7b** with pinacolborane (HBpin, 1.2 equiv.) using complex **4**.

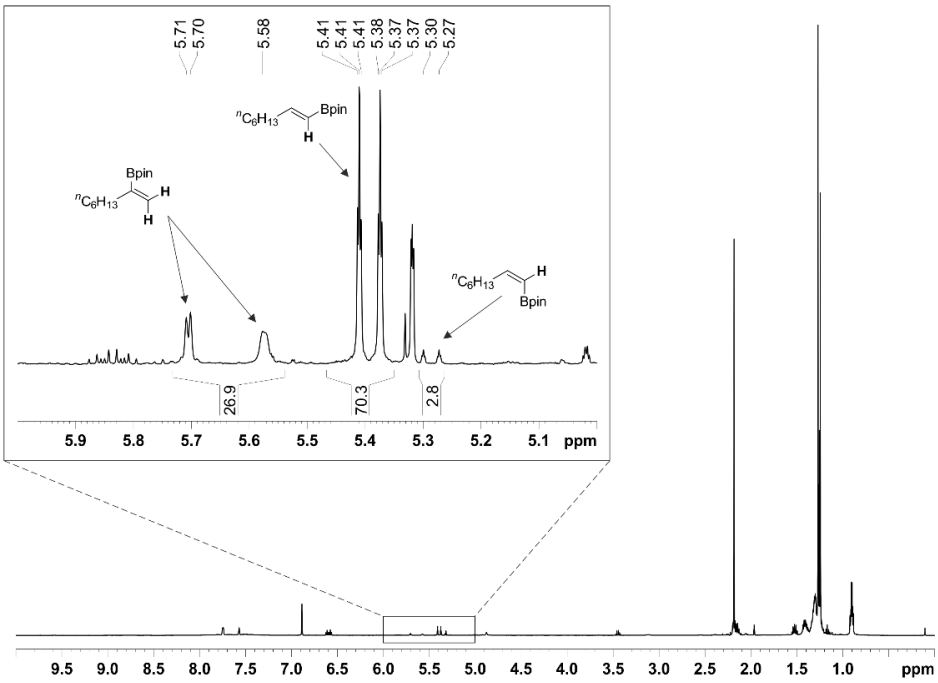

Figure SI 13. Reaction mixture ^{1}H NMR (400 MHz, CD_2Cl_2) of the catalytic hydroboration of **7b** and HBpin using complex **4**.

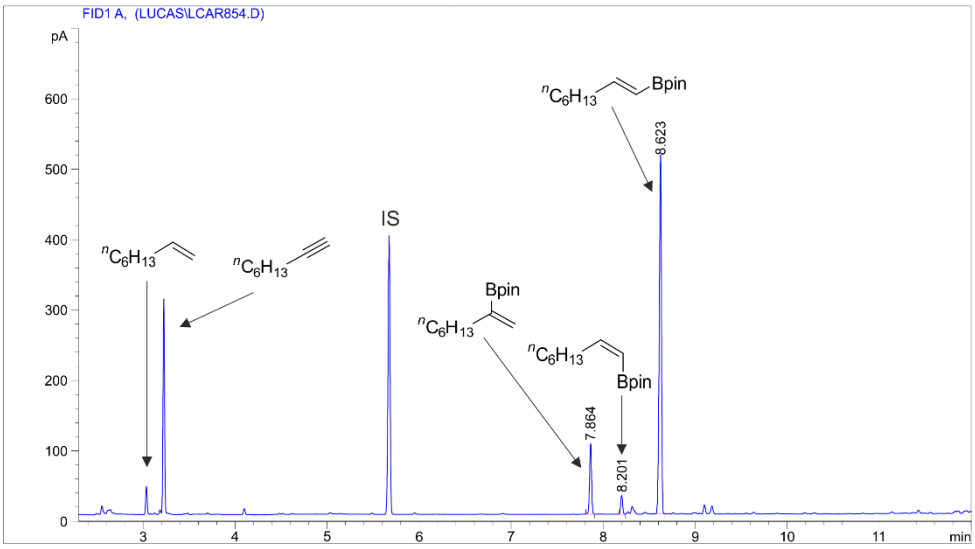

Figure SI 14. Reaction mixture GC-FID of the catalytic hydroboration of **7b** and HBpin using complex **4**. Peak 1 (rt = 7.864): Area%: 14.4. Peak 2 (rt = 8.201): Area%: 3.8. Peak 3 (rt = 8.623): Area%: 81.8.

5.3.8. Catalytic hydroboration of 7b with HBpin using complex 5:

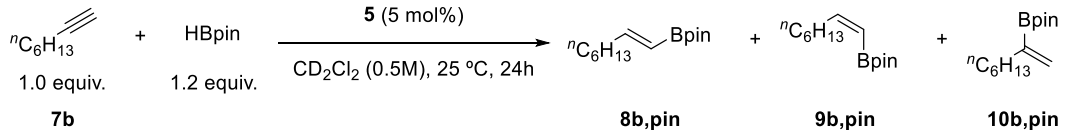

Scheme SI 9. Catalytic hydroboration of **7b** with pinacolborane (HBpin, 1.2 equiv.) using complex **5**.

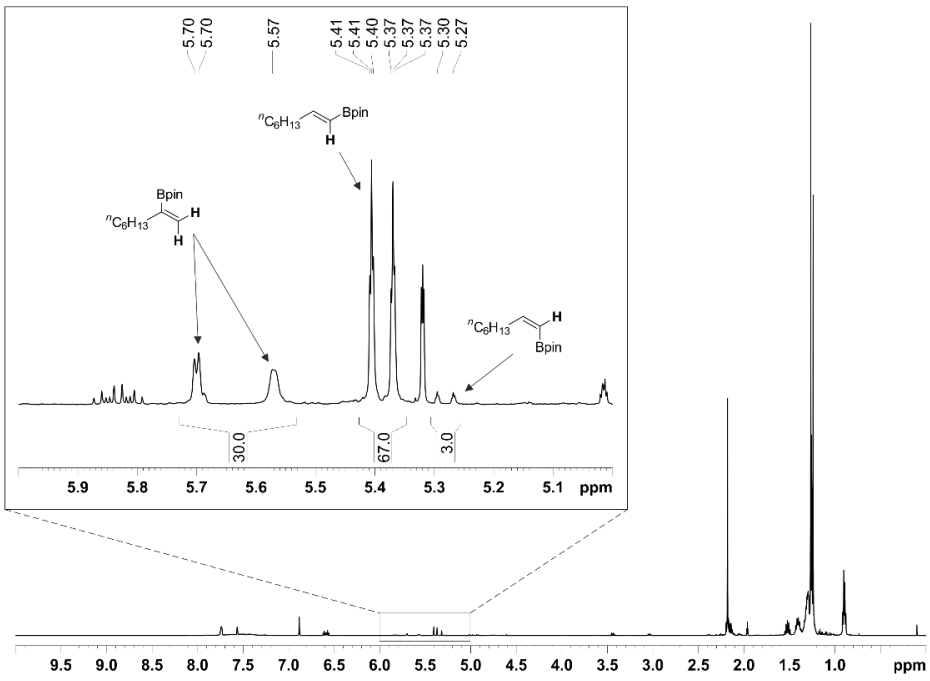

Figure SI 15. Reaction mixture ^{1}H NMR (400 MHz, CD_2Cl_2) of the catalytic hydroboration of **7b** and HBpin using complex **5**.

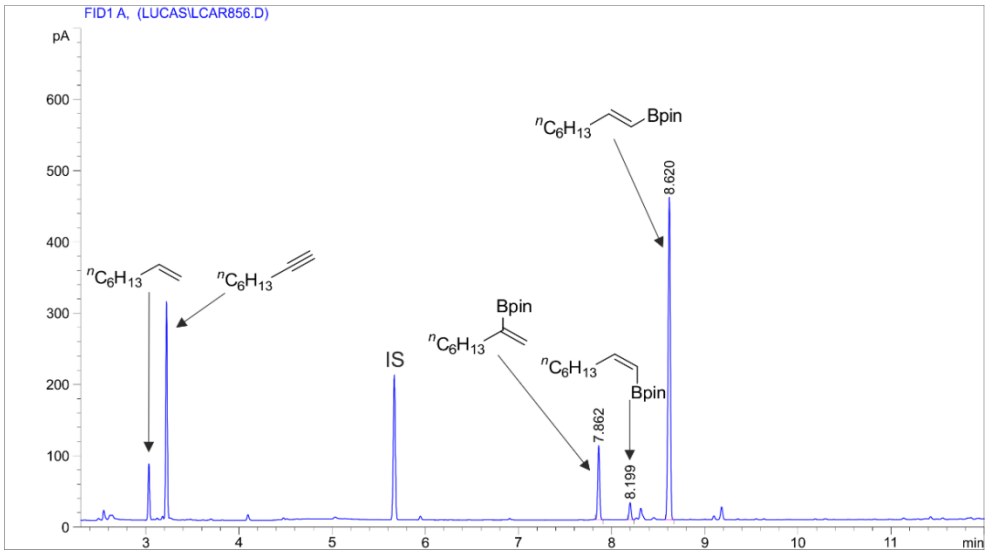

Figure SI 16. Reaction mixture GC-FID of the catalytic hydroboration of **7b** and HBpin using complex **5**. Peak 1 (rt = 7.862): Area%: 16.2. Peak 2 (rt = 8.199): Area%: 3.8. Peak 3 (rt = 8.620): Area%: 80.0.

5.3.9. Catalytic hydroboration of 7b with HBpin using complex 6:

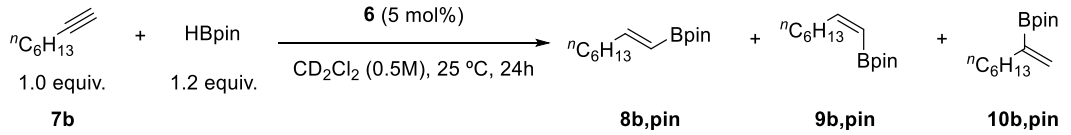

Scheme SI 10. Catalytic hydroboration of **7b** with pinacolborane (HBpin, 1.2 equiv.) using complex **6**.

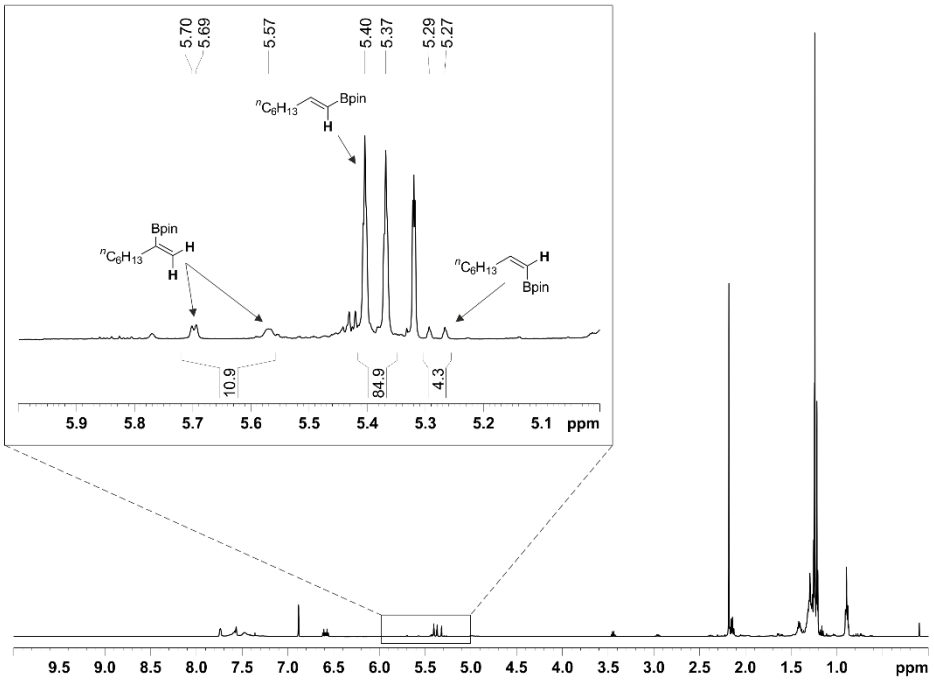

Figure SI 17. Reaction mixture ^{1}H NMR (400 MHz, CD_2Cl_2) of the catalytic hydroboration of **7b** and HBpin using complex **6**.

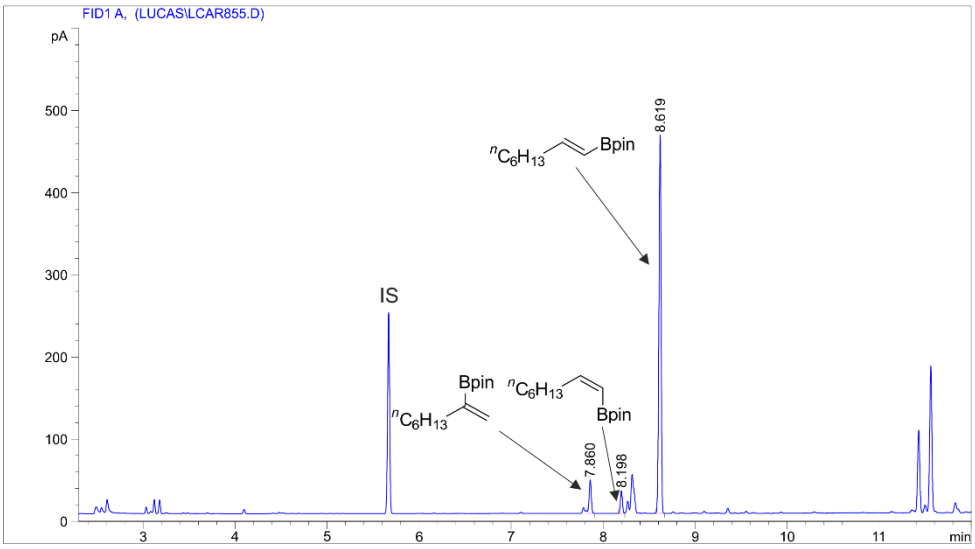

Figure SI 18. Reaction mixture GC-FID of the catalytic hydroboration of **7b** and HBpin using complex **6**. Peak 1 (rt = 7.860): Area%: 7.5. Peak 2 (rt = 8.198): Area%: 4.7. Peak 3 (rt = 8.619): Area%: 87.8.

5.3.10. Catalytic hydroboration of 7a with HBcat using complex 4:

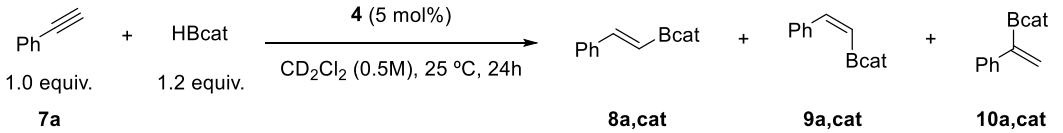

Scheme SI 11. Catalytic hydroboration of **7a** with catecholborane (HBcat, 1.2 equiv.) using complex **4**.

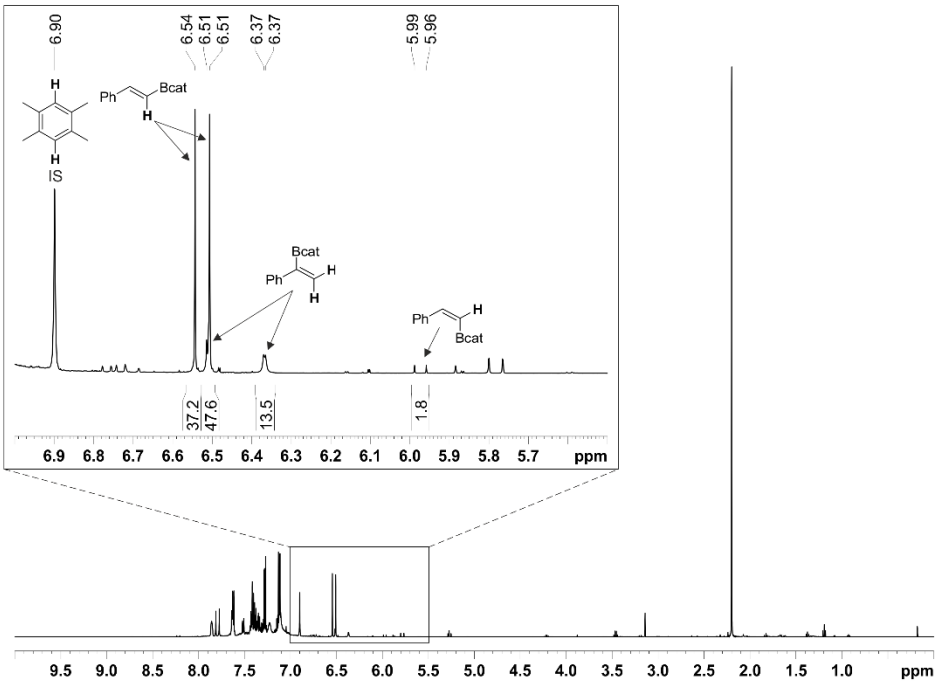

Figure SI 19. Reaction mixture ^{1}H NMR (400 MHz, CD_2Cl_2) of the catalytic hydroboration of **7a** and HBcat using complex **4**.

5.3.11. Catalytic hydroboration of 7a with HBcat using complex 5:

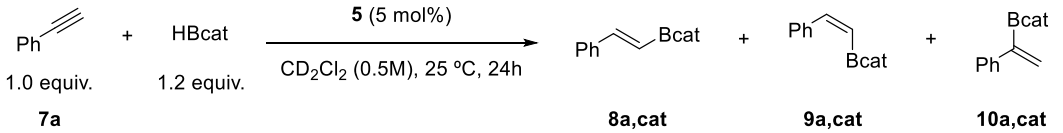

Scheme SI 12. Catalytic hydroboration of **7a** with catecholborane (HBcat, 1.2 equiv.) using complex **5**.

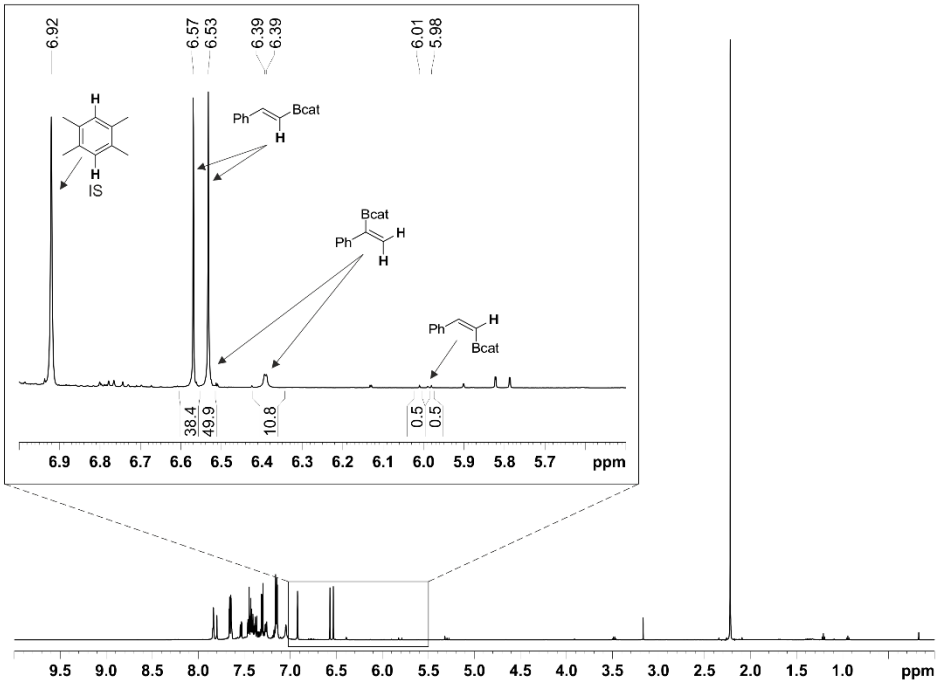

Figure SI 20. Reaction mixture ^{1}H NMR (400 MHz, CD_2Cl_2) of the catalytic hydroboration of **7a** and HBcat using complex **5**.

5.3.12. Catalytic hydroboration of 7a with HBcat using complex 6:

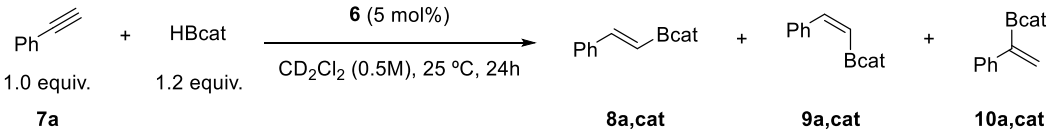

Scheme SI 13. Catalytic hydroboration of **7a** with catecholborane (HBcat, 1.2 equiv.) using complex **6**.

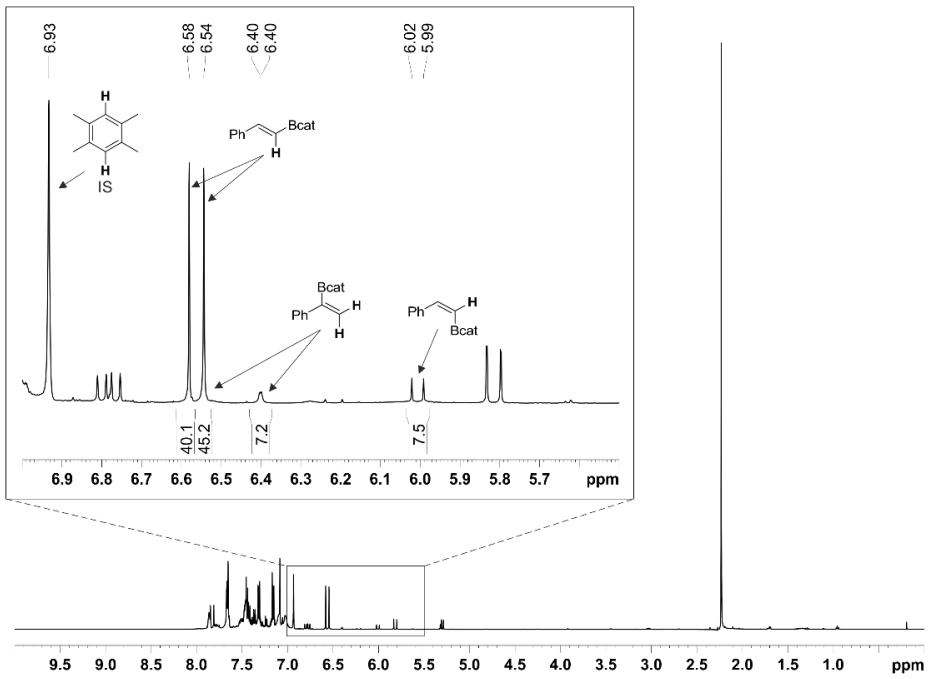

Figure SI 21. Reaction mixture ^{1}H NMR (400 MHz, CD_2Cl_2) of the catalytic hydroboration of **7a** and HBcat using complex **6**.

5.3.13. Catalytic hydroboration of 7b with HBcat using complex 4:

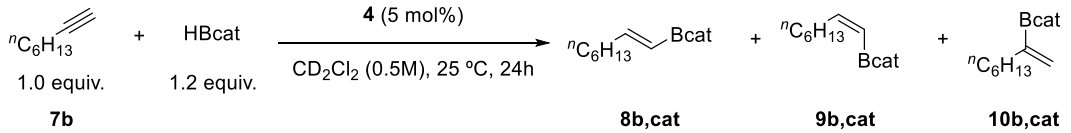

Scheme SI 14. Catalytic hydroboration of **7b** with catecholborane (HBcat, 1.2 equiv.) using complex **4**.

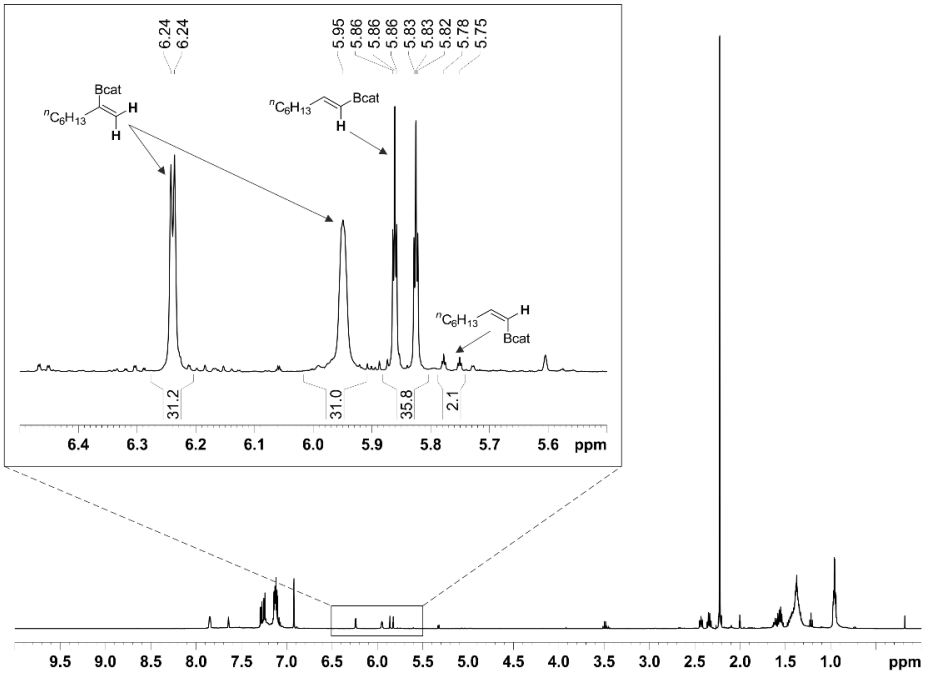

Figure SI 22. Reaction mixture ^{1}H NMR (400 MHz, CD_2Cl_2) of the catalytic hydroboration of **7b** and HBcat using complex **4**.

5.3.14. Catalytic hydroboration of 7b with HBcat using complex 5:

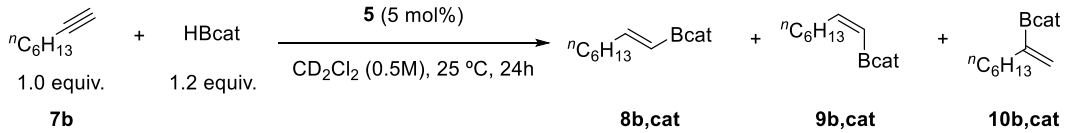

Scheme SI 15. Catalytic hydroboration of **7b** with catecholborane (HBcat, 1.2 equiv.) using complex **5**.

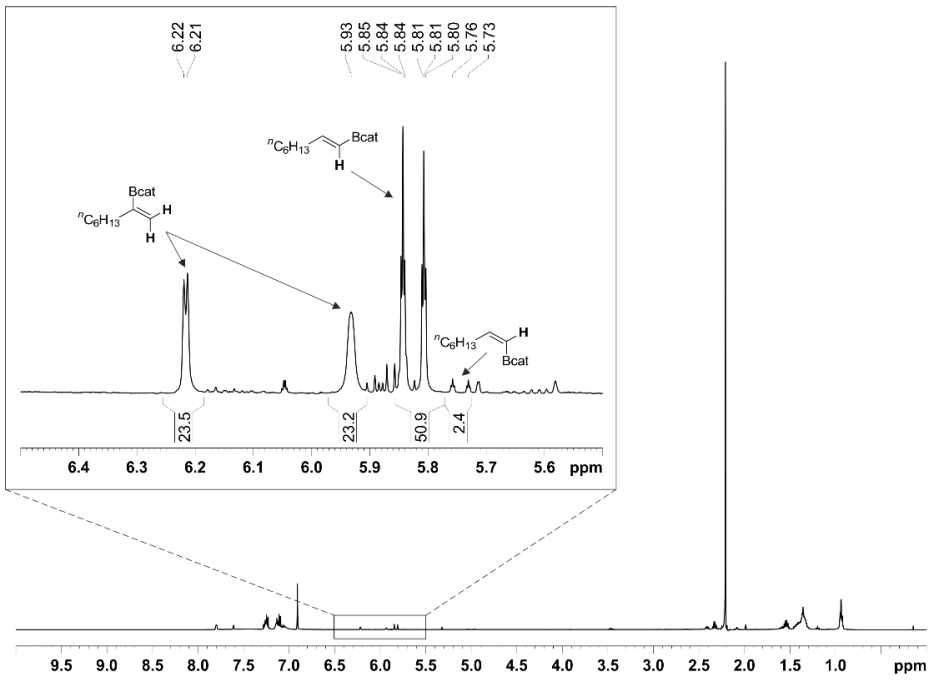

Figure SI 23. Reaction mixture ^{1}H NMR (400 MHz, CD_2Cl_2) of the catalytic hydroboration of **7b** and HBcat using complex **5**.

5.3.15. Catalytic hydroboration of 7b with HBcat using complex 6:

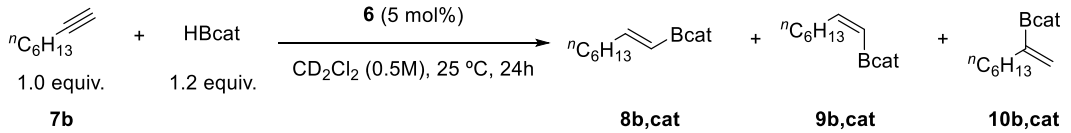

Scheme SI 16. Catalytic hydroboration of **7b** with catecholborane (HBcat, 1.2 equiv.) using complex **6**.

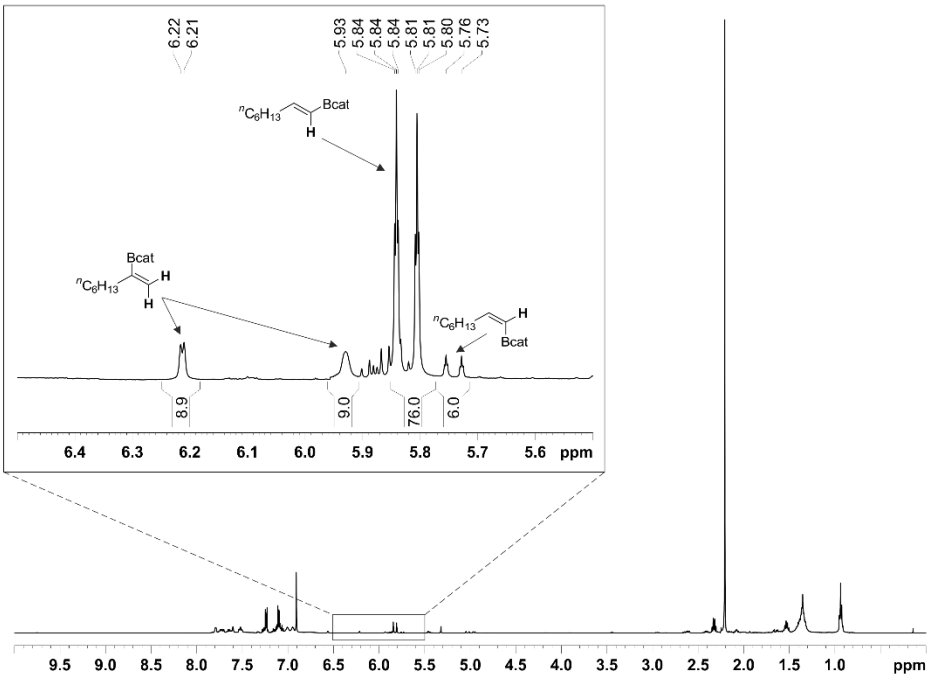

Figure SI 24. Reaction mixture ^{1}H NMR (400 MHz, CD_2Cl_2) of the catalytic hydroboration of **7b** and HBcat using complex **6**.

5.3.16 Catalytic hydroboration of 7a with HBpin using complex 11:

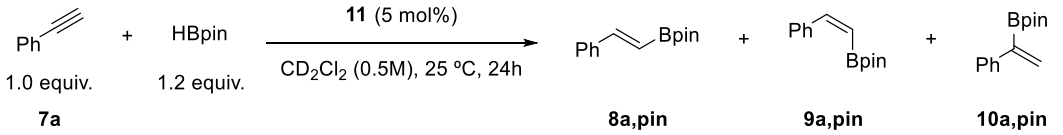

Scheme SI 17. Catalytic hydroboration of **7a** with pinacolborane (HBpin, 1.2 equiv.) using complex **11**.

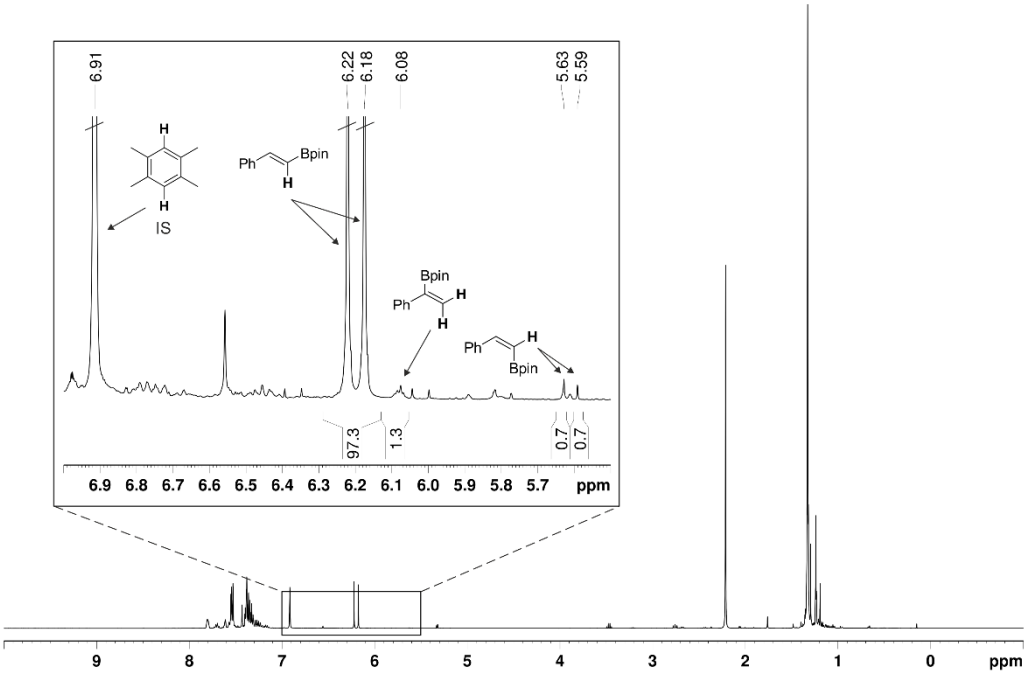

Figure SI 25. Reaction mixture ^{1}H NMR (400 MHz, CD_2Cl_2) of the catalytic hydroboration of **7a** and HBpin using complex **11**.

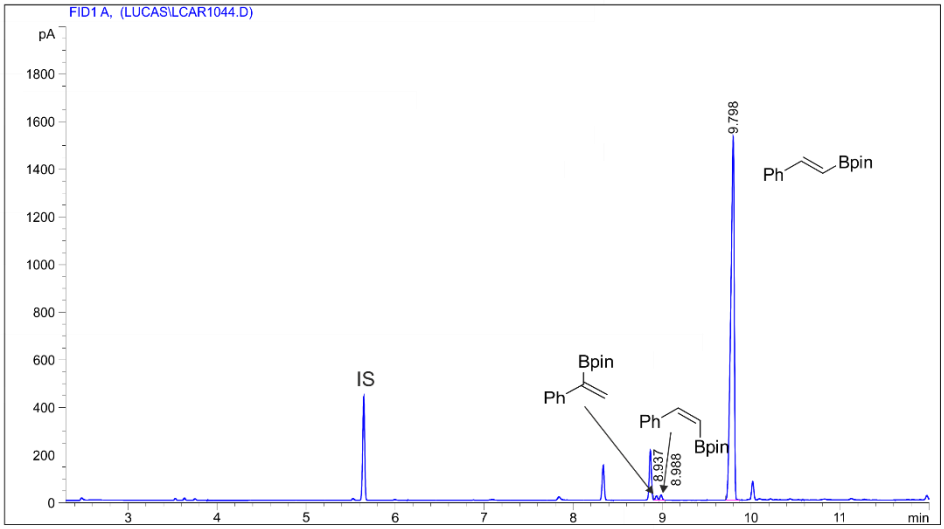

Figure SI 26. Reaction mixture GC-FID of the catalytic hydroboration of **7a** and HBpin using complex **11**. Peak 1 (rt = 8.937): Area%: 0.7. Peak 2 (rt = 8.988): Area%: 0.9. Peak 3 (rt = 9.798): Area%: 98.4.

5.4. Characterization of the *E* / branched hydroboration products. Vinylboronic esters were isolated from the crude reactions using boric acid impregnated silica gel.[19] As mentioned in section 5.3, catechol boronic esters were not isolated,[17] but directly assigned from the reaction mixture in agreement with previous reports in the literature. ^{1}H NMR and ^{13}C{^{1}H} NMR spectra and GC-FID chromatograms of the isolated products can be found in section 7.3.

Boric acid impregnated silica gel: A 1000 mL round bottom flask equipped with a stir bar was charged with silica gel (300 mL), boric acid (28 g) and ethanol (550 mL) under air. The suspension was stirred at rt for 2 h at which time ethanol and excess boric acid were removed by filtration. The impregnated silica gel was washed with ethanol (3 x 200 mL) and dried in a vacuum oven at 140 °C for 48 h. Once dried, the boric acid impregnated silica gel was stored in a desiccator until used.

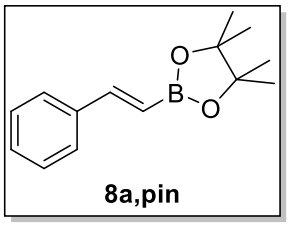

***E*-2-(4,4,5,5-Tetramethyl-1,3,2-dioxaborolan-2-yl)styrene** (**8a,pin**): The reaction crude mixture was purified by column chromatography using $B(OH)_3$ impregnated SiO_2 and *n*-hexane and AcOEt as the eluents (30:1→10:1, *n*-hexane:AcOEt), to afford the compound as a yellow oil. ^{1}H NMR (400 MHz, CD_2Cl_2) δ: 7.55-7.48(m, 2H), 7.43-7.27 (m, 4H), 6.17 (d, *J* = 18.4 Hz, 1H), 1.30 (s, 12H) ppm. ^{13}C{^{1}H} NMR (100 MHz, CD_2Cl_2) δ:[20] 149.6, 138.0, 129.3, 129.0, 127.4, 83.7, 25.1 ppm. GC-FID: rt = 9.783 min. ^{1}H NMR and ^{13}C{^{1}H} NMR data were in agreement with those previously reported.[21]

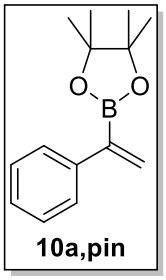

4,4,5,5-Tetramethyl-2-(1-phenylvinyl)-1,3,2-dioxaborolane (**10a,pin**): The reaction crude mixture was purified by column chromatography using $B(OH)_3$ impregnated SiO_2 and *n*-hexane and AcOEt as the eluents (30:1→10:1, *n*-hexane:AcOEt), to afford the compound as a yellow oil. ^{1}H NMR (400 MHz, CD_2Cl_2) δ: 7.50-7.45 (m, 2H), 7.37-7.27 (m, 3H), 6.06 (m, 2H), 1.34 (s, 12H) ppm. ^{13}C{^{1}H} NMR (100 MHz, CD_2Cl_2) δ:

[19] Boronic esters are known to partially decompose with SiO_2. Boric acid impregnated silica is known to decrease this decomposition. See: S. Hitosugi, D. Tanimoto, W. Nakanishi and H. Isobe, *Chem. Lett.*, 2012, **41**, 972-973.

[20] The C–B signal in ^{13}C{^{1}H} NMR was not observed in the spectra. For details, see: B. Wrackmeyer, *Prog. Nucl. Magn. Reson. Spectrosc.*, 1979, **12**, 227-259. This observation also applies to the rest of vinyl boronic esters.

[21] A. Grirrane, A. Corma and H. García, *Chem. -Eur. J.*, 2011, **17**, 2467-2478.

142.0, 131.1, 128.5, 127.6, 127.4, 84.2, 25.0 ppm. GC-FID: rt = 8.977 min. ^{1}H NMR and ^{13}C{^{1}H} NMR data were in agreement with those previously reported.[22]

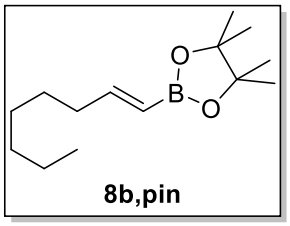

***E*-4,4,5,5-tetramethyl-2-(oct-1-en-1-yl)-1,3,2-dioxaborolane** (**8b,pin**): The reaction crude mixture was purified by column chromatography using $B(OH)_3$ impregnated SiO_2 and *n*-hexane and AcOEt as the eluents (30:1, *n*-hexane:AcOEt), to afford the compound as a colourless oil. ^{1}H NMR (400 MHz, CD_2Cl_2) δ: 6.57 (dt, *J* = 17.9, 6.5 Hz, 1H), 5.37 (dt, *J* = 17.9, 1.5 Hz, 1H), 2.14 (m, 2H), 1.46-1.19 (m, 20H), 0.88 (m, 3H) ppm. ^{13}C{^{1}H} NMR (100 MHz, CD_2Cl_2) δ: 155.0, 83.3, 36.2, 32.2, 29.4, 28.8, 25.0, 23.0, 14.3 ppm. GC-FID: rt = 8.605 min. ^{1}H NMR and ^{13}C{^{1}H} NMR data were in agreement with those previously reported.[21]

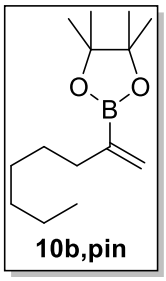

4,4,5,5-tetramethyl-2-(oct-1-en-2-yl)-1,3,2-dioxaborolane (**10b,pin**): The reaction crude mixture was purified by column chromatography using $B(OH)_3$ impregnated SiO_2 and *n*-hexane and AcOEt as the eluents (30:1, *n*-hexane:AcOEt), to afford the compound as a colourless oil. ^{1}H NMR (500 MHz, CD_2Cl_2) δ: 5.68 (d, *J* = 3.7 Hz, 1H), 5.56 (br s, 1H), 2.10 (m, 2H), 1.46-1.22 (m, 20H), 0.88 (m, 3H) ppm. ^{13}C{^{1}H} NMR (126 MHz, CD_2Cl_2) δ: 128.6, 83.6, 35.8, 32.2, 29.7, 29.4, 24.9, 23.1, 14.3 ppm. GC-FID: rt = 7.855 min. ^{1}H NMR and ^{13}C{^{1}H} NMR data were in agreement with those previously reported.[23]

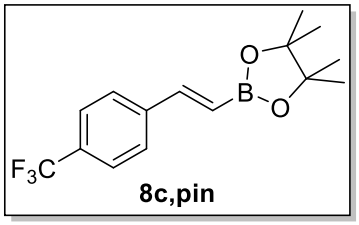

***E*-4,4,5,5-tetramethyl-2-(4-(trifluoromethyl)styryl)-1,3,2 dioxaborolane** (**8c,pin**): The reaction crude mixture was purified by column chromatography using $B(OH)_3$ impregnated SiO_2 and *n*-hexane and AcOEt as the eluents (30:1→10:1, *n*-hexane:AcOEt), to afford the compound as a yellow oil. ^{1}H NMR (400 MHz, CD_2Cl_2) δ: 7.61 (s, 4H), 7.38 (d, *J* = 18.4 Hz, 1H), 6.26 (d, *J* = 18.4 Hz, 1H), 1.29 (s, 12H) ppm. ^{13}C{^{1}H} NMR (126 MHz, CD_2Cl_2) δ: 147.7, 141.4, 130.5 (q, J_{C-F} = 32.3 Hz), 127.6, 125.9 (q, J_{C-F} = 3.9 Hz), 124.6 (q, J_{C-F} =

[22] H. Jang, A. R. Zhugralin, Y. Lee and A. H. Hoveyda, *J. Am. Chem. Soc.*, 2011, **133**, 7859-7871.
[23] D. P. Ojha and K. R. Prabhu, *Org. Lett.*, 2016, **18**, 432-435.

272.1 Hz), 83.9, 25.0 ppm. GC-FID: rt = 9.603 min. ^{1}H NMR and ^{13}C{^{1}H} NMR data were in agreement with those previously reported.[22]

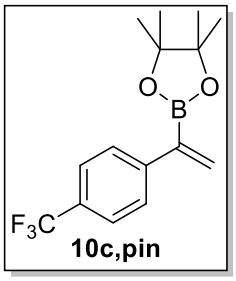

4,4,5,5-tetramethyl-2-(1-(4-(trifluoromethyl)phenyl)vinyl)-1,3,2 dioxaborolane (**10c,pin**): The reaction crude mixture was purified by column chromatography using $B(OH)_3$ impregnated SiO_2 and *n*-hexane and AcOEt as the eluents (30:1→10:1, *n*-hexane:AcOEt), to afford the compound as a yellow oil. ^{1}H NMR (400 MHz, CD_2Cl_2) δ: 7.58 (s, 4H), 6.14 (br m, 2H), 1.31 (s, 12H) ppm. ^{13}C{^{1}H} NMR (126 MHz, CD_2Cl_2) δ: 145.8, 133.2, 129.0 (q, $J_{C–F}$ = 32.2 Hz), 128.0, 125.3 (q, $J_{C–F}$ = 3.7 Hz), 124.9 (q, $J_{C–F}$ = 271.6 Hz), 84.6, 25.0 ppm. ^{19}F{^{1}H} NMR (376 MHz, CD_2Cl_2) δ: -62.4 (s, 3F) ppm. GC-FID: rt = 8.784 min. ^{1}H NMR and ^{13}C{^{1}H} NMR data were in agreement with those previously reported.[22]

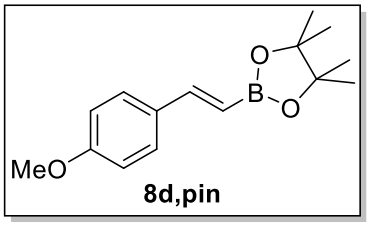

***E*-2-(4-methoxystyryl)-4,4,5,5-tetramethyl-1,3,2 dioxaborolane** (**8d,pin**): The reaction crude mixture was purified by column chromatography using $B(OH)_3$ impregnated SiO_2 and *n*-hexane and AcOEt as the eluents (30:1→10:1, *n*-hexane:AcOEt), to afford the compound as a yellow oil. ^{1}H NMR (400 MHz, CD_2Cl_2) δ: 7.45 (dm, *J* = 8.8 Hz, 2H), 7.30 (d, *J* = 18.4 Hz, 1H), 6.88 (dm, *J* = 8.8 Hz, 2H), 5.98 (d, *J* = 18.3 Hz, 1H), 3.81 (s, 3H), 1.28 (s, 12H) ppm. ^{13}C{^{1}H} NMR (100 MHz, CD_2Cl_2) δ: 160.8, 149.2, 130.8, 128.9, 114.3, 83.5, 55.7, 25.0 ppm. GC-FID: rt = 11.530 min. ^{1}H NMR and ^{13}C{^{1}H} NMR data were in agreement with those previously reported.[24]

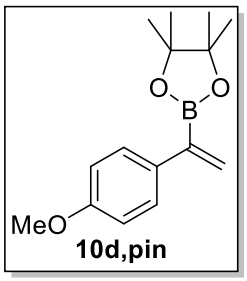

2-(1-(4-methoxyphenyl)vinyl)-4,4,5,5-tetramethyl-1,3,2 dioxaborolane (**10d,pin**): The reaction crude mixture was purified by column chromatography using $B(OH)_3$ impregnated SiO_2 and *n*-hexane and AcOEt as the eluents (30:1→10:1, *n*-hexane:AcOEt), to afford the compound as a yellow oil. ^{1}H NMR (400 MHz, CD_2Cl_2) δ: 7.41 (dm, *J* = 8.8 Hz, 2H), 6.84 (dm, *J* = 8.8 Hz, 2H), 5.98 (d, *J* = 2.8 Hz, 1H), 5.91 (d, *J* = 3.0 Hz, 1H), 3.79 (s, 3H), 1.31 (s,

[24] W. B. Reid, J. J. Spillane, S. B. Krause and D. A. Watson, *J. Am. Chem. Soc.*, 2016, **138**, 5539-5542.

12H) ppm. $^{13}C\{^{1}H\}$ NMR (100 MHz, CD_2Cl_2) δ: 159.4, 134.4, 129.1, 128.8, 113.9, 84.1, 55.6, 25.0 ppm. GC-FID: rt = 10.679 min. ^{1}H NMR and $^{13}C\{^{1}H\}$ NMR data were in agreement with those previously reported.[25]

[25] W. Guan, A. K. Michael, M. L. McIntosh, L. Koren-Selfridge, J. P. Scott and T. B. Clark, *J. Org. Chem.*, 2014, **79**, 7199-7204.

6. Details of the DFT Computational Studies:

6.1. Computational method. Geometry optimizations of compounds **4MePy** (4-methylpyridine), **IPFB** (iodopentafluorobenzene), **4MePy·IPFB**, **1**, **2**, **3**, **Rh[(CO)$_2$]$^+$**, **CO**, **Rh[(CO)(1)(2)]$^+$** and **Rh[(CO)(1)(3)]$^+$** were carried out using the TPSS[26]-D3[27] functional and the def2-TZVP basis set[28] as implemented in Gaussian 09, Revision D.01.[29] The TPSS-D3/def2-TZVP level of theory offers a good compromise between the size of the system (up to 70 atoms for **Rh[(CO)(1)(2)]$^+$** and **Rh[(CO)(1)(3)]$^+$**), the computational cost and the accuracy in describing halogen bonding.[30] Solvent effects (toluene) were incorporated employing the Polarizable Continuum Model (PCM) with the integral equation formalism (IEFPCM calculations)[31] with radii and non-electrostatic terms[32] as implemented in Gaussian 09, Revision D.01. Energies in solution (toluene) include corrections for zero-point energy and free energy (incorporating temperature and entropic effects corrected to 298.15 K). Electrostatic potential surfaces were calculated with Gaussian 09 at the TPSS-D3-def2TZVP level of theory considering the effects of toluene as the solvent and have been plotted with GaussView 5.0 using an isovalue of 0.001 a.u.

[26] J. Tao, J. P. Perdew, V. N. Staroverov and G. E. Scuseria, *Phys. Rev. Lett.*, 2003, **91**, 146401/1-146401/4.
[27] (a) S. Grimme, J. Antony, S. Ehrlich and H. Krieg, *J. Chem. Phys.*, 2010, **132**, 154104/1-154104/19. (b) S. Grimme, S. Ehrlich and L. Goerigk, *J. Comput. Chem.*, 2011, **32**, 1456-1465.
[28] (a) F. Weigend and R. Ahlrichs, *Phys. Chem. Chem. Phys.*, 2005, **7**, 3297-3305. (b) F. Weigend, *Phys. Chem. Chem. Phys.*, 2006, **8**, 1057-1065.
[29] Gaussian 09, Revision D.01, M. J. Frisch, G. W. Trucks, H. B. Schlegel, G. E. Scuseria, M. A. Robb, J. R. Cheeseman, G. Scalmani, V. Barone, B. Mennucci, G. A. Petersson, H. Nakatsuji, M. Caricato, X. Li, H. P. Hratchian, A. F. Izmaylov, J. Bloino, G. Zheng, J. L. Sonnenberg, M. Hada, M. Ehara, K. Toyota, R. Fukuda, J. Hasegawa, M. Ishida, T. Nakajima, Y. Honda, O. Kitao, H. Nakai, T. Vreven, J. A. Montgomery, Jr., J. E. Peralta, F. Ogliaro, M. Bearpark, J. J. Heyd, E. Brothers, K. N. Kudin, V. N. Staroverov, T. Keith, R. Kobayashi, J. Normand, K. Raghavachari, A. Rendell, J. C. Burant, S. S. Iyengar, J. Tomasi, M. Cossi, N. Rega, J. M. Millam, M. Klene, J. E. Knox, J. B. Cross, V. Bakken, C. Adamo, J. Jaramillo, R. Gomperts, R. E. Stratmann, O. Yazyev, A. J. Austin, R. Cammi, C. Pomelli, J. W. Ochterski, R. L. Martin, K. Morokuma, V. G. Zakrzewski, G. A. Voth, P. Salvador, J. J. Dannenberg, S. Dapprich, A. D. Daniels, O. Farkas, J. B. Foresman, J. V. Ortiz, J. Cioslowski and D. J. Fox, Gaussian, Inc., Wallingford CT, 2013.
[30] For example, see: R. Sure and S. Grimme, *Chem. Commun.*, 2016, **52**, 9893-9896.
[31] G. Scalmani and M. J. Frisch, *J. Chem. Phys.*, 2010, **132**, 114110/1-114110/15.
[32] A. V. Marenich, C. J. Cramer and D. G. Truhlar, *J. Phys. Chem. B*, 2009, **113**, 6378-6396.

6.2. Cartesian coordinates.

4MePy:

N	5.34583000	-0.17944600	0.01358300
C	6.06506500	0.95331300	-0.00650600
C	7.45857100	0.98703300	-0.02169700
C	8.17849700	-0.21299300	-0.01508900
C	7.43006400	-1.39630300	0.00295200
C	6.03855300	-1.32963100	0.01757800
H	5.49456900	1.88098700	-0.01361800
H	7.97755500	1.94254300	-0.04180600
H	7.92622500	-2.36410700	0.00346500
H	5.44607300	-2.24334900	0.03023600
C	9.68422500	-0.23310500	-0.00219200
H	10.05566300	-0.32122900	1.02711700
H	10.07523500	-1.08690100	-0.56500400
H	10.09951800	0.68621800	-0.42636900

IPFB:

C	-2.37992600	-0.13924200	-0.00019100
C	-1.67803600	1.06396800	-0.00075200
C	-0.28547200	1.05163300	-0.00077500
C	0.42695100	-0.14798100	-0.00025700
C	-0.29285100	-1.34320900	0.00029000
C	-1.68549100	-1.34679300	0.00033700
F	-3.72033100	-0.13513100	-0.00015900
F	-2.34709200	2.22865100	-0.00126200
F	0.35759600	2.23230500	-0.00130400
I	2.51485200	-0.15393400	-0.00029500
F	0.34291200	-2.52785300	0.00078300
F	-2.36190700	-2.50721700	0.00088000

4MePy·IPFB:

C	-2.33943400	-0.14874300	-0.00355200

C	-1.64310300	1.05731200	-0.00711500
C	-0.25058500	1.04642900	-0.00230900
C	0.47652700	-0.14164500	0.00565800
C	-0.24479200	-1.33335400	0.00911600
C	-1.63717800	-1.35131100	0.00454200
F	-3.68286500	-0.15208200	-0.00795300
F	-2.32213300	2.22017400	-0.01508300
F	0.38366000	2.23882100	-0.00598900
I	2.61293200	-0.13900500	0.01058400
F	0.39515100	-2.52271100	0.01678700
F	-2.31026100	-2.51765400	0.00796800
N	5.32654500	-0.16137100	0.01099400
C	6.03872400	0.97535500	-0.00849000
C	7.42986500	0.99347100	-0.02271500
C	8.13937600	-0.21352100	-0.01594800
C	7.38524600	-1.39403000	0.00214900
C	5.99660400	-1.32438500	0.01591500
H	5.46457300	1.89894900	-0.01591200
H	7.95567000	1.94441200	-0.04252000
H	7.87534500	-2.36407600	0.00296700
H	5.38762100	-2.22540500	0.02819400
C	9.64375500	-0.24393700	-0.00349300
H	10.01191200	-0.33133300	1.02698200
H	10.02803000	-1.10297800	-0.56237000
H	10.06522300	0.67119900	-0.42975000

Compound **1**:

P	6.97005454	3.29558891	13.40575589
C	5.24920690	2.70249267	13.13830743
C	4.56869794	3.22901623	12.02882245
C	3.26920694	2.82035621	11.73065917
H	2.75772556	3.23546465	10.86606943
C	2.62340813	1.89271533	12.55009205
H	1.60652428	1.58151607	12.32565559

C	3.28573753	1.37354334	13.66421320
H	2.78618466	0.65426346	14.30848841
C	4.59081790	1.77186282	13.95609827
C	7.28530215	2.74955448	15.14265294
C	8.22935600	1.78732710	15.52227263
C	8.41009088	1.52451038	16.87973648
H	9.13561188	0.78189033	17.20184688
C	7.64253113	2.21925351	17.81183378
C	6.72321986	3.15908233	17.34130451
H	6.10224676	3.72352012	18.03528046
N	6.54719466	3.43322903	16.04328807
C	7.96471567	2.08033292	12.44048108
C	7.48791829	0.83528335	12.00395573
H	6.46643999	0.53877487	12.22570063
C	8.31530444	-0.02576197	11.28198095
C	9.63110769	0.34060907	10.99111365
H	10.27313924	-0.33227998	10.42869338
C	10.11520221	1.57899345	11.41690739
H	11.13540271	1.87528691	11.18655135
C	9.28420507	2.44605362	12.12652096
H	5.06203706	3.96475614	11.39722189
H	5.09434986	1.35866496	14.82519559
H	8.80311934	1.25230382	14.77210329
H	7.75106496	2.04316631	18.87803820
H	7.93130850	-0.98625547	10.94719262
H	9.66010232	3.41704979	12.44259509

Compound **2**:

P	6.79655400	7.72906500	12.36275900
I	5.84793500	6.15913700	15.34126200
C	5.95897300	8.76475800	13.65445500
C	5.68702200	10.12292100	13.46335500
C	5.02830000	10.89918600	14.41187300
C	4.61871500	10.31133500	15.60318800

C	4.87467800	8.96069100	15.82670400
C	5.53485600	8.19184700	14.87079600
F	6.06928100	10.74997600	12.33289800
F	4.78864400	12.20233100	14.19017500
F	3.98276200	11.04430700	16.52911500
F	4.45904100	8.43617700	16.99618000
C	5.69255500	8.01014800	10.91383200
C	5.86763500	8.99009100	9.92641800
C	4.96872300	9.08558000	8.86441900
H	5.11426600	9.84914400	8.10458800
C	3.87986500	8.21485700	8.78114300
C	3.69741100	7.23598600	9.75948500
H	2.85705900	6.54967900	9.69714500
C	4.60566300	7.12594300	10.81159800
H	4.47452600	6.34932100	11.56232300
C	8.32034000	8.68273200	12.00102700
C	8.90830300	9.54917600	12.93444500
C	10.14459400	10.14042600	12.67517000
H	10.57985300	10.81512000	13.40779600
C	10.81588000	9.87428600	11.48133400
H	11.77610500	10.34035800	11.27782400
C	10.24657600	9.00173400	10.55115300
H	10.76383500	8.78348000	9.62039600
C	9.01545600	8.40234300	10.81111200
H	6.70123300	9.68213800	9.99053100
H	3.17936000	8.29599600	7.95424300
H	8.39962800	9.77000300	13.86898600
H	8.58878600	7.71767600	10.08177000

Compound **3**:

P	6.59965900	7.60239000	12.31505400
I	7.83686700	7.13237500	15.47306300
C	5.85280500	8.63792200	13.64882300
C	4.81834100	9.55944400	13.40824200

C	4.23073200	10.28363400	14.44396800
C	4.67043300	10.10796200	15.75540200
C	5.69943500	9.20560300	16.02744400
C	6.27054700	8.48021000	14.98186600
C	5.63002400	8.14064100	10.84089000
C	5.99962300	9.20034000	10.00008500
C	5.21629800	9.53322200	8.89415600
H	5.51700900	10.35539000	8.24955700
C	4.05070800	8.81673000	8.61717100
C	3.67473800	7.75711100	9.44574200
H	2.77228300	7.19019700	9.23166700
C	4.46452100	7.41501400	10.54307100
H	4.17615800	6.57996700	11.17828000
C	8.21115300	8.45294900	12.04283500
C	8.49513100	9.75498700	12.47958100
C	9.74234500	10.32838500	12.22962400
H	9.95030900	11.33775200	12.57556300
C	10.71890300	9.61124900	11.53611600
H	11.68981900	10.05951900	11.34237400
C	10.44636300	8.31329000	11.09910200
H	11.20484700	7.74682000	10.56491900
C	9.20425100	7.73499700	11.35891300
H	6.90245300	9.76648900	10.21026700
H	3.44194500	9.07710500	7.75523100
H	7.74044900	10.32190800	13.01778900
H	9.00099700	6.71725700	11.03296100
H	4.47448900	9.71016800	12.38923800
H	3.43301200	10.98749000	14.22251200
H	4.21866900	10.66614700	16.57094100
H	6.05090500	9.06435200	17.04436500

$Rh[(CO)_2]^+$:

Rh	6.93262700	5.64698000	13.00866000
C	7.65138400	5.22630200	11.24288900

O	8.06938200	4.98165400	10.21413700
C	6.21285500	6.07133900	14.77392300
O	5.79292400	6.32120400	15.80071100

CO:

C	7.63602800	5.23213500	11.30104400
O	8.03195300	5.03147900	10.25733400

Rh[(CO)(1)(2)]$^{+}$:

Rh	7.00081100	5.56019400	12.97277400
P	6.74771300	7.78423100	12.35878100
P	6.93987300	3.26863200	13.39878700
I	6.07404500	6.15567100	15.39088700
C	5.96528700	8.78653200	13.69046500
C	5.67557200	10.14182000	13.50548900
C	5.04998500	10.90339200	14.48913000
C	4.70683300	10.30707100	15.70066700
C	4.99925500	8.95991500	15.90438600
C	5.61830700	8.20770200	14.91730300
F	6.00512000	10.76465600	12.35908000
F	4.78086400	12.19788000	14.28088100
F	4.11047700	11.02778800	16.65534600
F	4.67187000	8.40887500	17.09254600
C	5.63275300	7.95285400	10.92200000
C	5.74541400	8.98156200	9.97667700
C	4.85084700	9.04244800	8.90902500
H	4.94630000	9.83742200	8.17485200
C	3.83715100	8.09078100	8.78348500
C	3.71749100	7.06826500	9.72705800
H	2.93184900	6.32375700	9.63208100
C	4.61577500	6.99364500	10.78889400
H	4.54216200	6.18661500	11.51553000
C	5.23309100	2.69836700	13.08541500
C	4.67927500	2.95167800	11.81787100

C	3.36856800	2.57475400	11.53885800
H	2.95152300	2.76798700	10.55448900
C	2.59229400	1.95600800	12.52266400
H	1.56697300	1.67002900	12.30617800
C	3.13540600	1.70726500	13.78257500
H	2.53620500	1.22508300	14.54981000
C	4.45232700	2.07347400	14.06667600
C	7.26272500	2.76903200	15.14574100
C	7.86662300	1.55923900	15.49422300
C	8.02750200	1.25887700	16.84723600
H	8.49757900	0.32688300	17.14695900
C	7.57847900	2.16671300	17.80288200
C	6.99290300	3.35540700	17.36997800
H	6.63810800	4.10298700	18.07516600
N	6.84519000	3.64972900	16.07196400
C	7.61139000	5.22010900	11.27734500
O	7.97399400	5.01595700	10.19794400
C	8.30084900	8.65338000	11.97076600
C	8.94311500	9.43156400	12.94412100
C	10.17916700	10.01491100	12.67061700
H	10.66390200	10.62444100	13.42788800
C	10.78674500	9.82086400	11.42958900
H	11.74739300	10.28078600	11.21611300
C	10.15688900	9.03582100	10.46162500
H	10.62633200	8.88078500	9.49432700
C	8.92242000	8.44759100	10.72847900
C	8.03387300	2.18207400	12.43293700
C	7.59537800	0.95765400	11.91042600
H	6.56474900	0.64314600	12.04578400
C	8.48572700	0.14424700	11.20910700
C	9.81113600	0.54422800	11.03256300
H	10.50056800	-0.09094200	10.48356700
C	10.25098300	1.76395700	11.55280000
H	11.28029700	2.07957300	11.40864000

C	9.36545700	2.58466300	12.24736200
H	6.52649400	9.72867700	10.06848200
H	3.14285000	8.14452400	7.94958100
H	5.27430500	3.43881600	11.04982700
H	4.86120200	1.87081900	15.05172400
H	8.20140900	0.87099200	14.72555200
H	7.68614000	1.96912900	18.86449700
H	8.48093400	9.58866900	13.91453600
H	8.44415600	7.83948400	9.96635500
H	8.14133500	-0.80101000	10.79923600
H	9.69971900	3.54349800	12.63806900

Rh[(CO)(1)(3)]$^{+}$:

Rh	7.03660200	5.53823500	12.98755300
P	6.75228700	7.75857100	12.38063800
P	6.97245900	3.24827700	13.42851500
I	6.09141700	6.18689800	15.39008500
C	5.90083100	8.75643300	13.66195500
C	5.54639100	10.09113100	13.39916200
C	4.88760100	10.85165400	14.36026600
C	4.56911400	10.28937600	15.59827700
C	4.91064700	8.96611600	15.87782300
C	5.57273900	8.21641400	14.90552200
C	5.69458500	7.94046600	10.90302400
C	5.81480400	9.00789100	10.00216500
C	4.93789200	9.10743900	8.92187400
H	5.03947700	9.93150600	8.22125800
C	3.93657100	8.15199400	8.73813900
C	3.81174500	7.08927300	9.63534200
H	3.03611200	6.34157600	9.49458800
C	4.68991700	6.98004200	10.71070800
H	4.60840500	6.14624500	11.40509900
C	5.24445300	2.72475800	13.14912200
C	4.71483200	2.89516500	11.85786500

C	3.38842300	2.56438000	11.59640700
H	2.98995200	2.69082700	10.59360000
C	2.57251300	2.07679000	12.62143200
H	1.53547200	1.82544900	12.41778800
C	3.09202400	1.91278900	13.90504600
H	2.46176900	1.53245000	14.70409400
C	4.42477000	2.23269300	14.17233600
C	7.33775600	2.72036700	15.15888300
C	7.97380600	1.51683600	15.47170700
C	8.17954700	1.20180500	16.81512800
H	8.67576500	0.27503600	17.08814800
C	7.74229400	2.08916200	17.79505700
C	7.12107700	3.27145800	17.39334100
H	6.77166900	4.00129700	18.11983900
N	6.92942400	3.58327300	16.10548500
C	7.63191000	5.19701300	11.28996400
O	7.98192500	4.99351300	10.20508200
C	8.29895800	8.66170200	12.03445800
C	8.87301800	9.50006900	13.00054700
C	10.10398600	10.10907500	12.75628800
H	10.53822300	10.76222000	13.50802300
C	10.77161200	9.88337000	11.55237400
H	11.72824000	10.36204400	11.36259500
C	10.20757400	9.04212800	10.58997100
H	10.72391800	8.86349900	9.65092400
C	8.98052200	8.42774800	10.82865800
C	8.00238200	2.14288100	12.41238800
C	7.53364700	0.90563000	11.94804900
H	6.51561000	0.59205400	12.15949500
C	8.37605500	0.07786300	11.20595800
C	9.68551600	0.47501500	10.92983400
H	10.33697900	-0.17095800	10.34798800
C	10.15639700	1.70565900	11.39294500
H	11.17269600	2.01956300	11.17261500

C	9.31757200	2.54026700	12.12823700
H	6.59419600	9.75276100	10.13543000
H	3.25759300	8.23309900	7.89396400
H	5.34354000	3.27966300	11.05895700
H	4.81598400	2.10022100	15.17605100
H	8.30050700	0.84467400	14.68575300
H	7.88526400	1.88007100	18.85044200
H	8.35989500	9.68273600	13.94009500
H	8.54981500	7.77701800	10.07292200
H	8.00675600	-0.87652600	10.84118100
H	9.67576700	3.50742400	12.47492300
H	4.66067000	8.52918600	16.84014500
H	4.05133600	10.87818800	16.35014000
H	4.61920400	11.88094700	14.14216700
H	5.78883300	10.53080900	12.43614700

6.3. Plots of electrostatic potential surfaces (EPS). Electrostatic potential surfaces were calculated with Gaussian 09 at the TPSS-D3-def2TZVP level of theory considering the effects of toluene as the solvent and have been plotted with GaussView 5.0 using an isovalue of 0.001 a.u. (in each case, dark blue indicates the highest positive electrostatic potential value for the corresponding molecule and dark red indicates the highest negative electrostatic potential value for the corresponding molecule).

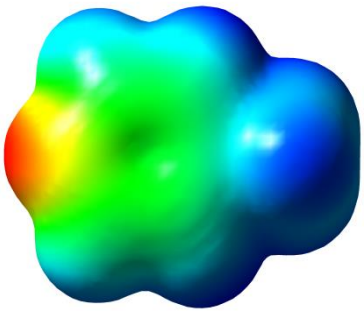

Figure SI 27. EPS plot for **4MePy**.
Max. EPS value = 0.032 a.u.
Min. EPS value = –0.066 a.u.

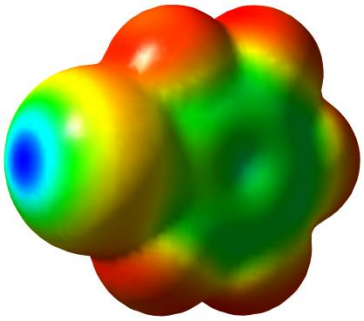

Figure SI 28. EPS plot for **IPFB**.
Max. EPS value = 0.056 a.u.
Min. EPS value = –0.013 a.u.

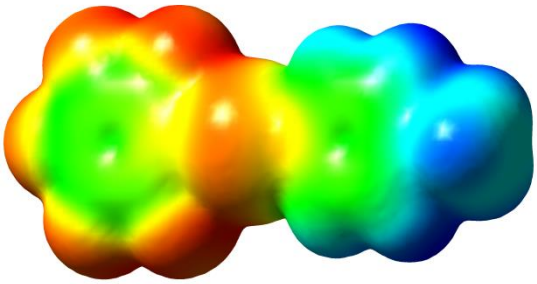

Figure SI 29. EPS plot for **4MePy·IPFB**.
Max. EPS value = 0.046 a.u.
Min. EPS value = –0.029 a.u.

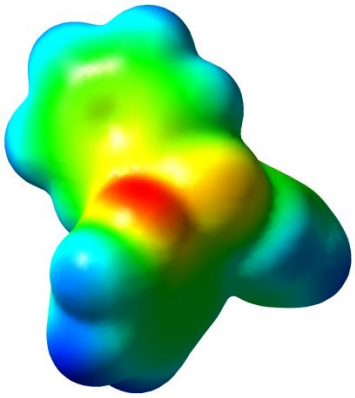

Figure SI 30. EPS plot for compound **1**.
Max. EPS value = 0.035 a.u.
Min. EPS value = –0.067 a.u.

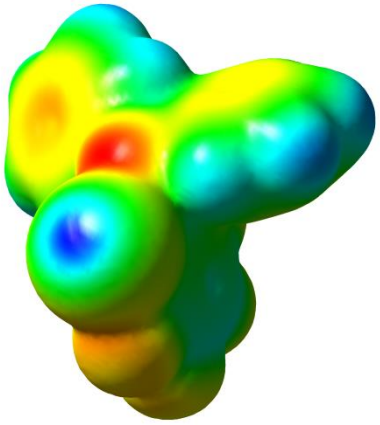

Figure SI 31. EPS plot for compound **2**.
Max. EPS value = 0.040 a.u.
Min. EPS value = –0.032 a.u.

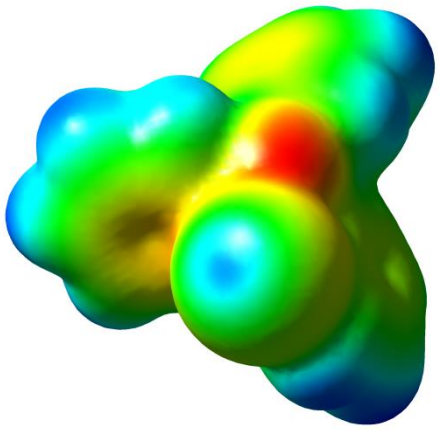

Figure SI 32. EPS plot for compound **3**.
Max. EPS value = 0.031 a.u.
Min. EPS value = –0.046 a.u.

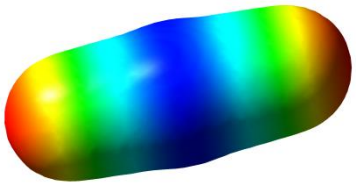

Figure SI 33. EPS plot for **Rh[(CO)$_2$]$^+$**.
Max. EPS value = 0.252 a.u.
Min. EPS value = 0.111 a.u.

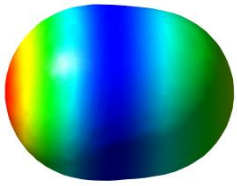

Figure SI 34. EPS plot for **CO**.
Max. EPS value = 0.018 a.u.
Min. EPS value = –0.023 a.u.

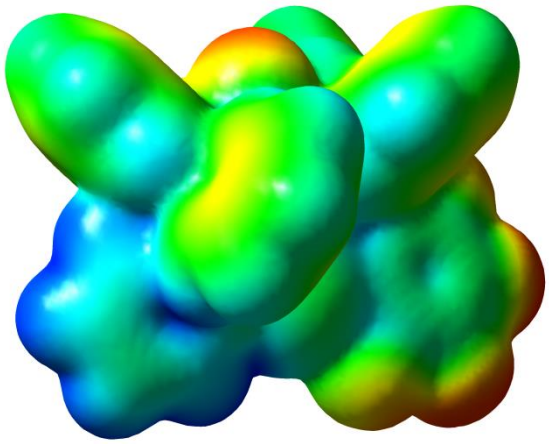

Figure SI 35. EPS plot for **Rh[(CO)(1)(2)]$^+$**.
Max. EPS value = 0.125 a.u.
Min. EPS value = 0.046 a.u.

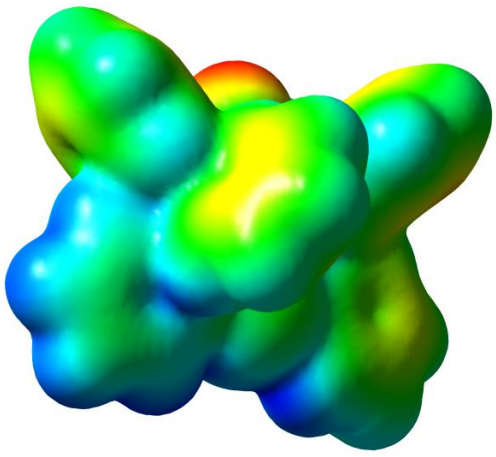

Figure SI 36. EPS plot for **Rh[(CO)(1)(3)]$^+$**.
Max. EPS value = 0.119 a.u.
Min. EPS value = 0.045 a.u.

7. Spectroscopic Data:

7.1. Spectroscopic NMR Data for ligands 1, 2 and 3.

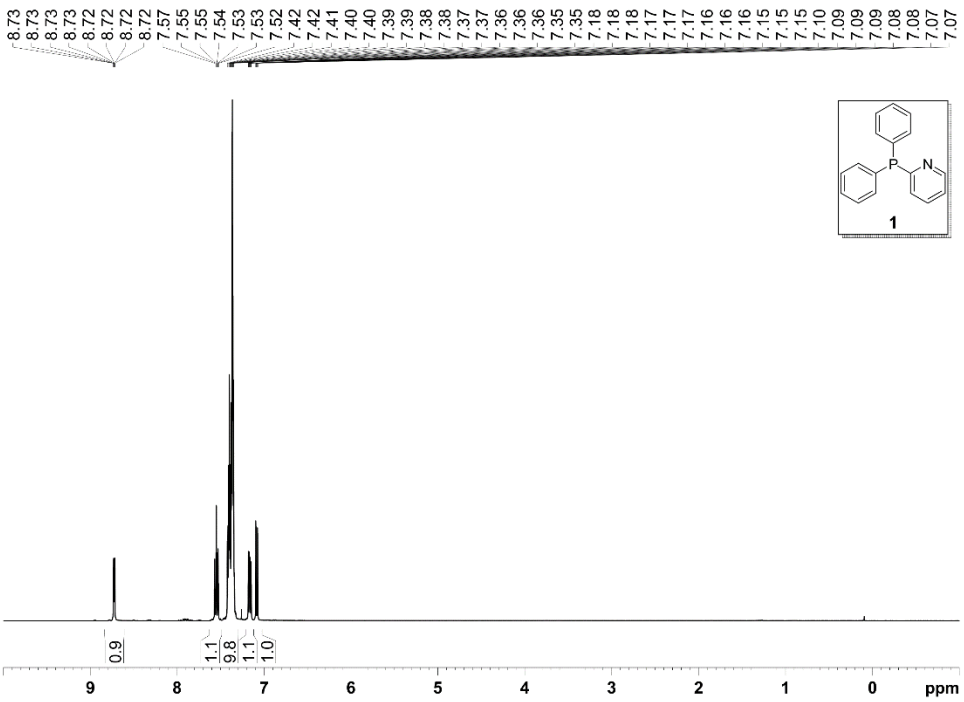

Figure SI 37. ^{1}H NMR (400 MHz, $CDCl_3$) for ligand **1**.

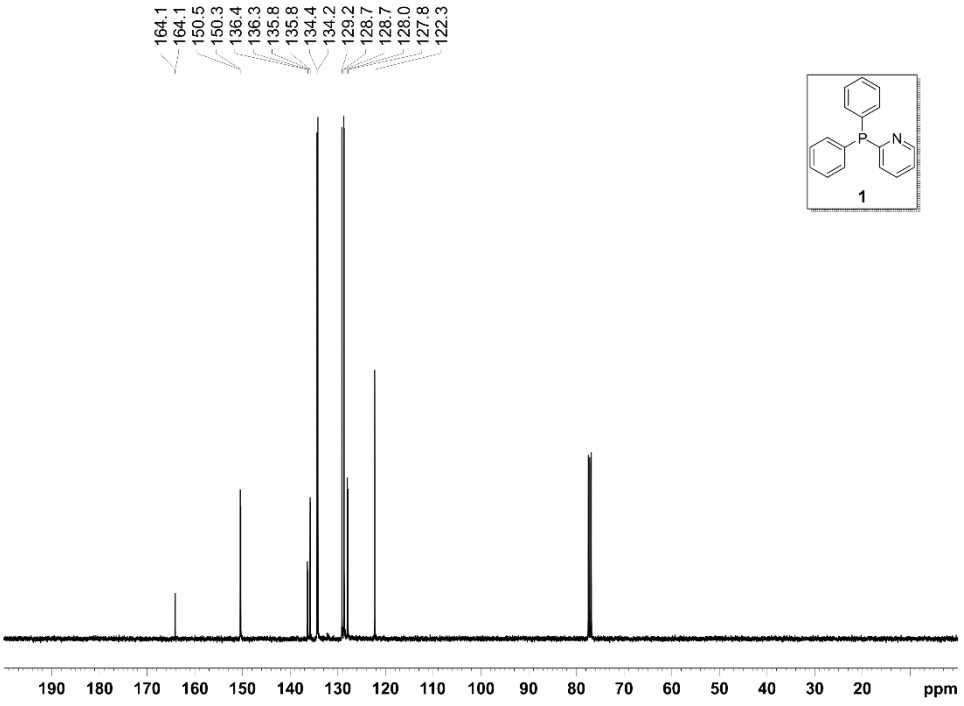

Figure SI 38. $^{13}C\{^{1}H\}$ NMR (100 MHz, $CDCl_3$) for ligand **1**.

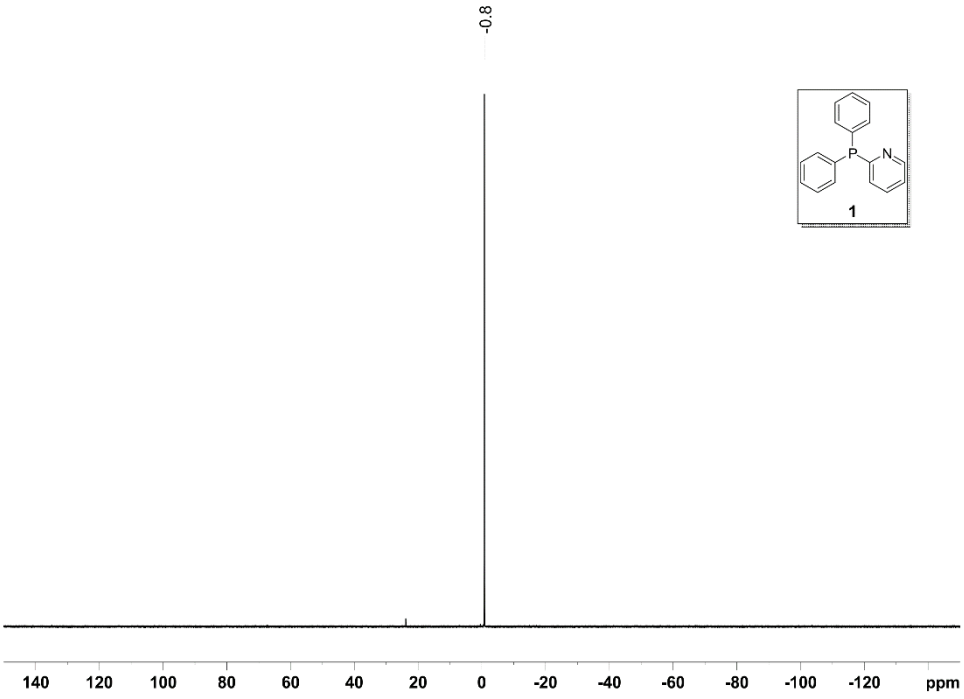

Figure SI 39. $^{31}P\{^{1}H\}$ NMR (162 MHz, $CDCl_3$) for ligand **1**.

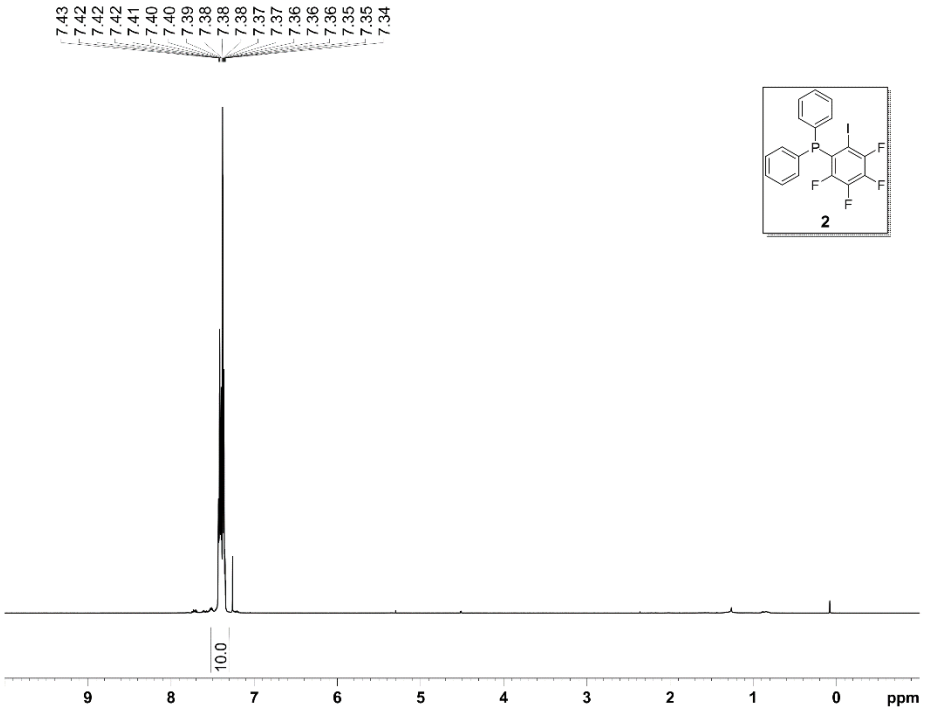

Figure SI 40. ^{1}H NMR (500 MHz, $CDCl_3$) for ligand **2**.

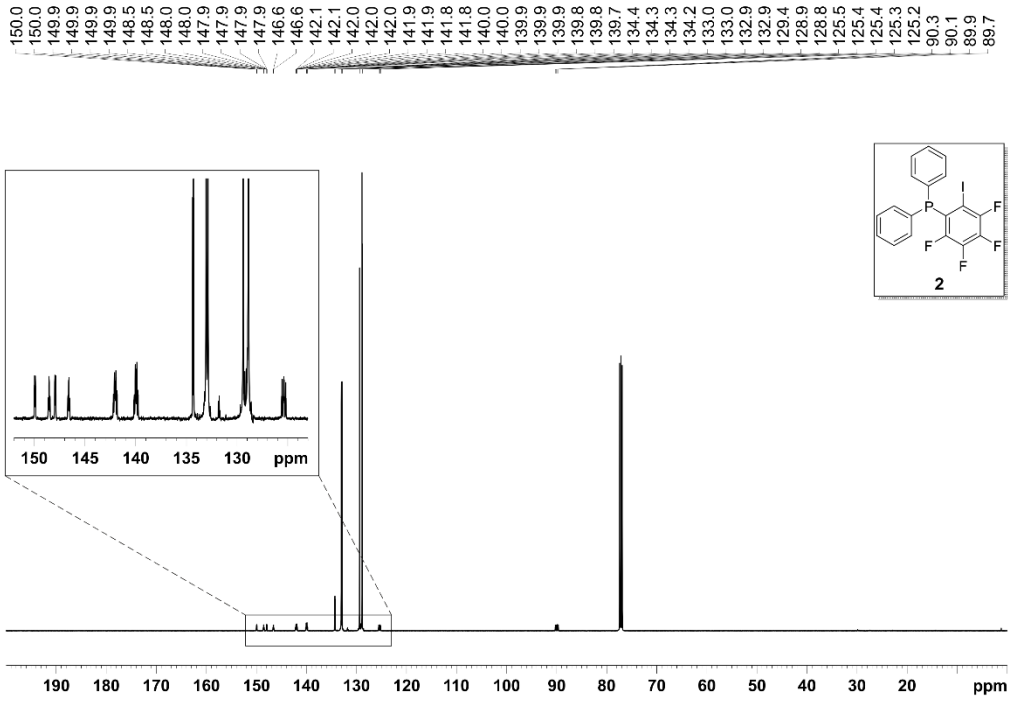

Figure SI 41. $^{13}C\{^{1}H\}$ NMR (126 MHz, $CDCl_3$) for ligand **2**.

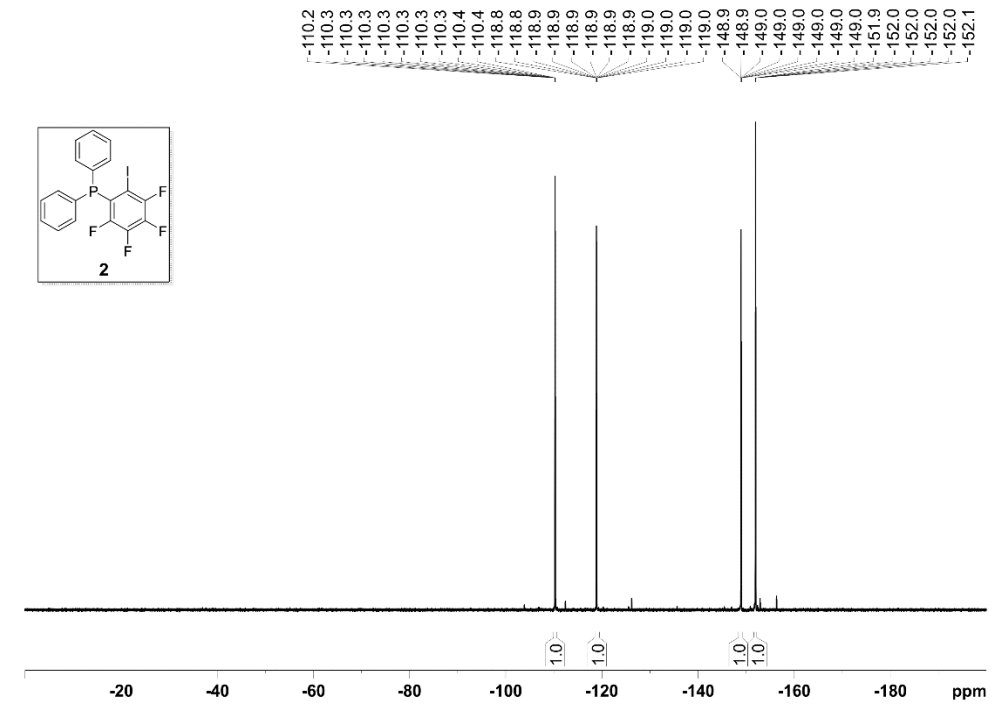

Figure SI 42. $^{19}F\{^{1}H\}$ NMR (376 MHz, $CDCl_3$) for ligand **2**.

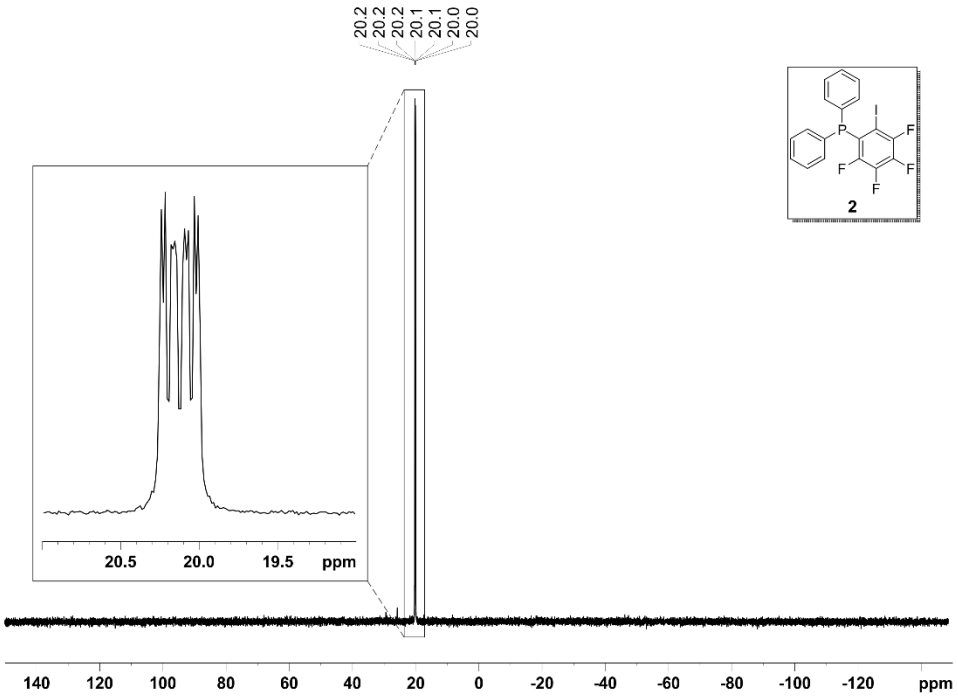

Figure SI 43. $^{31}P\{^{1}H\}$ NMR (162 MHz, $CDCl_3$) for ligand **2**.

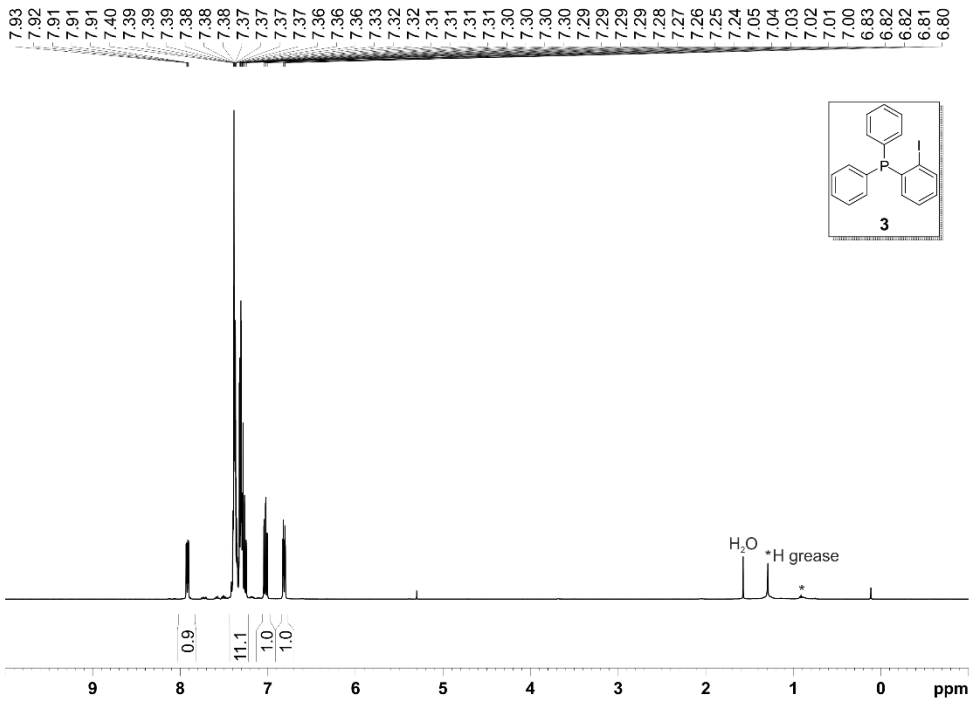

Figure SI 44. ^{1}H NMR (400 MHz, $CDCl_3$) for ligand **3**.

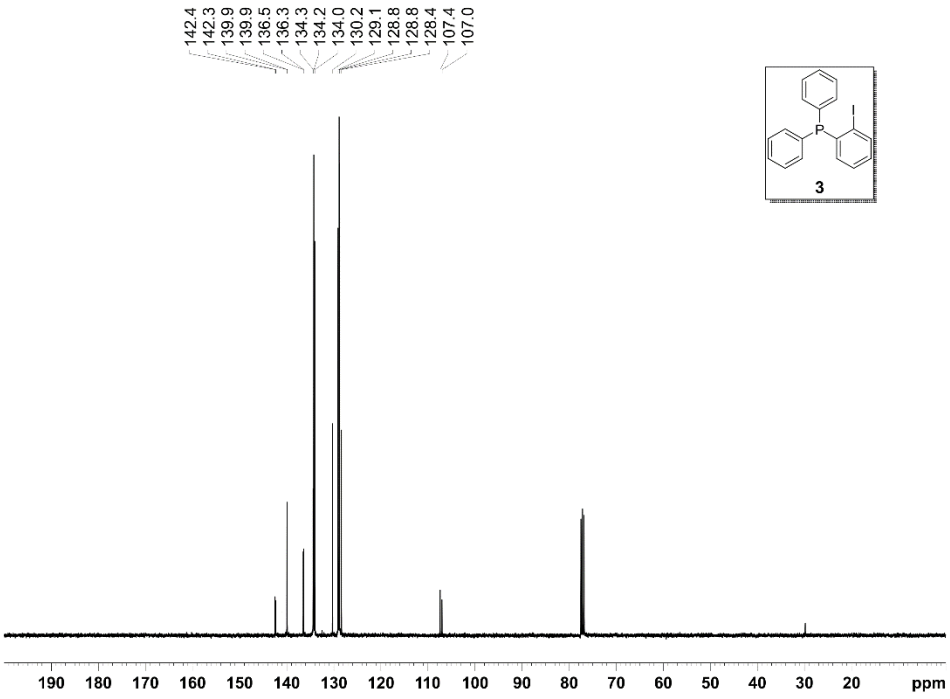

Figure SI 45. $^{13}C\{^{1}H\}$ NMR (100 MHz, $CDCl_3$) for ligand **3**.

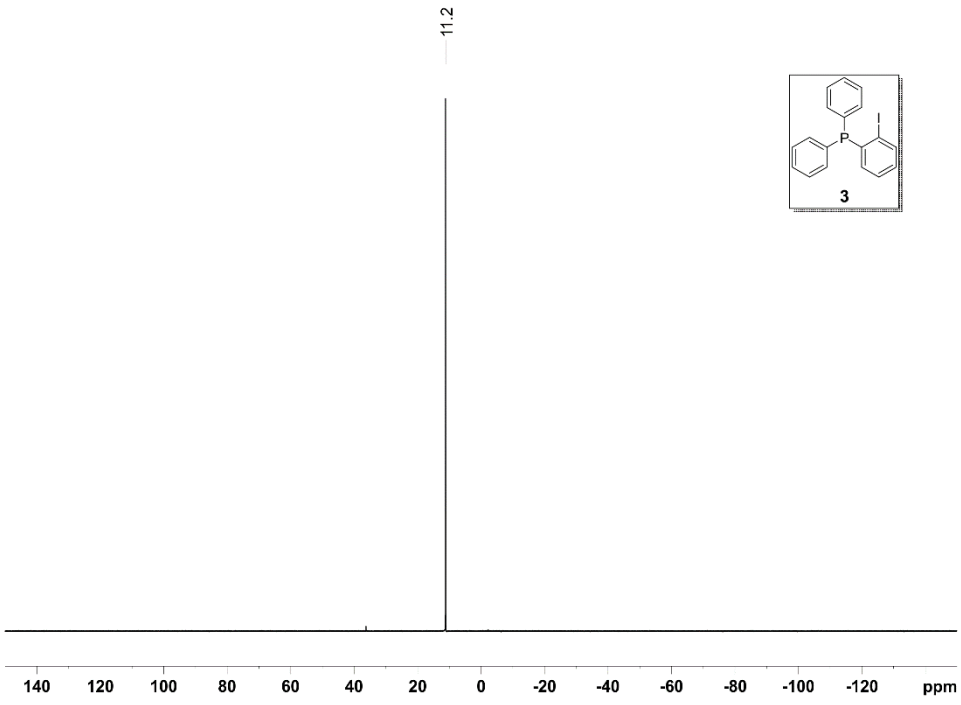

Figure SI 46. $^{31}P\{^{1}H\}$ NMR (162 MHz, $CDCl_3$) for ligand **3**.

7.2. Spectroscopic NMR and IR Data for complexes 4, 5, 6, 11 and 12.

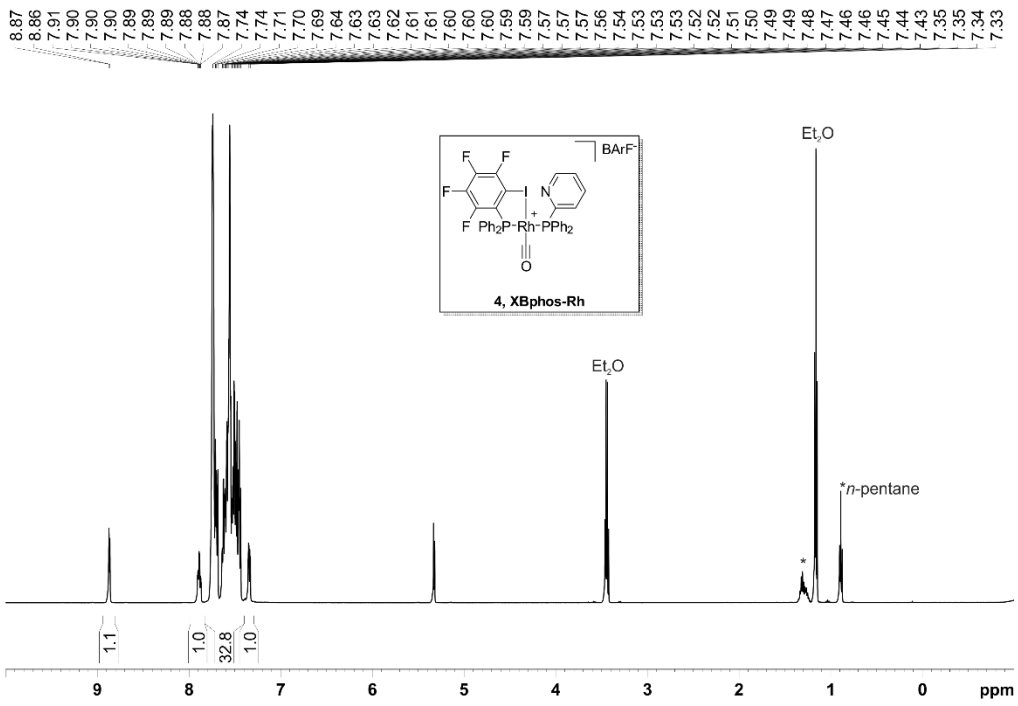

Figure SI 47. ^{1}H NMR (500 MHz, CD_2Cl_2) for complex **4**.

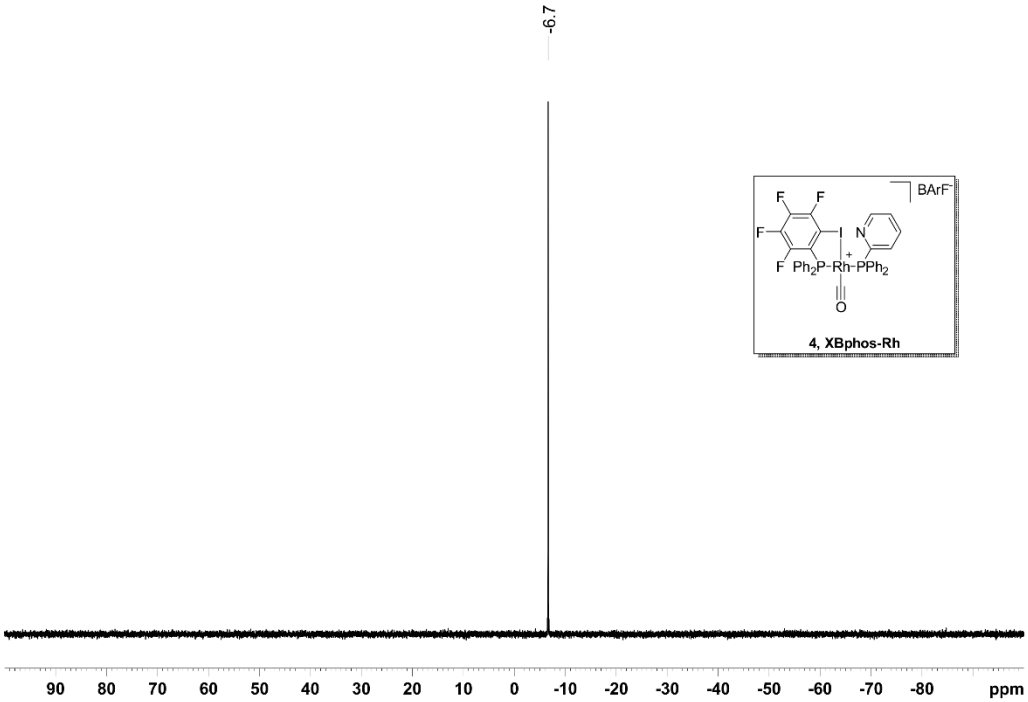

Figure SI 48. $^{11}B\{^{1}H\}$ NMR (160 MHz, CD_2Cl_2) for complex **4**.

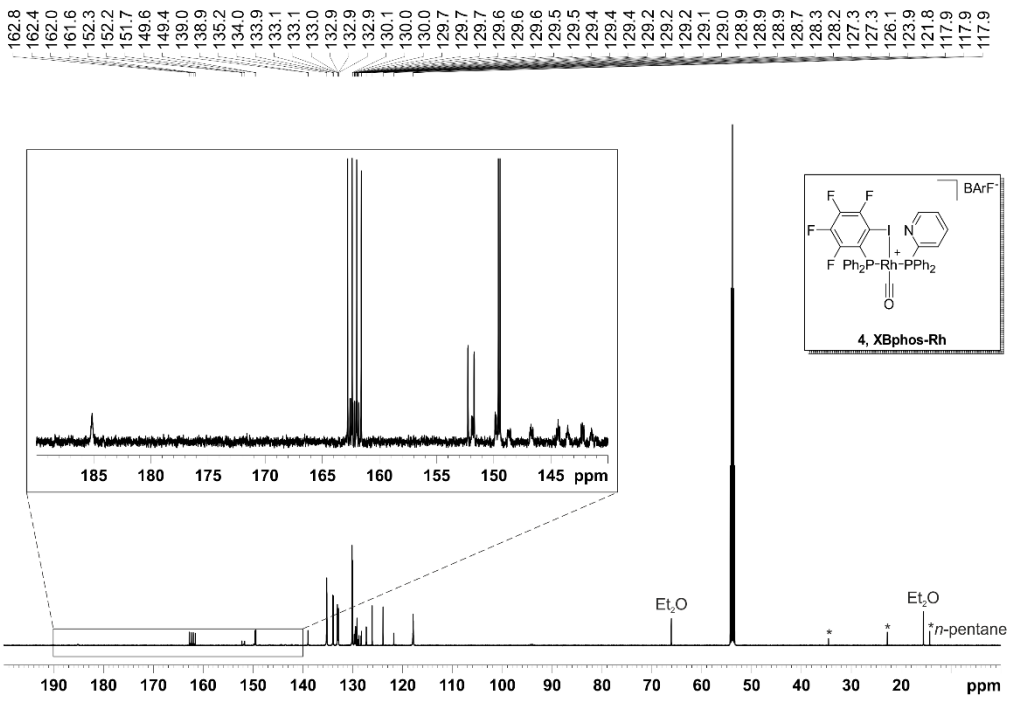

Figure SI 49. $^{13}C\{^{1}H\}$ NMR (126 MHz, CD_2Cl_2) for complex **4**.

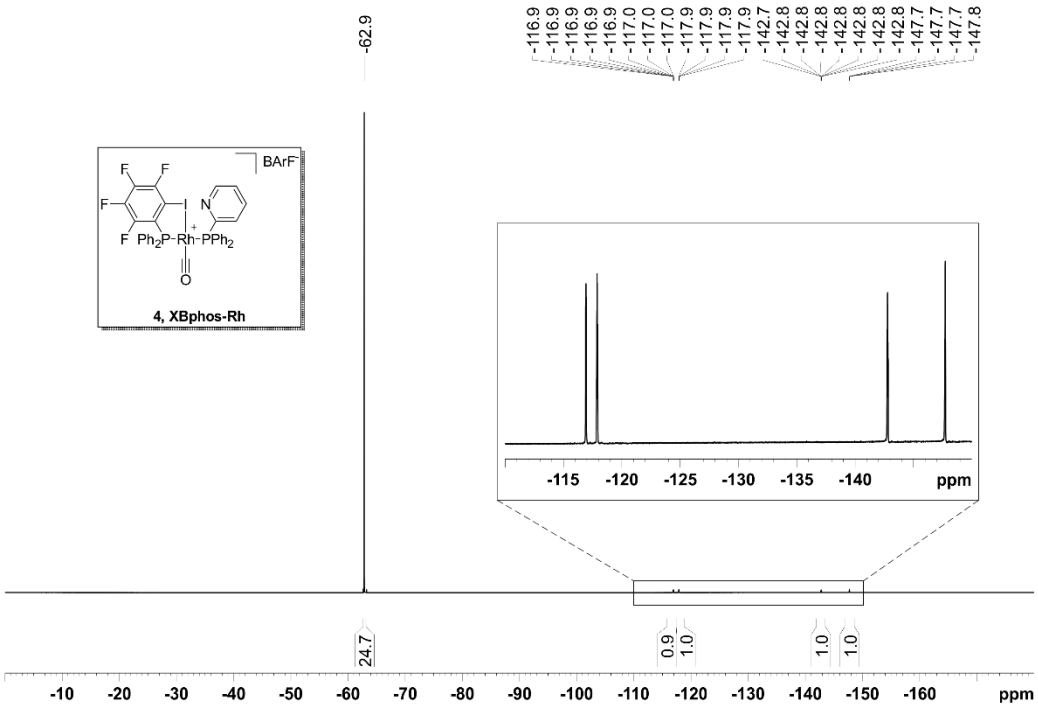

Figure SI 50. $^{19}F\{^{1}H\}$ NMR (471 MHz, CD_2Cl_2) for complex **4**.

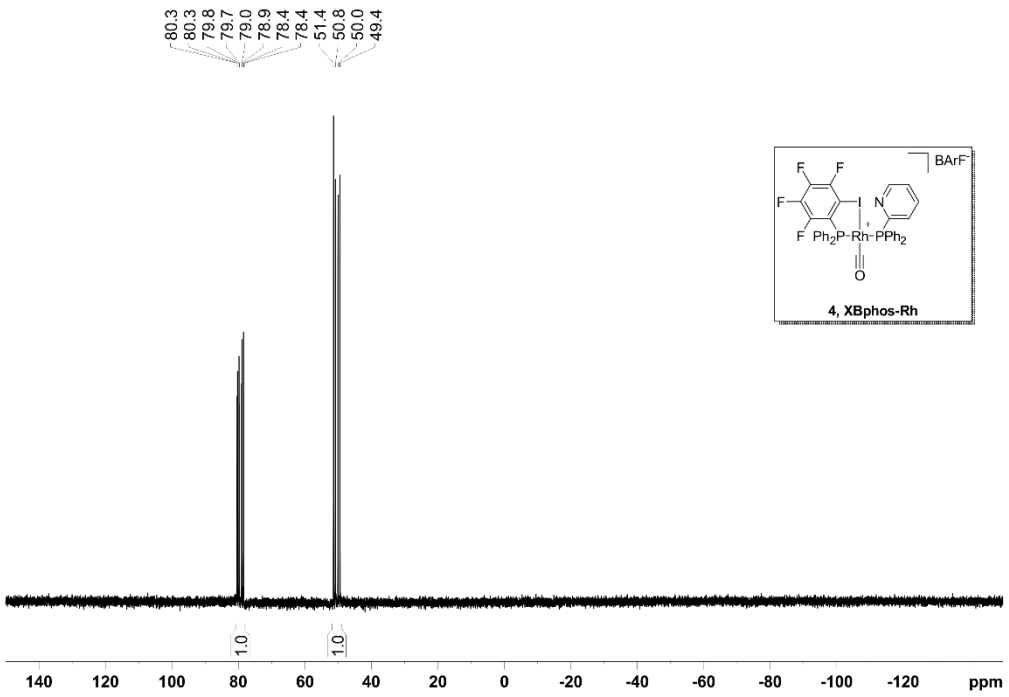

Figure SI 51. $^{31}P\{^{1}H\}$ NMR (203 MHz, CD_2Cl_2) for complex **4**.

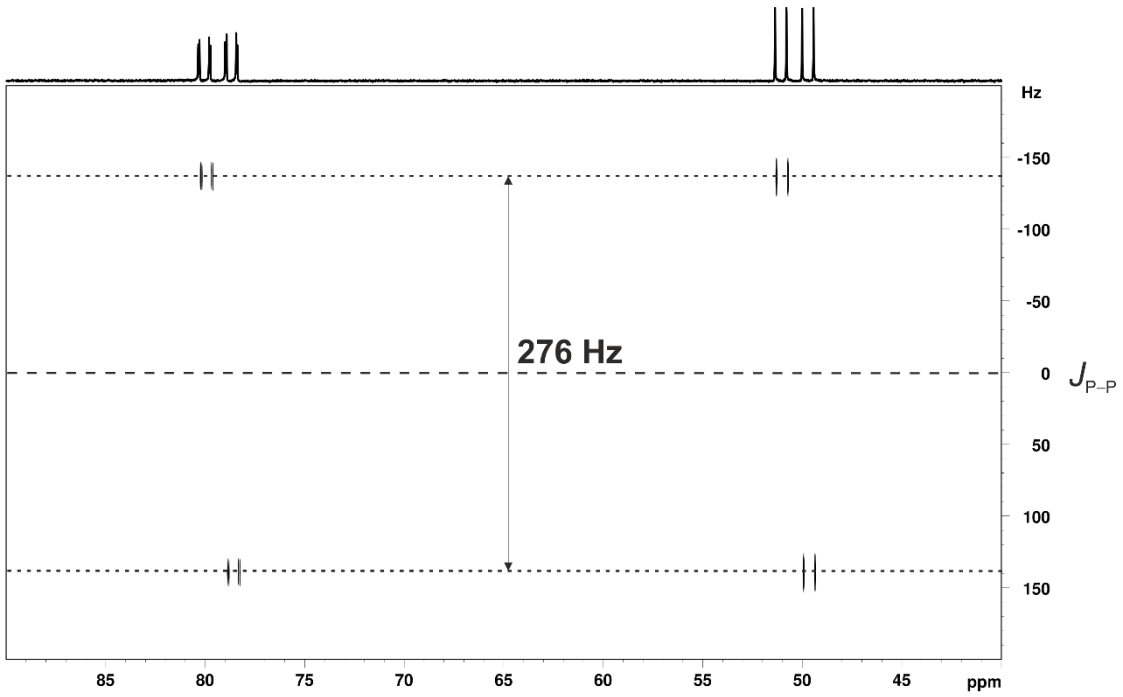

Figure SI 52. 2D heteronuclear $^{31}P\{^{1}H\}$ *J*-resolved NMR experiment (203 MHz, CD_2Cl_2) for complex **4**.

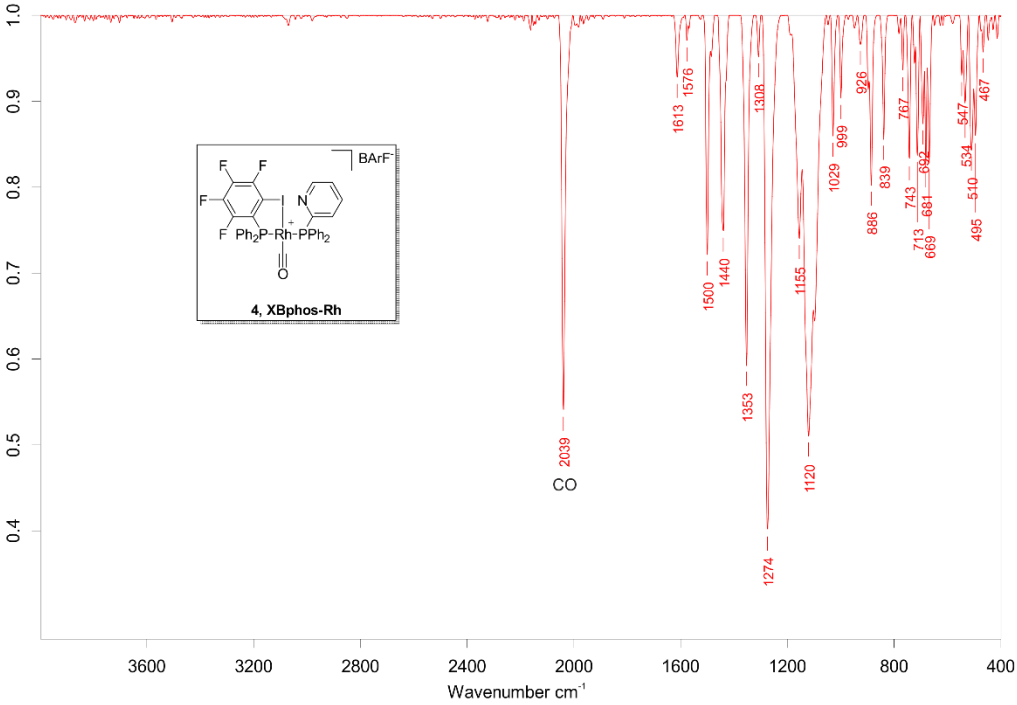

Figure SI 53. IR spectrum for complex **4**.

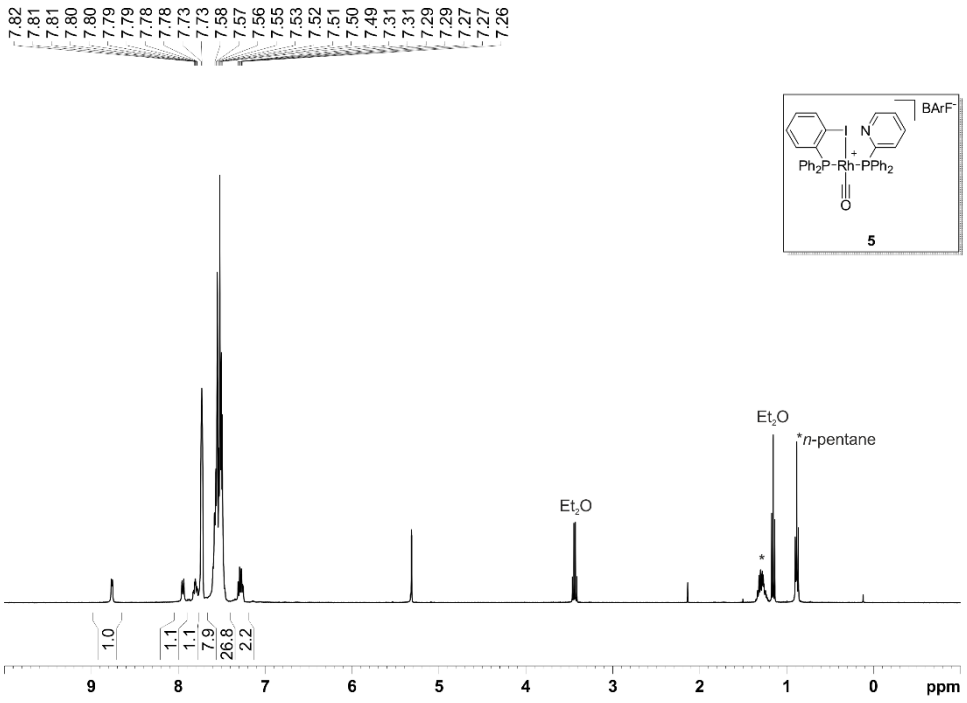

Figure SI 54. ^{1}H NMR (400 MHz, CD_2Cl_2) for complex **5**.

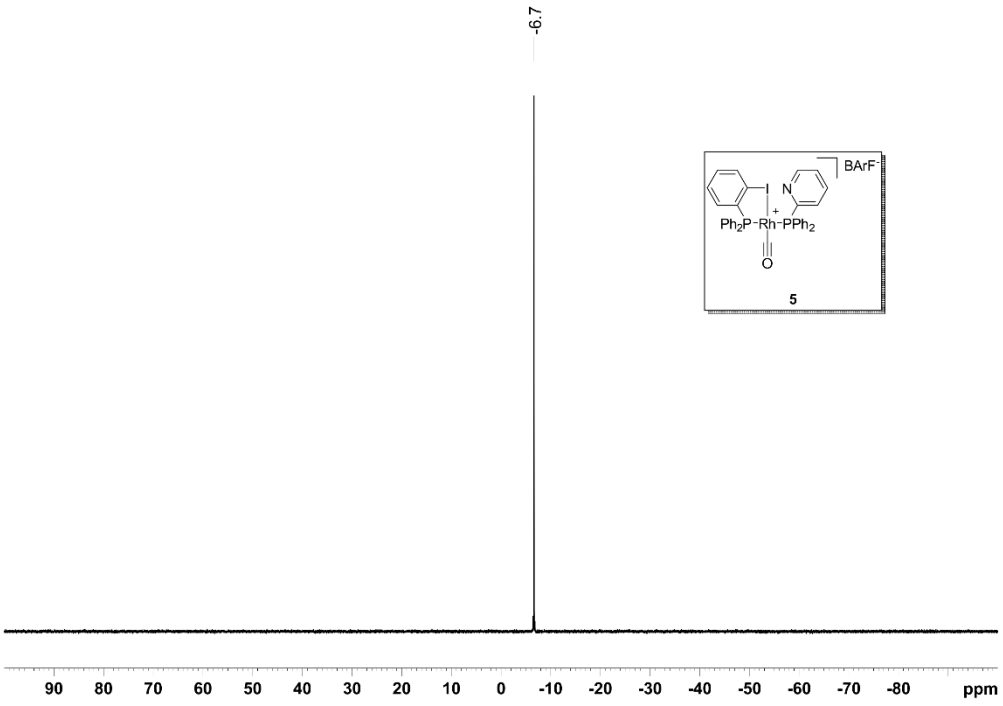

Figure SI 55. $^{11}B\{^{1}H\}$ NMR (128 MHz, CD_2Cl_2) for complex **5**.

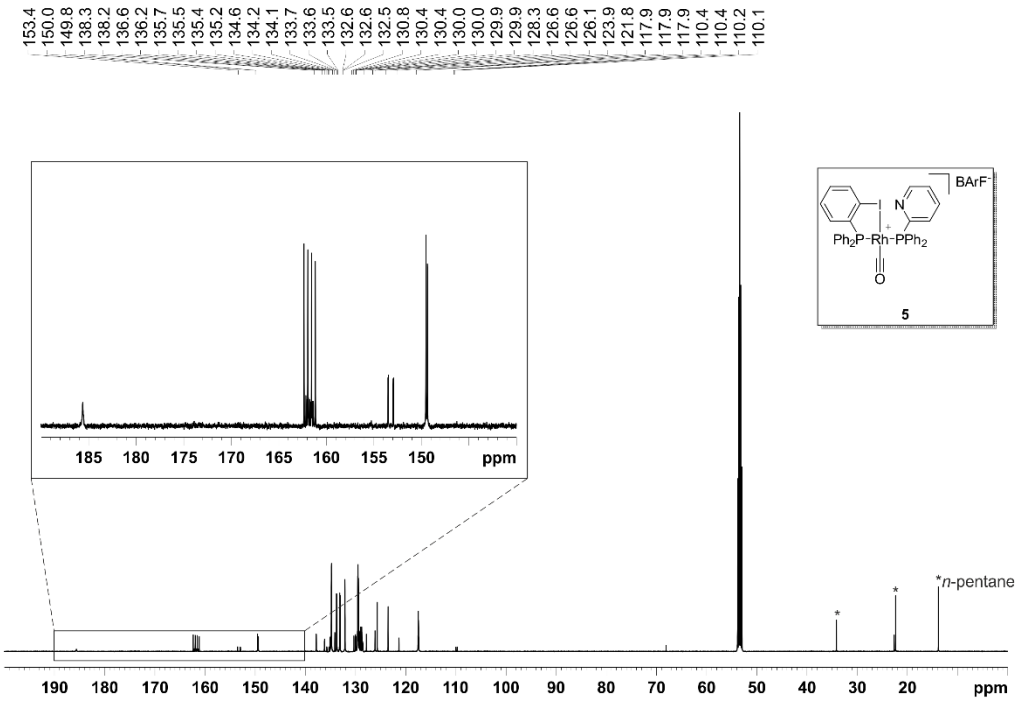

Figure SI 56. $^{13}C\{^{1}H\}$ NMR (126 MHz, CD_2Cl_2) for complex **5**.

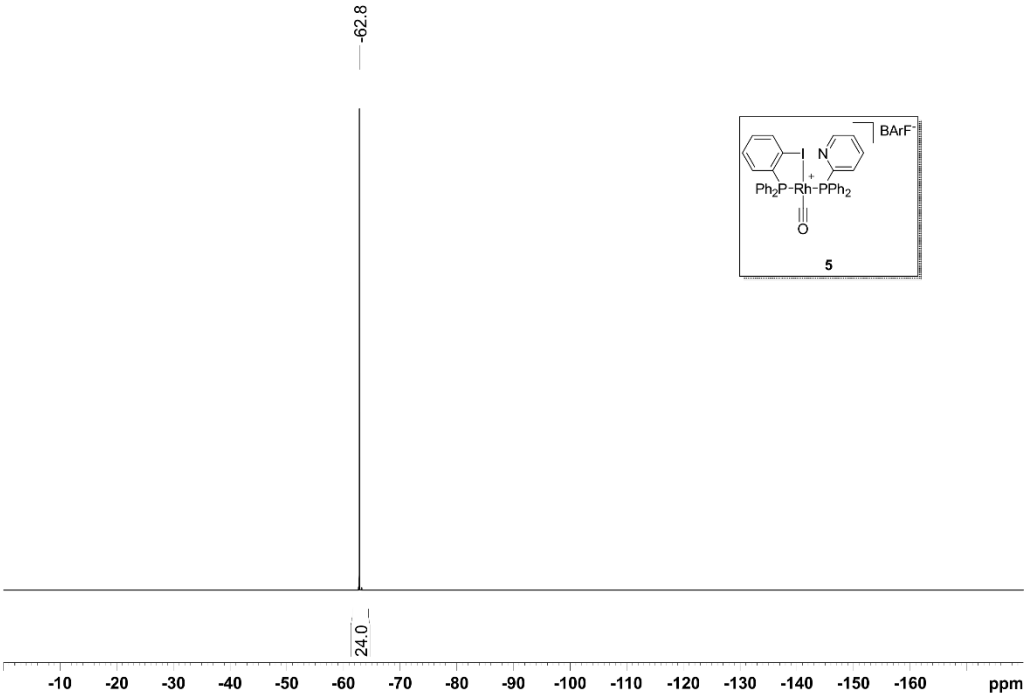

Figure SI 57. $^{19}F\{^{1}H\}$ NMR (471 MHz, CD_2Cl_2) for complex **5**.

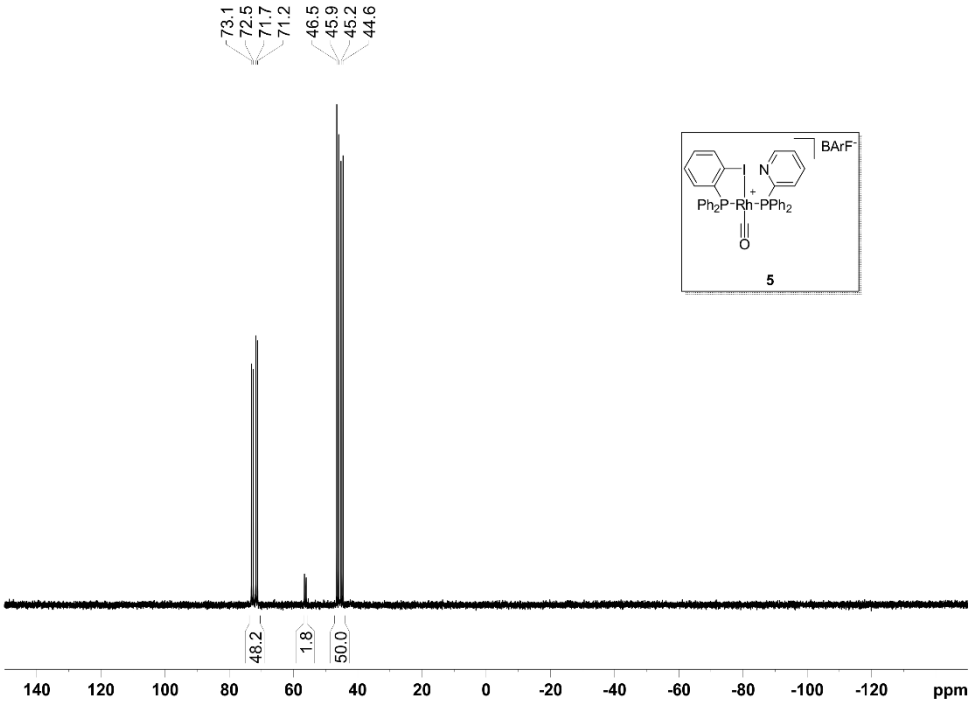

Figure SI 58. $^{31}P\{^{1}H\}$ IGD (inverse gated decoupling) NMR (203 MHz, CD_2Cl_2) for complex **5**.

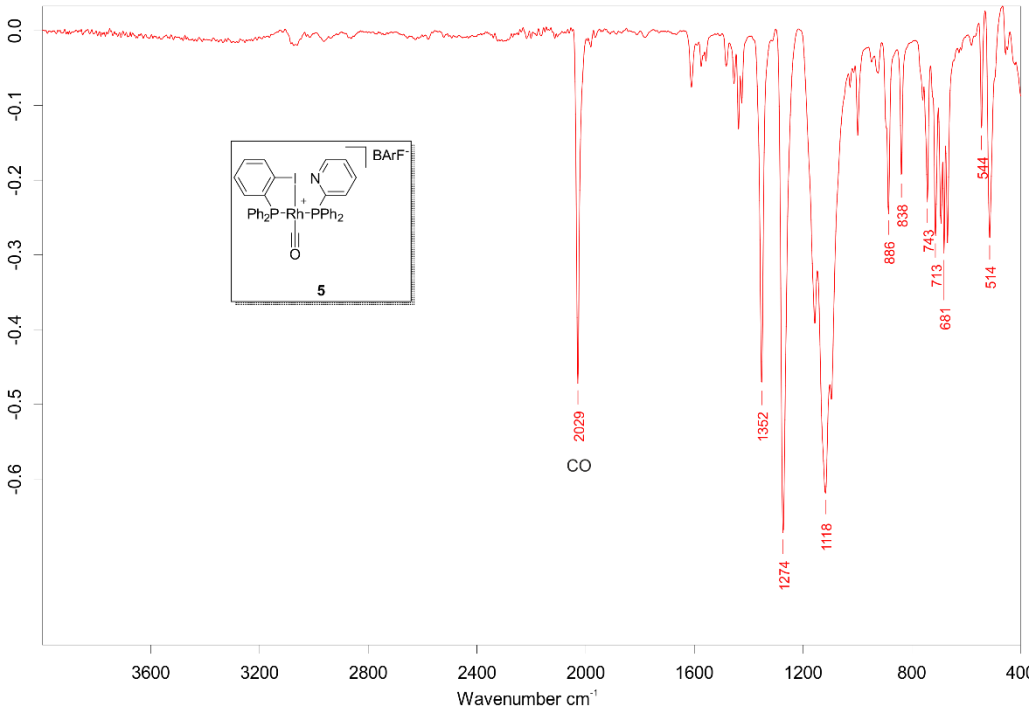

Figure SI 59. IR spectrum for complex **5**.

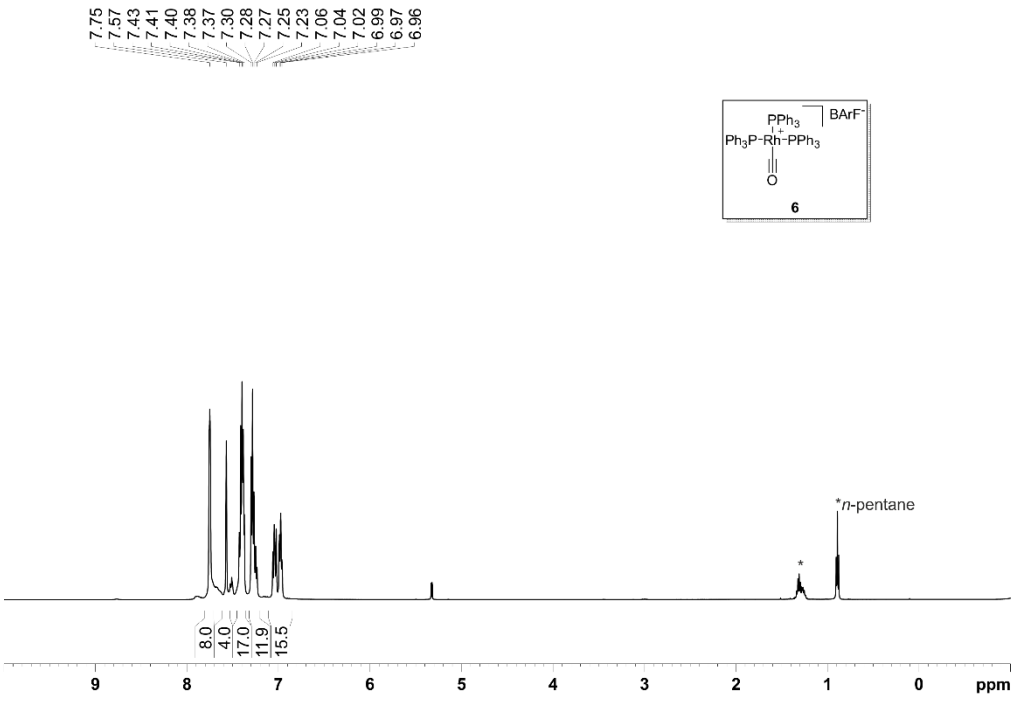

Figure SI 60. ^{1}H NMR (500 MHz, CD_2Cl_2) for complex **6**.

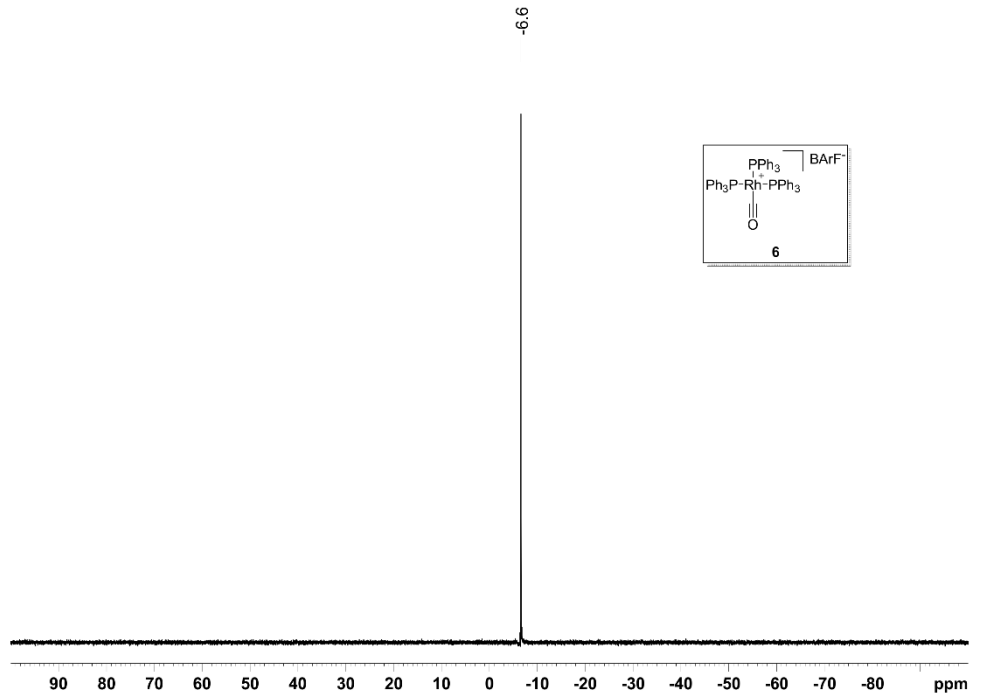

Figure SI 61. $^{11}B\{^{1}H\}$ NMR (128 MHz, CD_2Cl_2) for complex **6**.

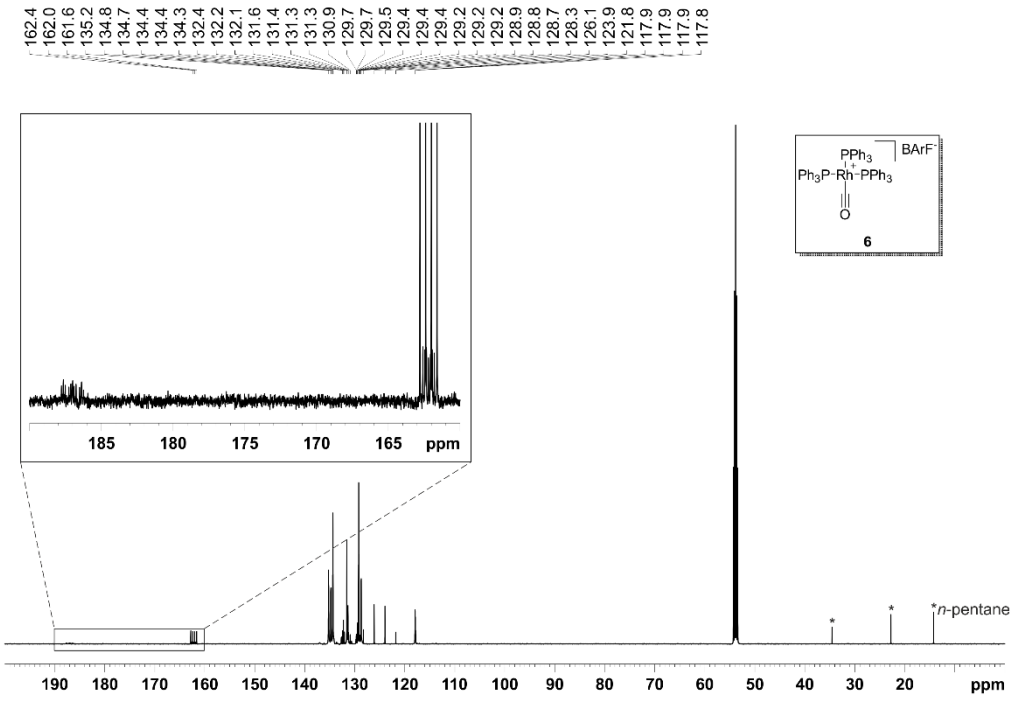

Figure SI 62. $^{13}C\{^{1}H\}$ NMR (126 MHz, CD_2Cl_2) for complex **6**.

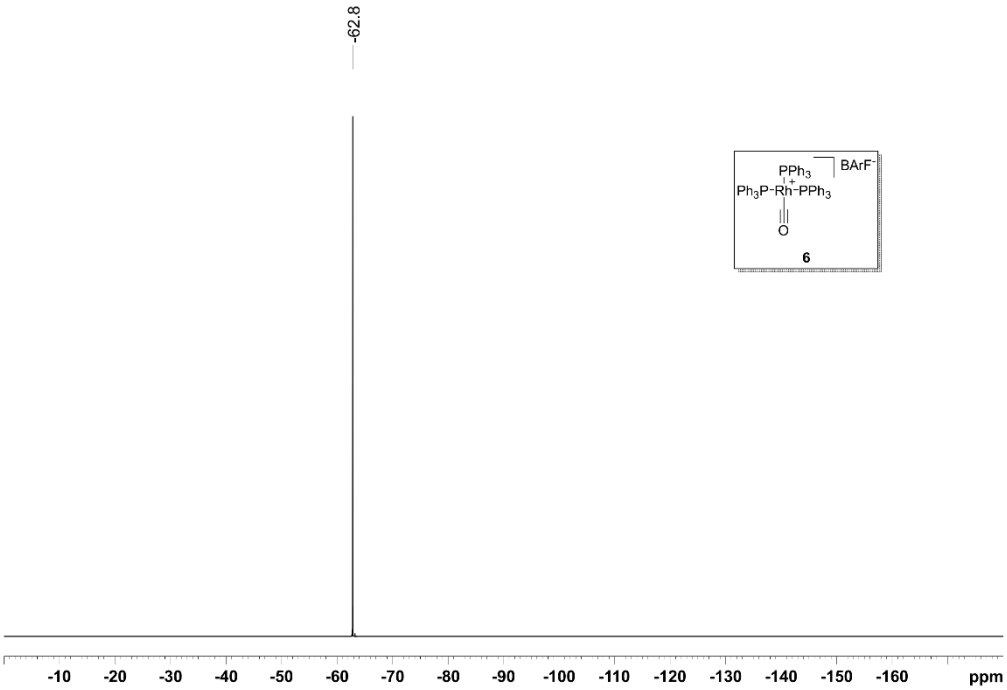

Figure SI 63. $^{19}F\{^{1}H\}$ NMR (471 MHz, CD_2Cl_2) for complex **6**.

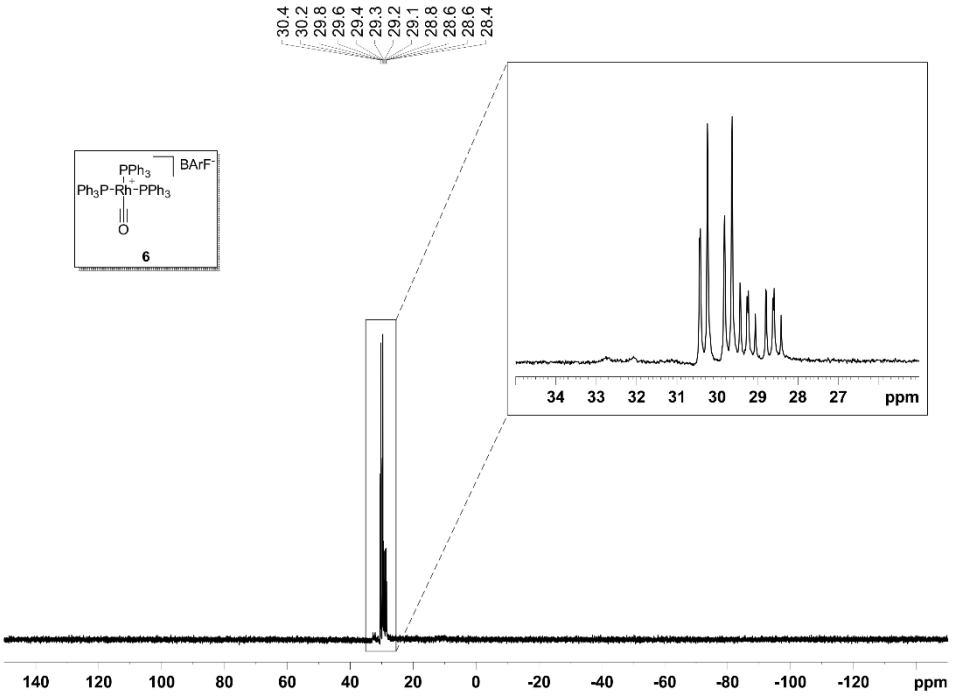

Figure SI 64. $^{31}P\{^{1}H\}$ NMR (203 MHz, CD_2Cl_2) for complex **6**.

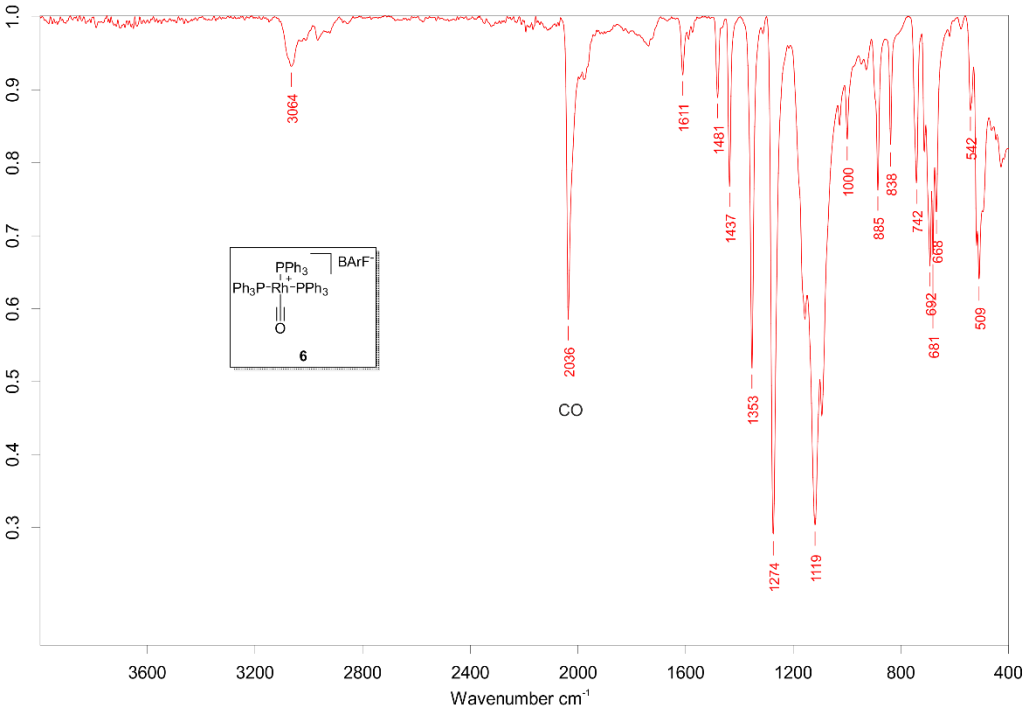

Figure SI 65. IR spectrum for complex **6**.

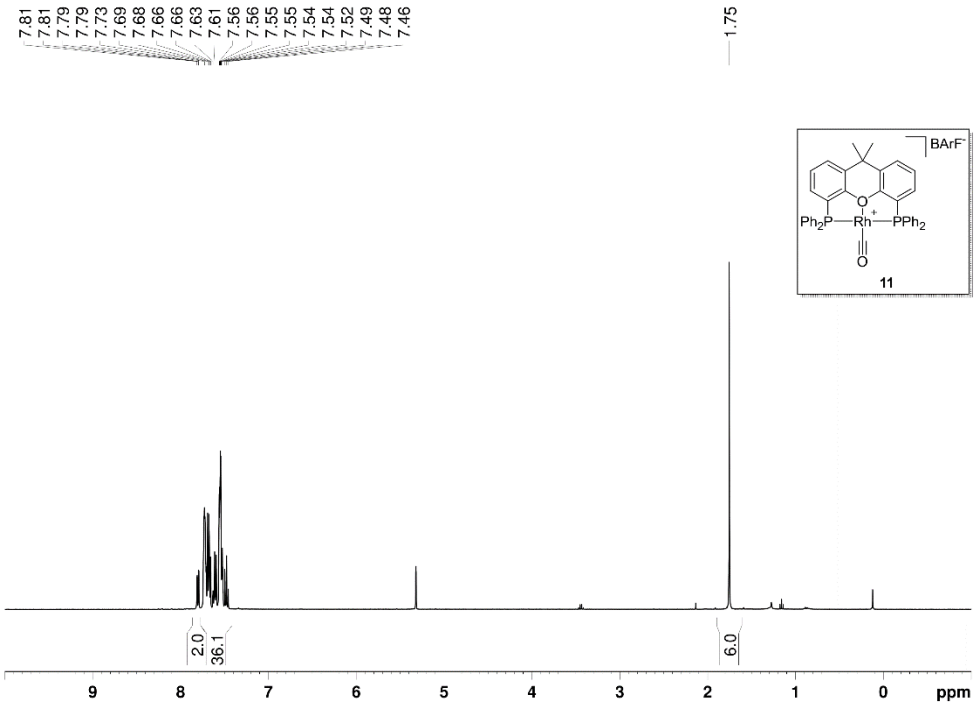

Figure SI 66. ^{1}H NMR (400 MHz, CD_2Cl_2) for complex **11**.

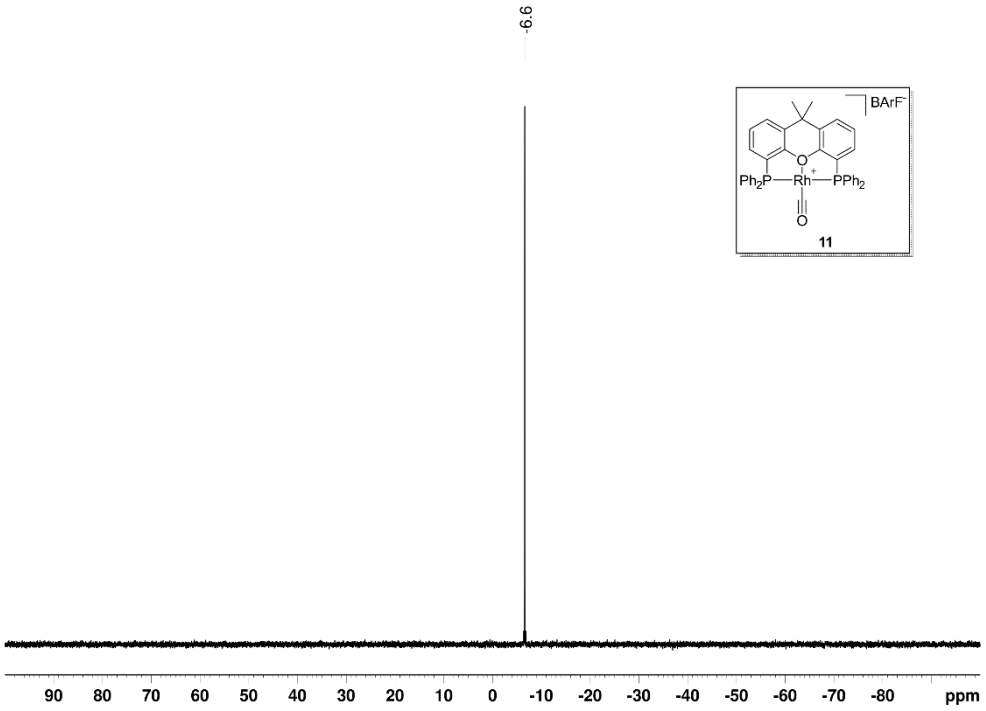

Figure SI 67. $^{11}B\{^{1}H\}$ NMR (128 MHz, CD_2Cl_2) for complex **11**.

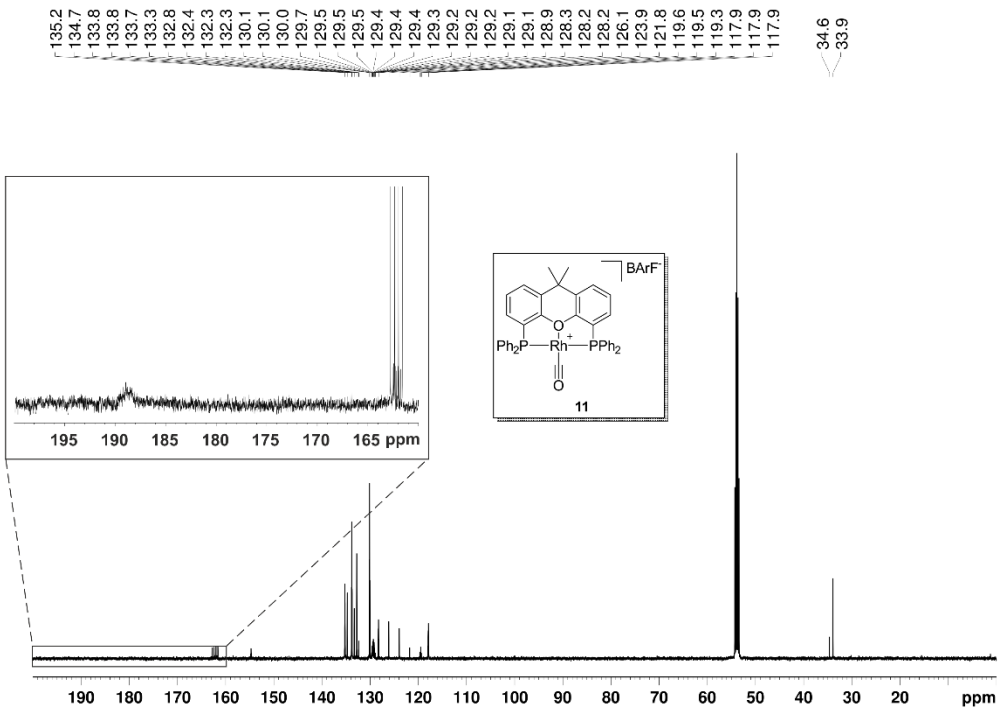

Figure SI 68. $^{13}C\{^{1}H\}$ NMR (126 MHz, CD_2Cl_2) for complex **11**.

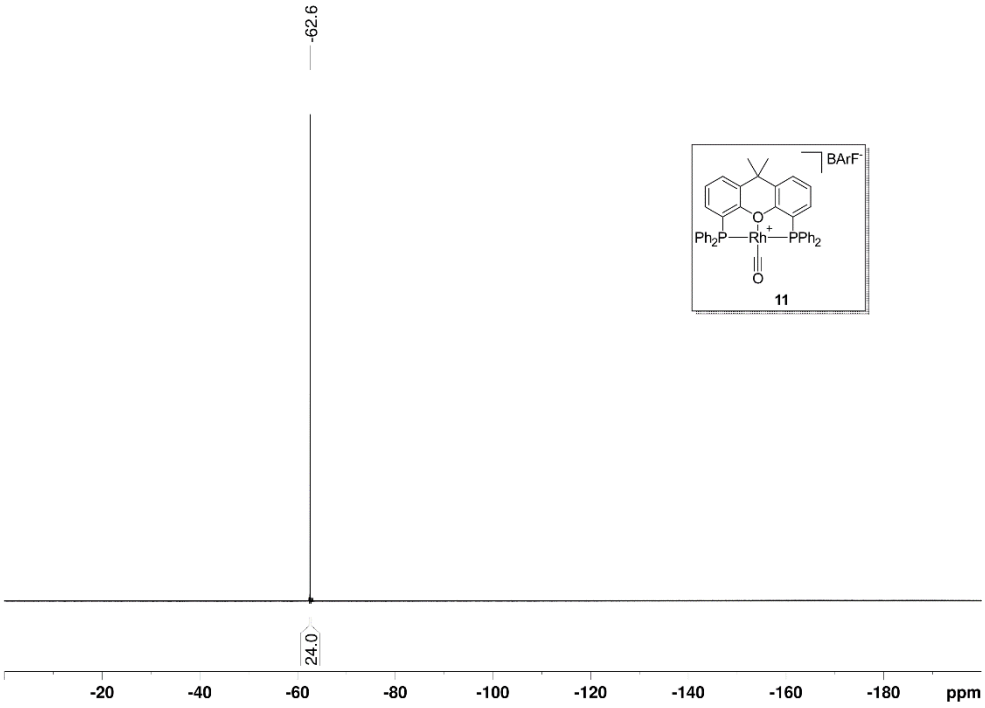

Figure SI 69. $^{19}F\{^{1}H\}$ NMR (376 MHz, CD_2Cl_2) for complex **11**.

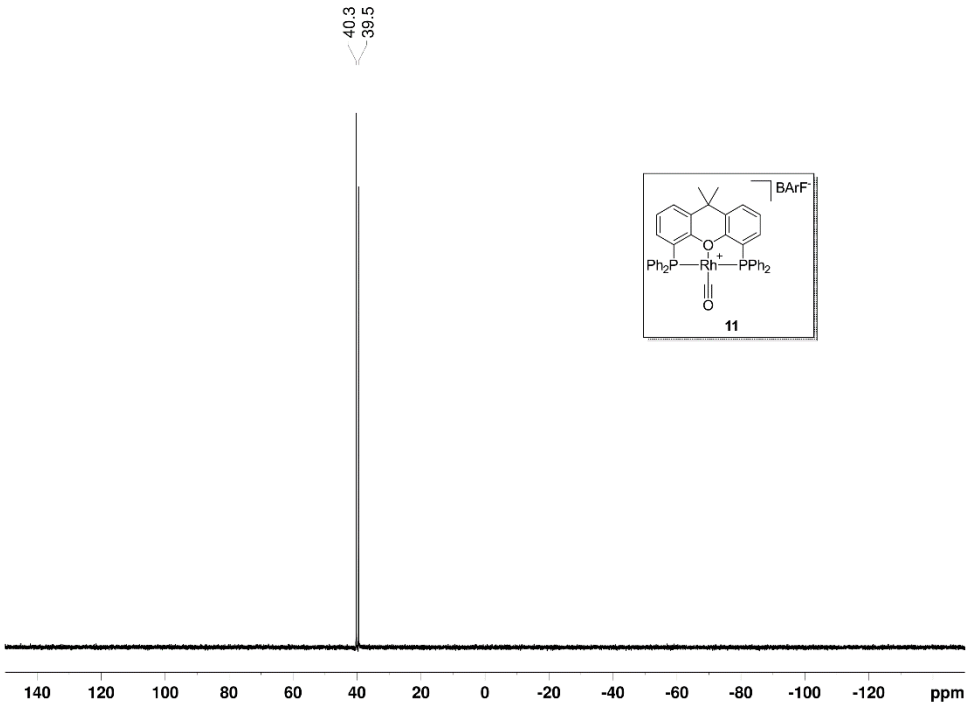

Figure SI 70. $^{31}P\{^{1}H\}$ NMR (162 MHz, CD_2Cl_2) for complex **11**.

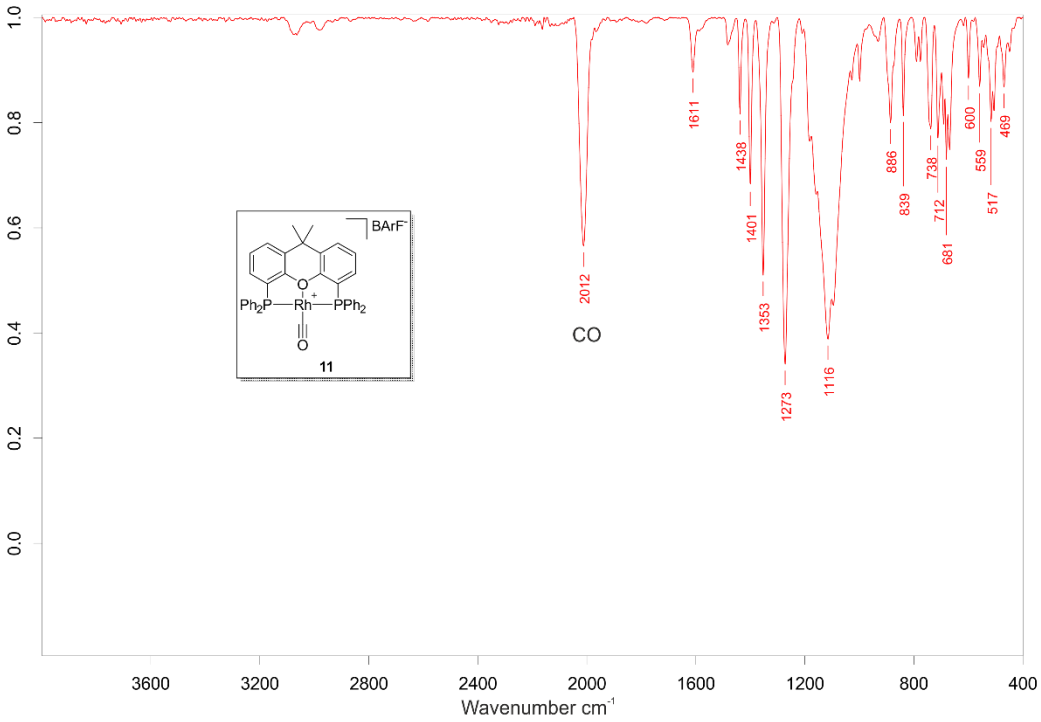

Figure SI 71. IR spectrum for complex **11**.

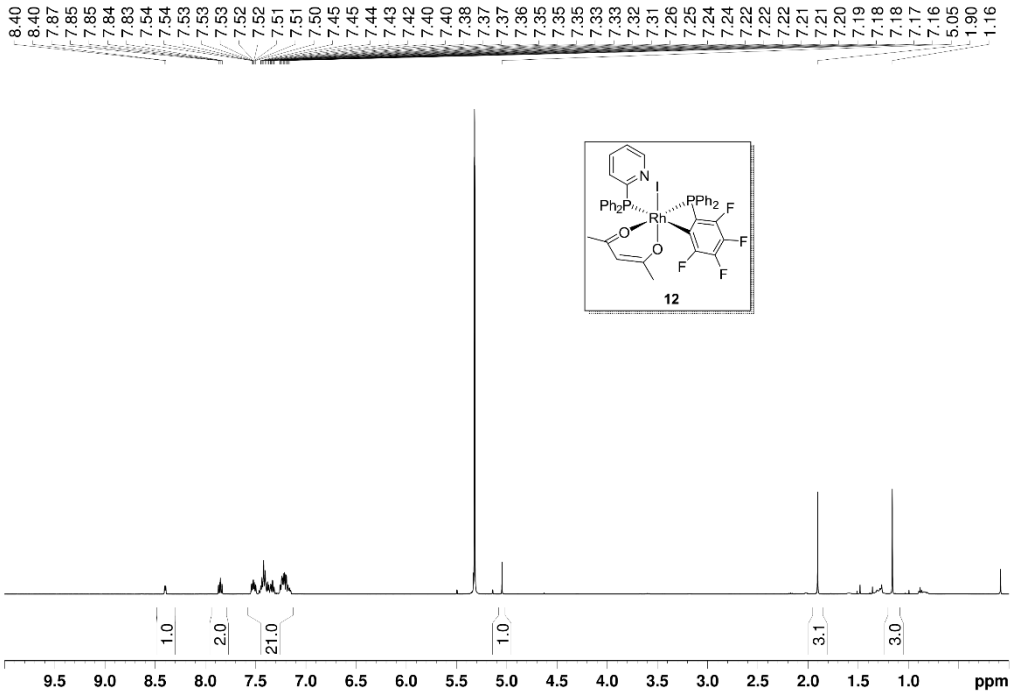

Figure SI 72. ^{1}H NMR (500 MHz, CD_2Cl_2) for complex **12**.

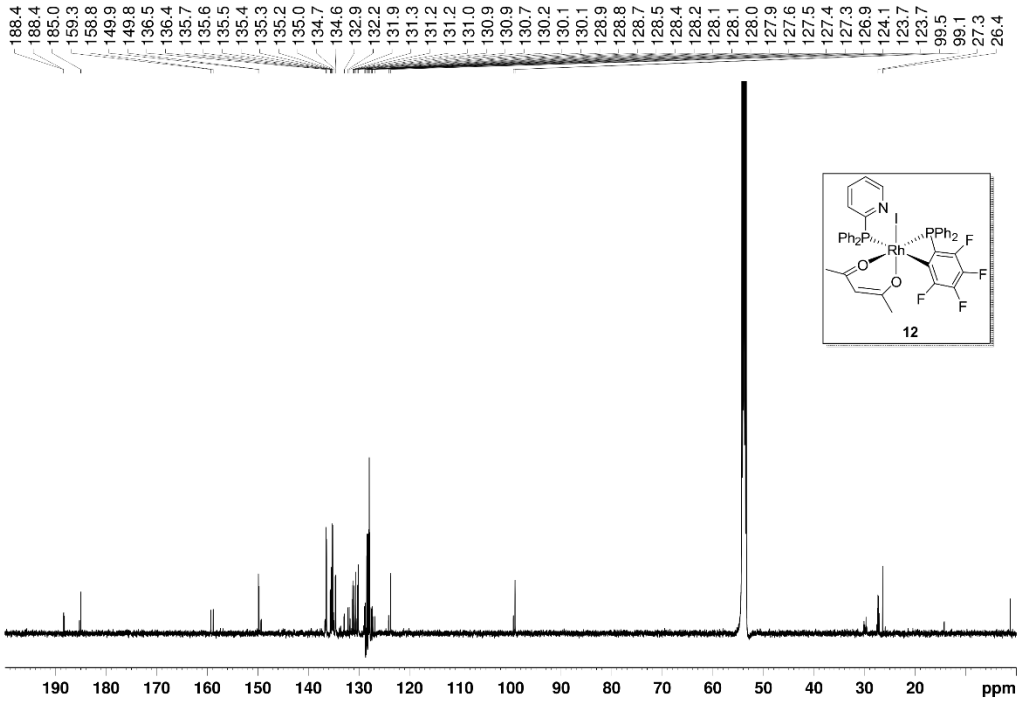

Figure SI 73. $^{13}C\{^{1}H\}$ NMR (126 MHz, CD_2Cl_2) for complex **12**.

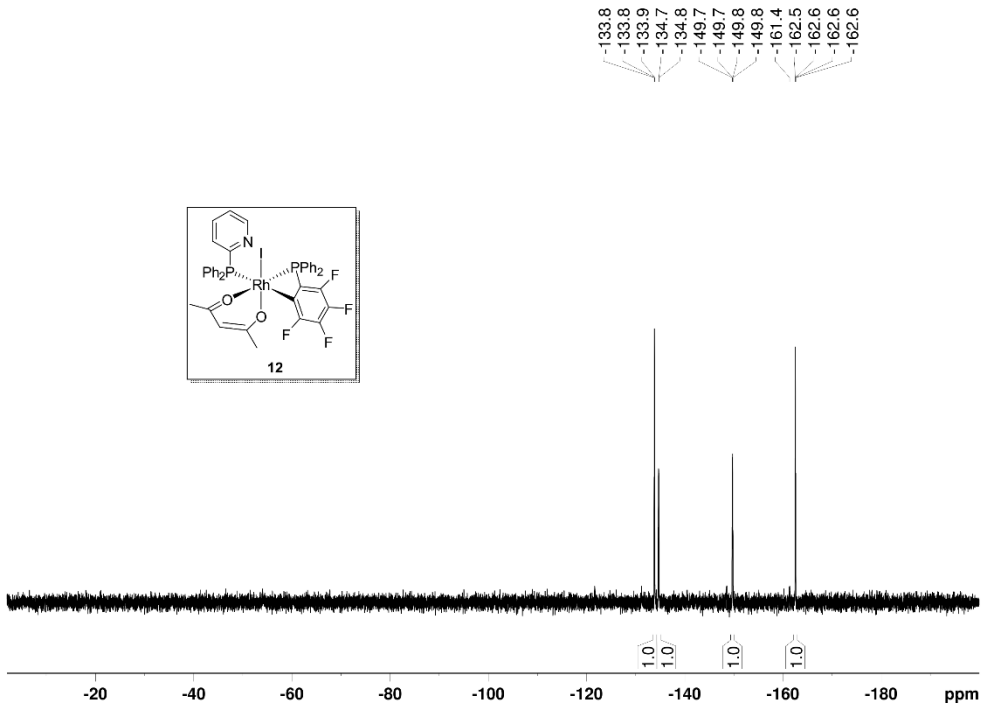

Figure SI 74. $^{19}F\{^{1}H\}$ NMR (376 MHz, CD_2Cl_2) for complex **12**.

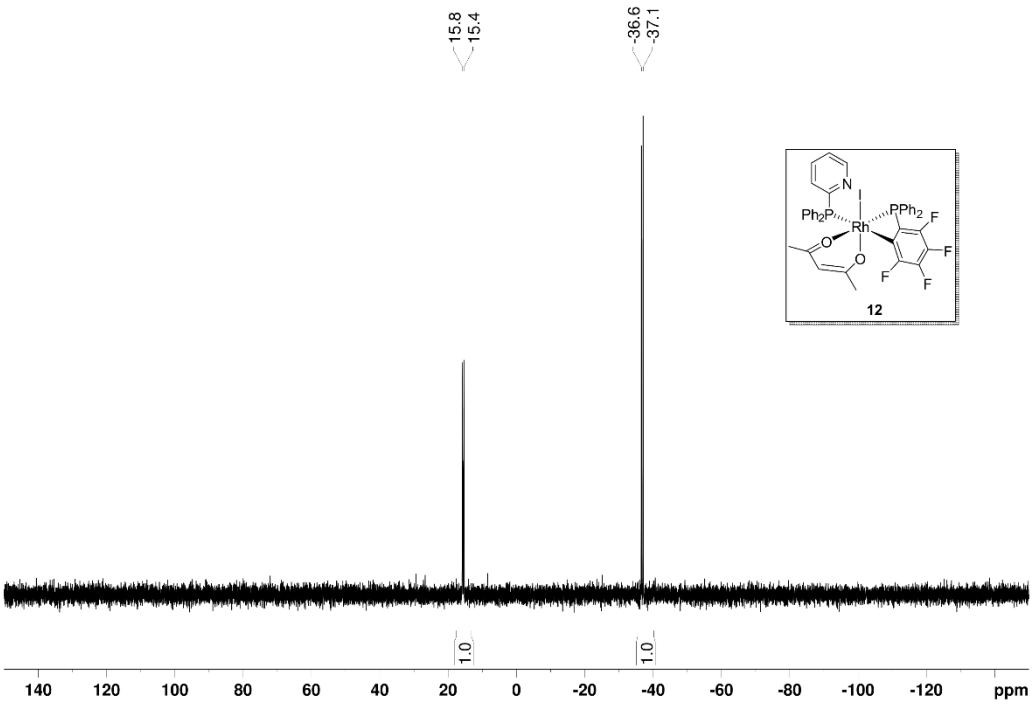

Figure SI 75. $^{31}P\{^{1}H\}$ NMR (203 MHz, CD_2Cl_2) for complex **12**.

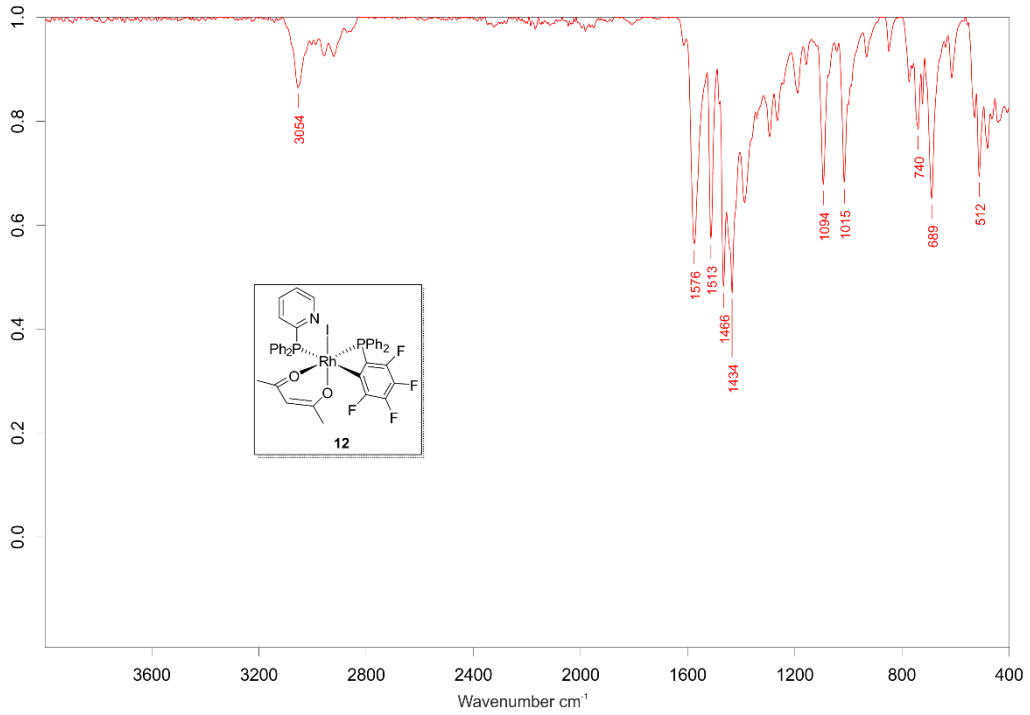

Figure SI 76. IR spectrum for complex **12**.

7.3. Spectroscopic NMR data and GC-FID chromatograms for *E* and branched hydroboration products.

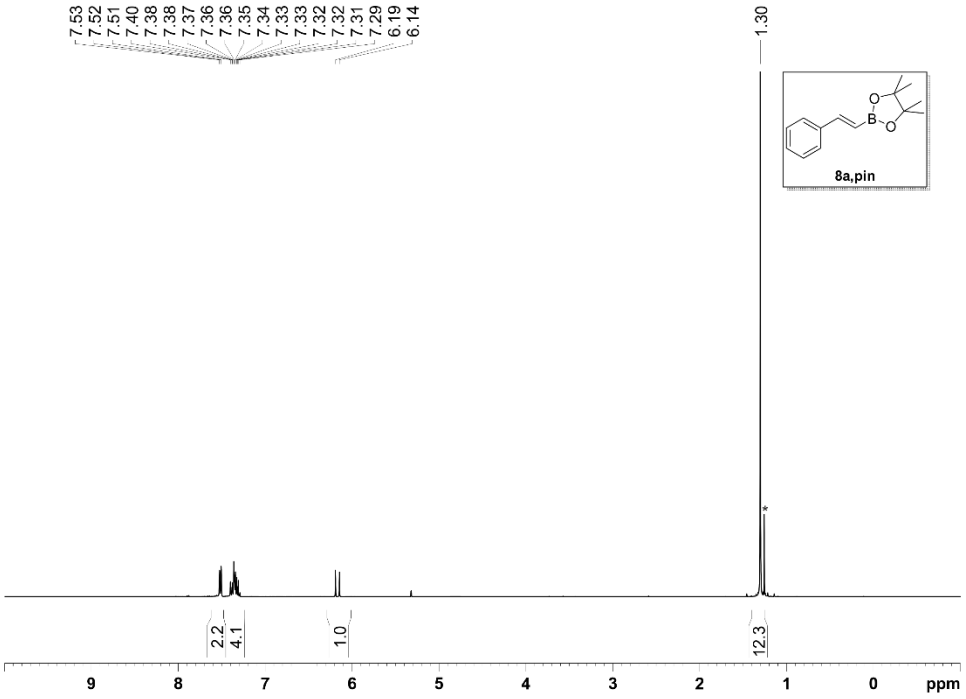

Figure SI 77. ^{1}H NMR (400 MHz, CD_2Cl_2) for product **8a,pin**.

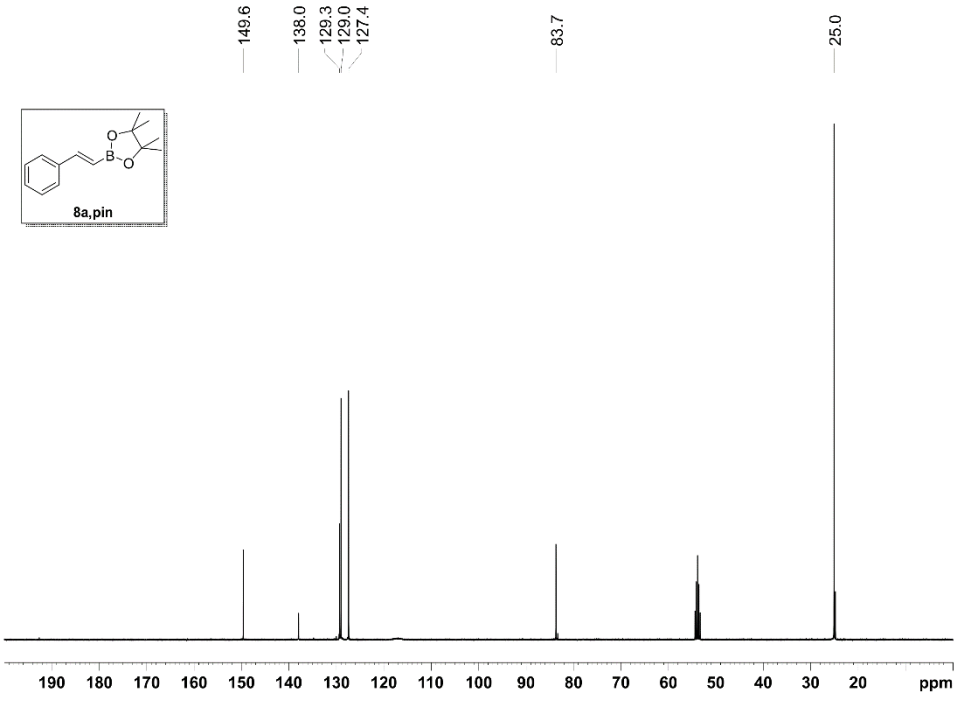

Figure SI 78. ^{13}C{^{1}H} NMR (100 MHz, CD_2Cl_2) for product **8a,pin**.

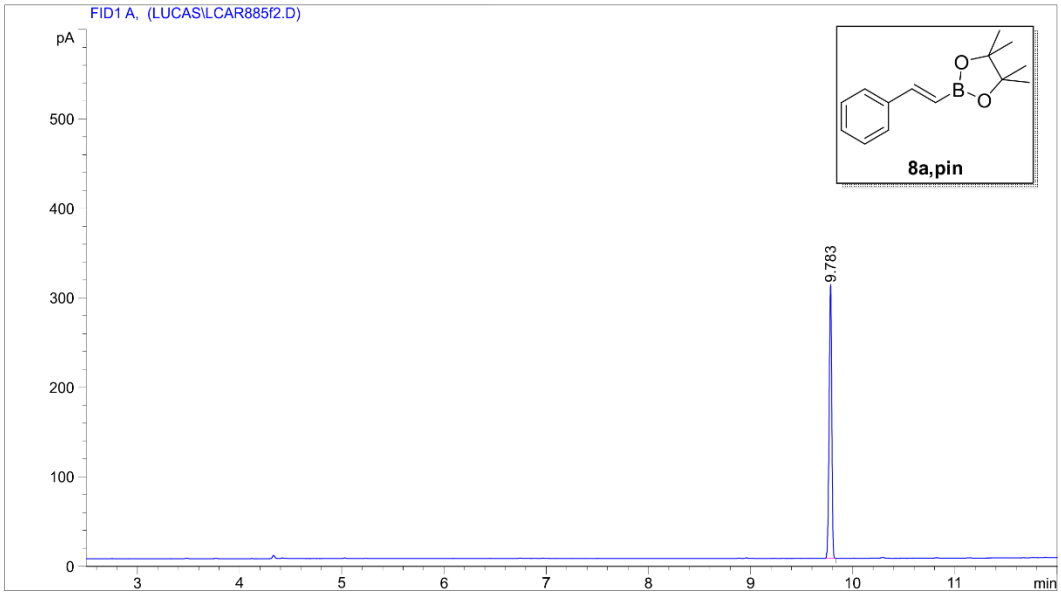

Figure SI 79. GC-FID for product **8a,pin**.

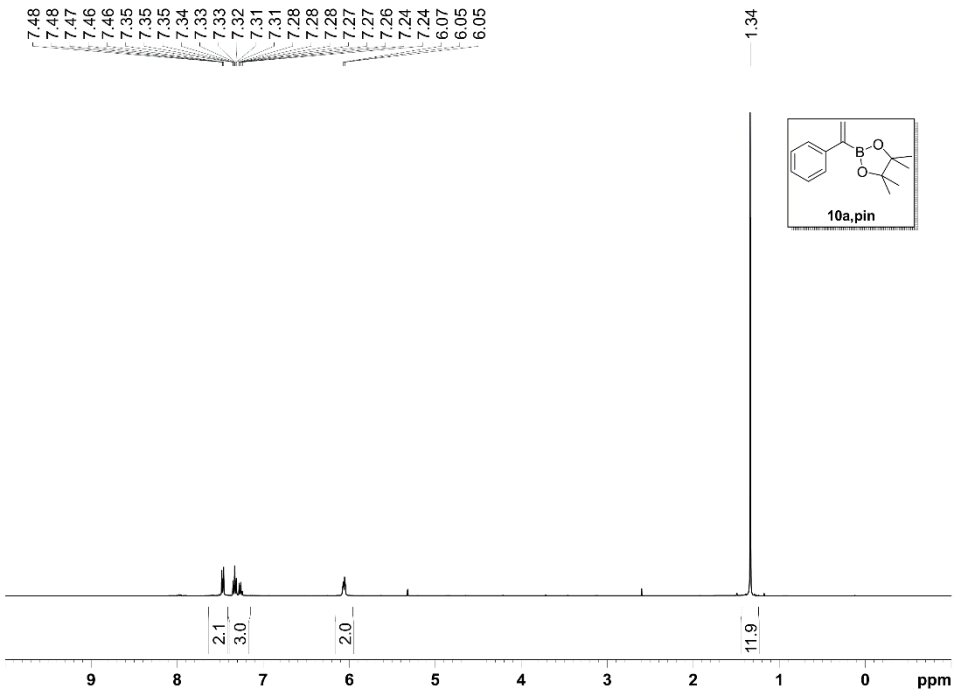

Figure SI 80. ^{1}H NMR (400 MHz, CD_2Cl_2) for product **10a,pin**.

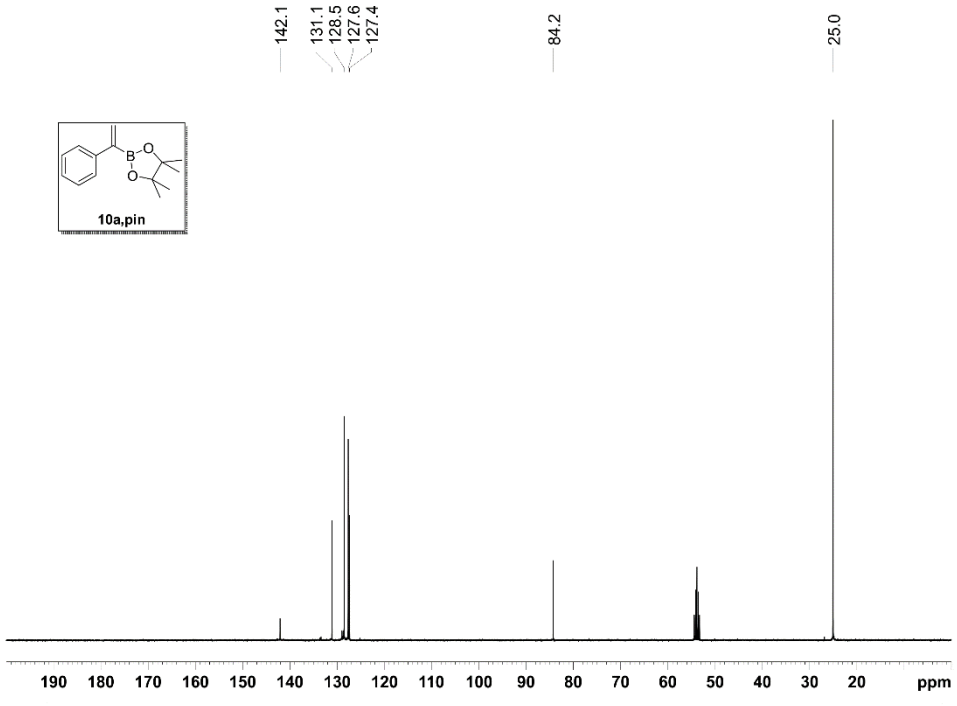

Figure SI 81. $^{13}C\{^{1}H\}$ NMR (100 MHz, CD_2Cl_2) for product **10a,pin**.

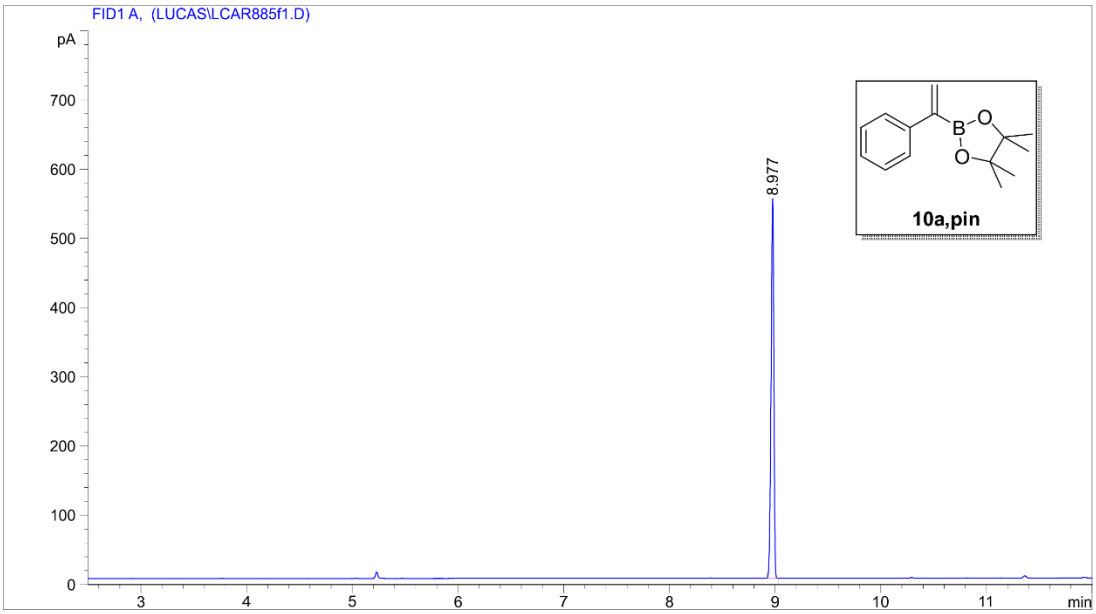

Figure SI 82. GC-FID for product **10a,pin**.

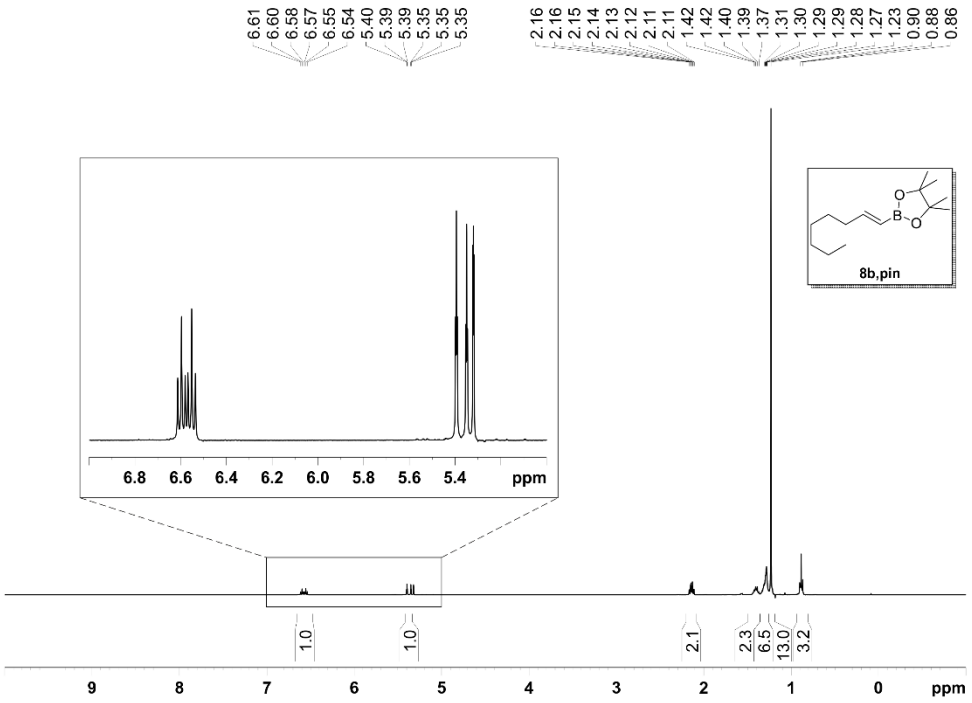

Figure SI 83. ^{1}H NMR (400 MHz, CD_2Cl_2) for product **8b,pin**.

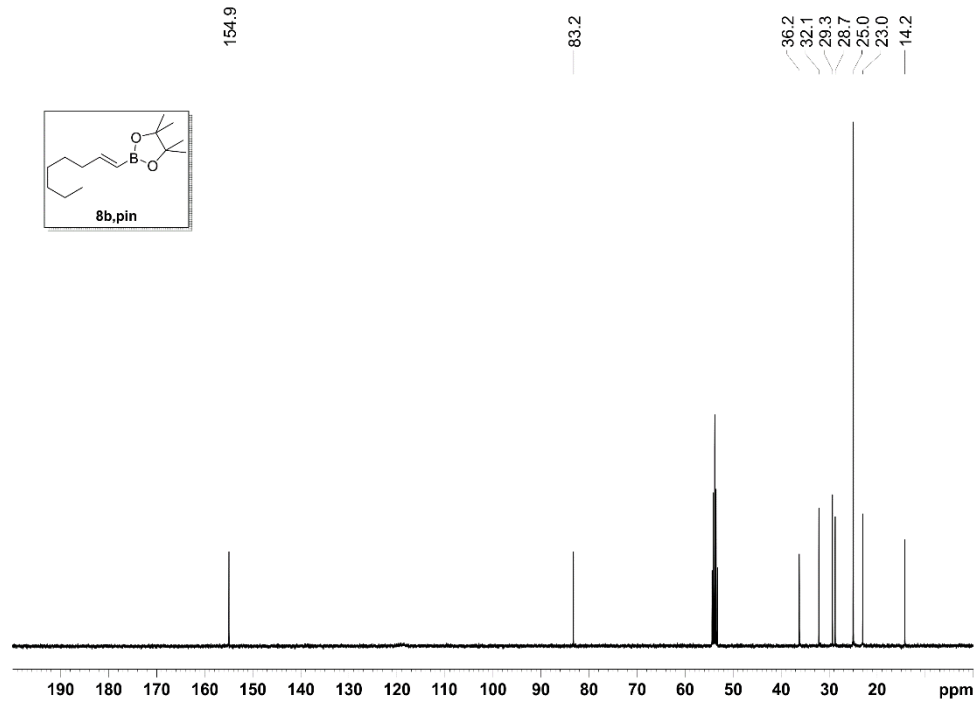

Figure SI 84. $^{13}C\{^{1}H\}$ NMR (100 MHz, CD_2Cl_2) for product **8b,pin**.

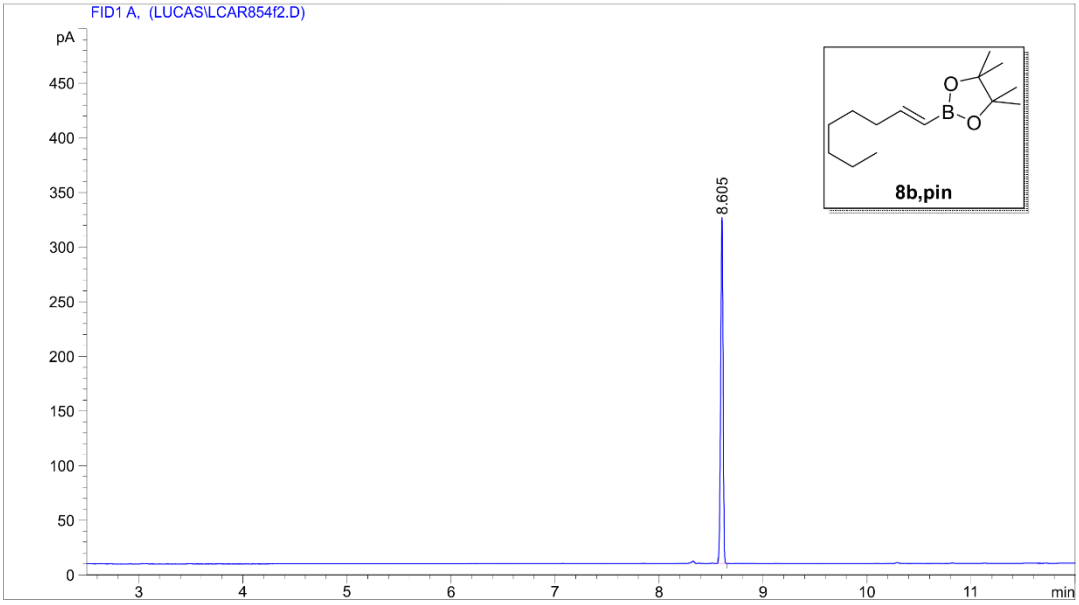

Figure SI 85. GC-FID for product **8b,pin**.

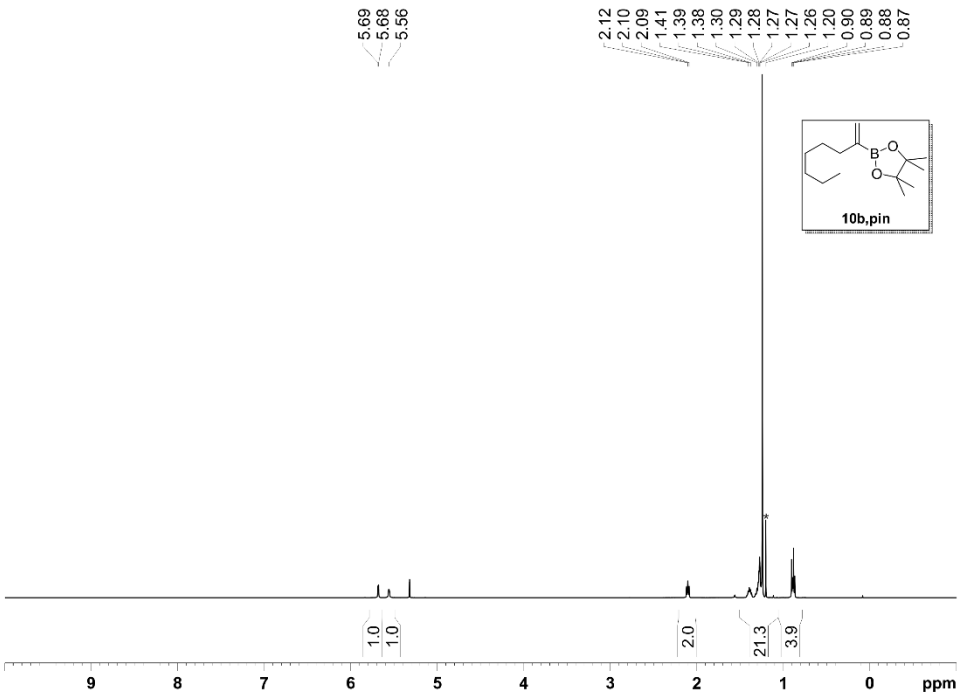

Figure SI 86. ^{1}H NMR (400 MHz, CD_2Cl_2) for product **10b,pin**.

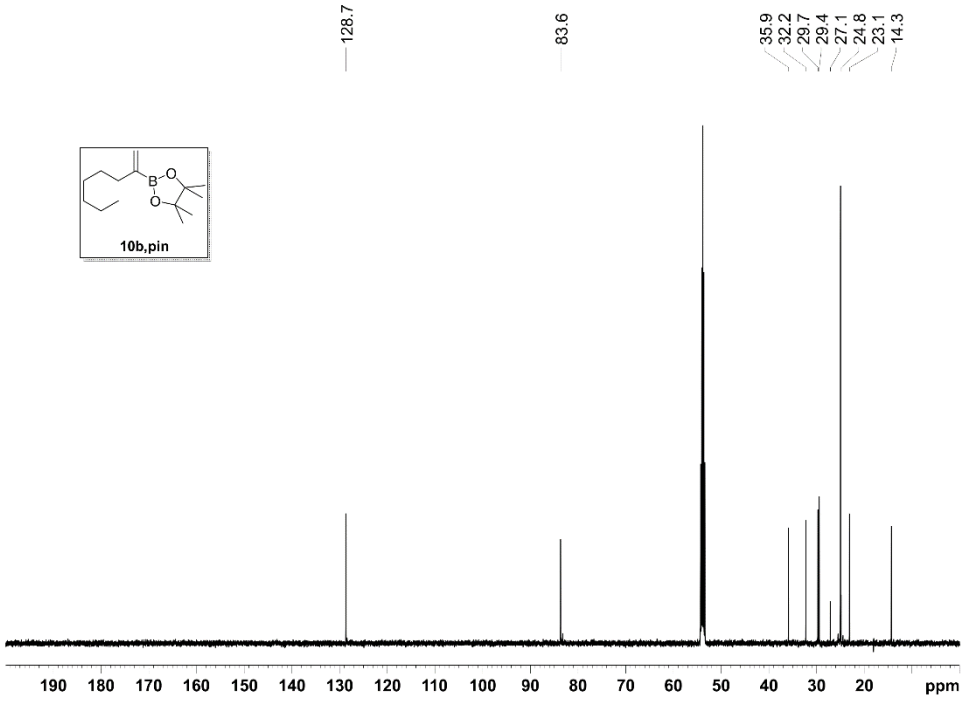

Figure SI 87. $^{13}C\{^{1}H\}$ NMR (100 MHz, CD_2Cl_2) for product **10b,pin**.

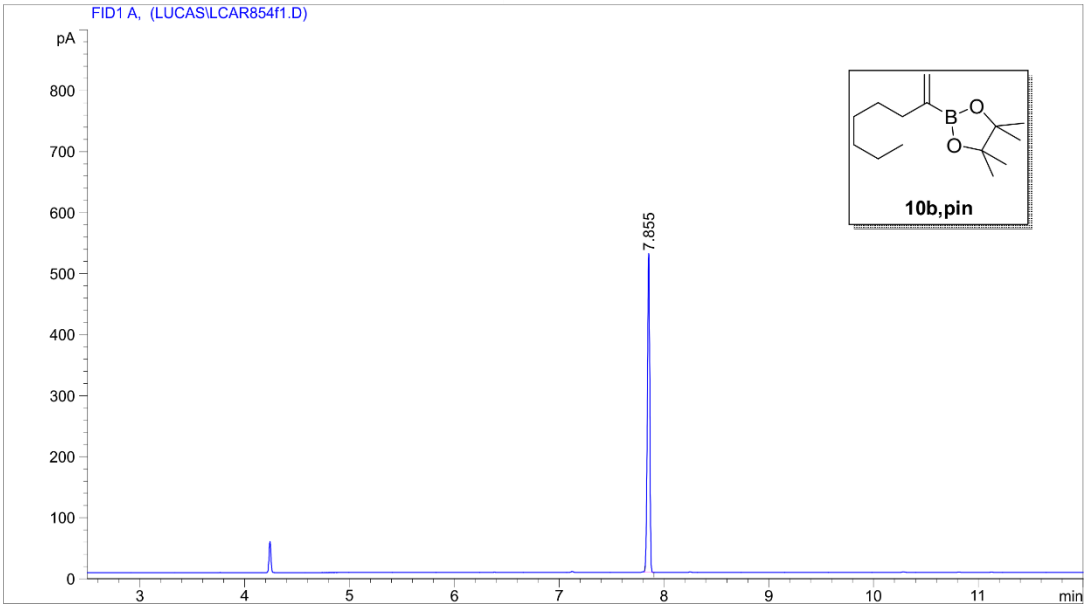

Figure SI 88. GC-FID for product **10b,pin**.

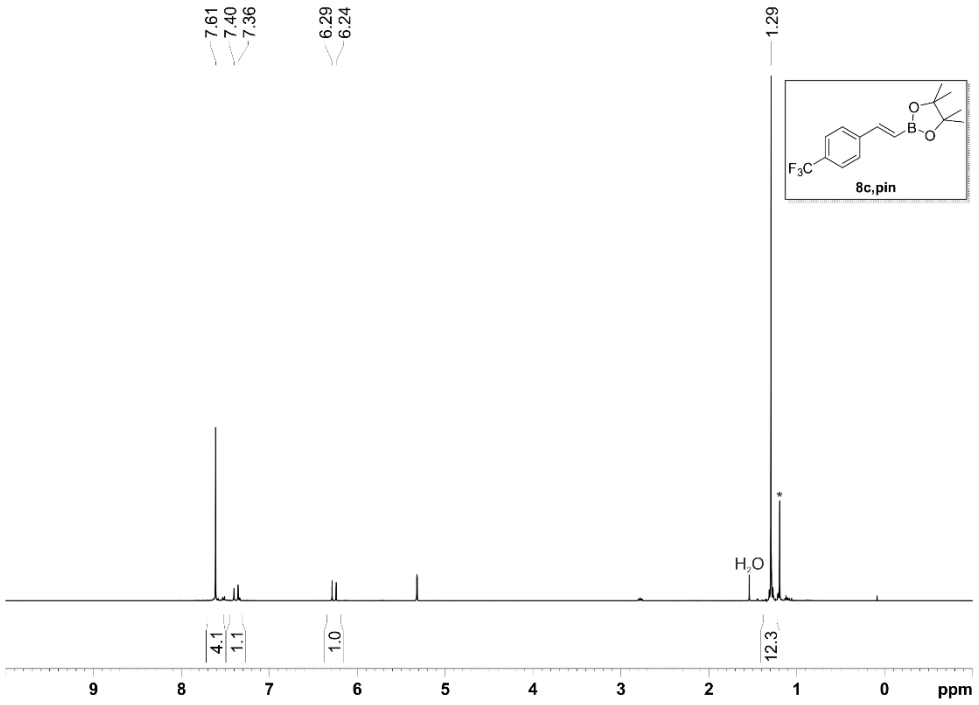

Figure SI 89. ^{1}H NMR (400 MHz, CD_2Cl_2) for product **8c,pin**.

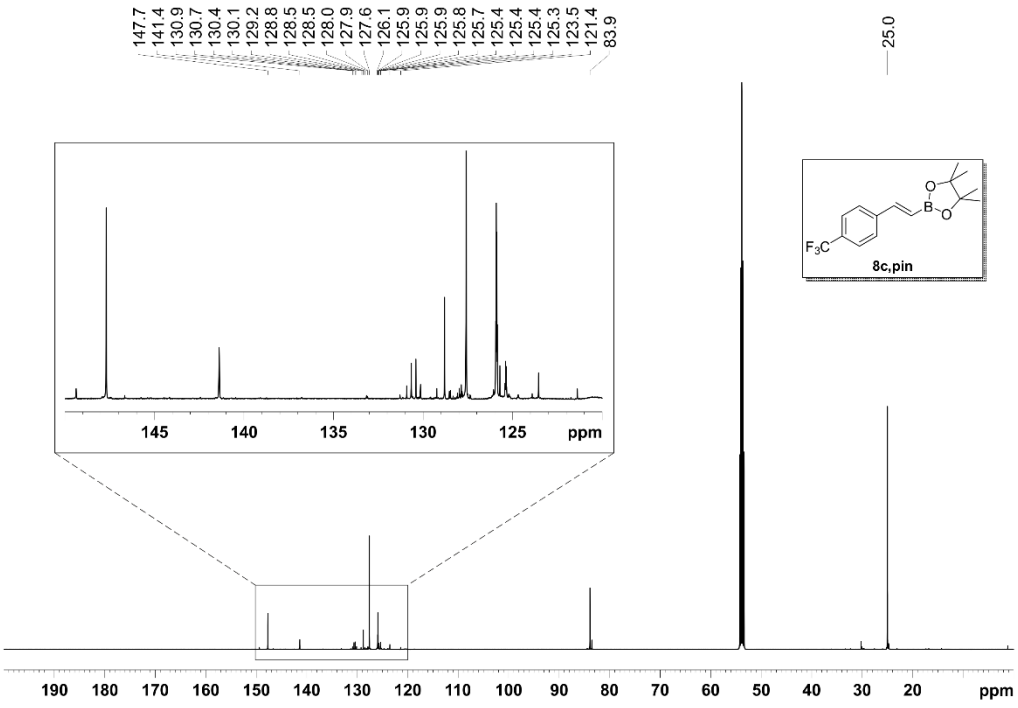

Figure SI 90. $^{13}C\{^{1}H\}$ NMR (126 MHz, CD_2Cl_2) for product **8c,pin**.

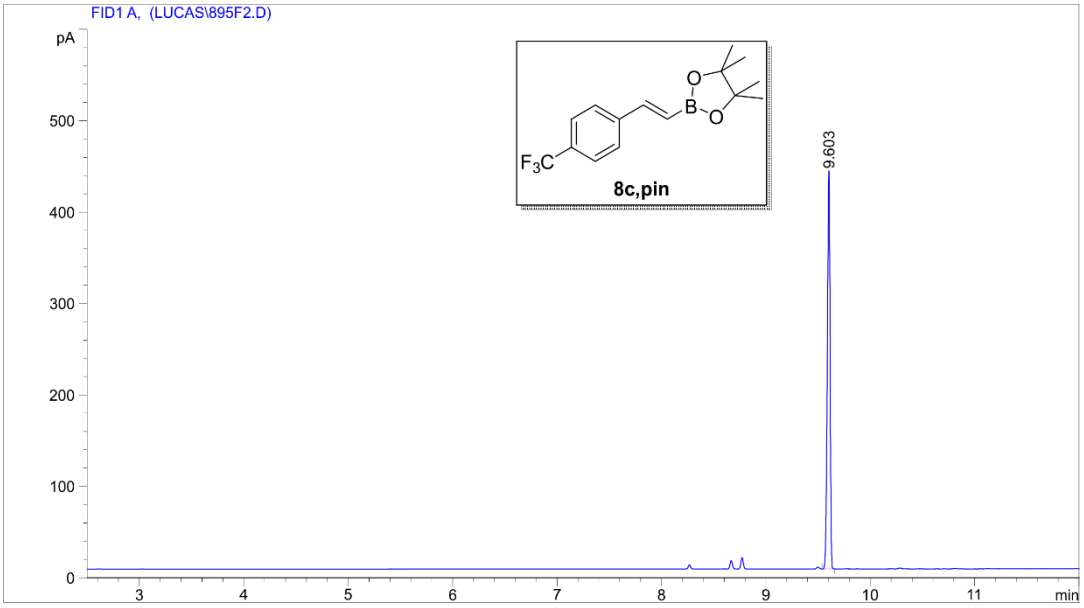

Figure SI 91. GC-FID for product **8c,pin**.

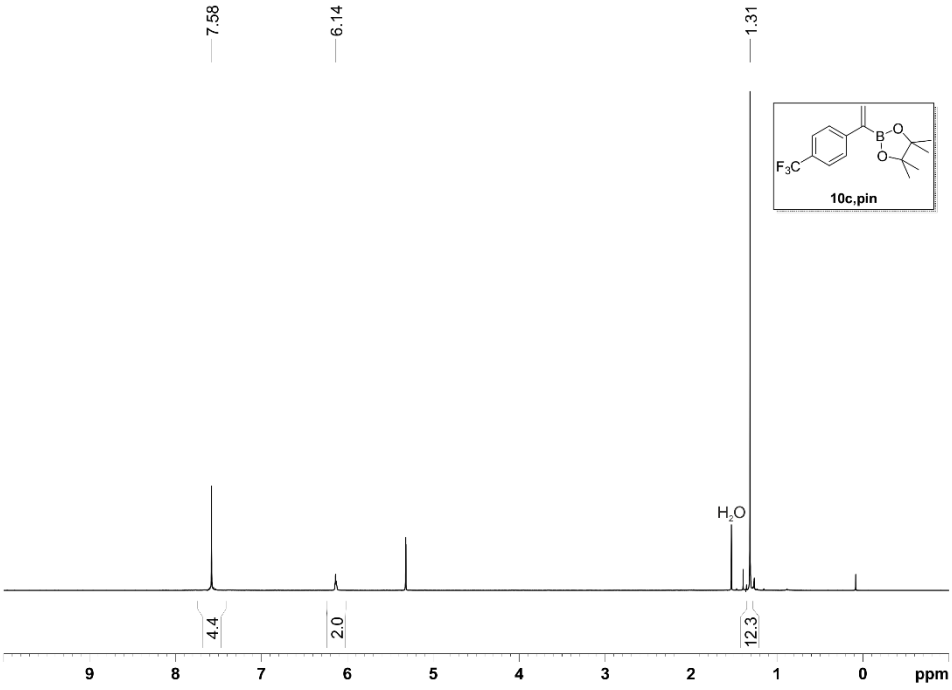

Figure SI 92. ^{1}H NMR (400 MHz, CD_2Cl_2) for product **10c,pin**.

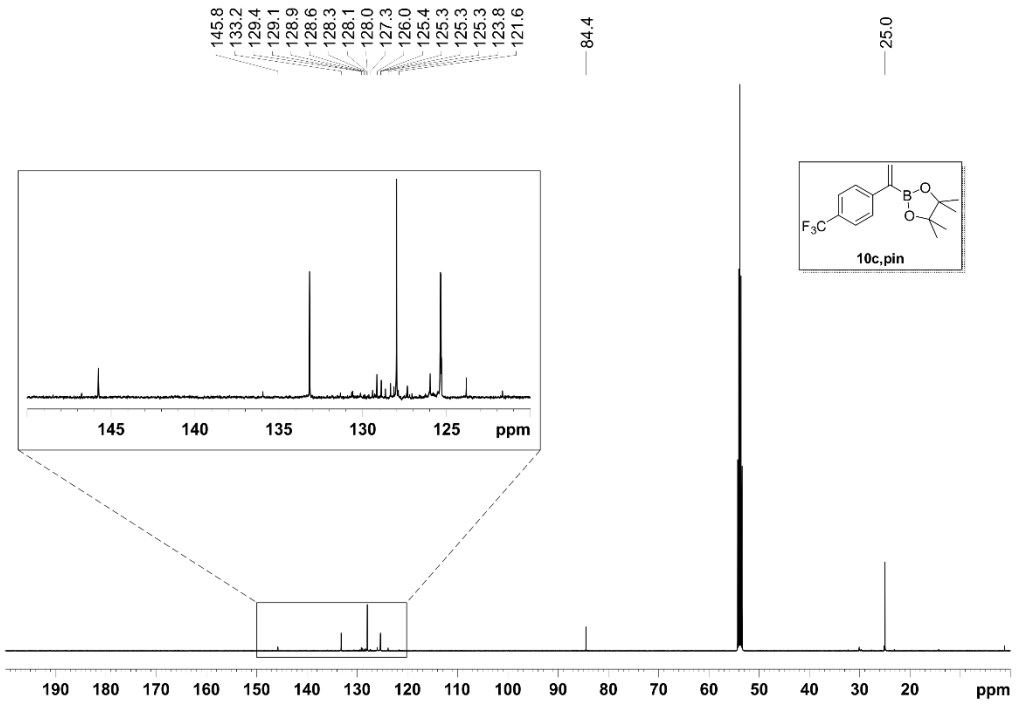

Figure SI 93. $^{13}C\{^{1}H\}$ NMR (126 MHz, CD_2Cl_2) for product **10c,pin**.

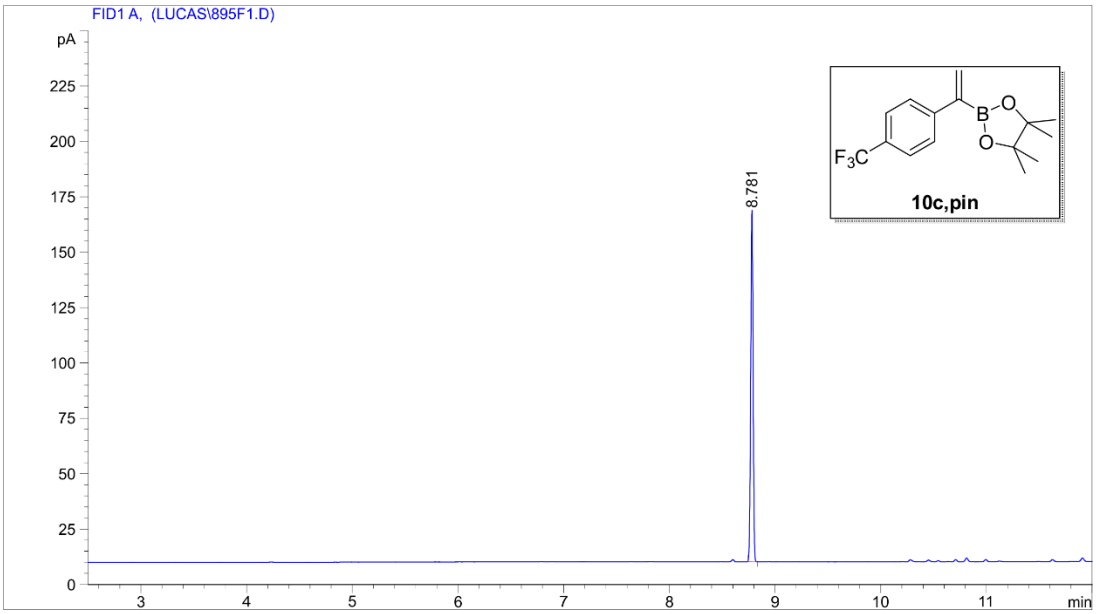

Figure SI 94. GC-FID for product **10c,pin**.

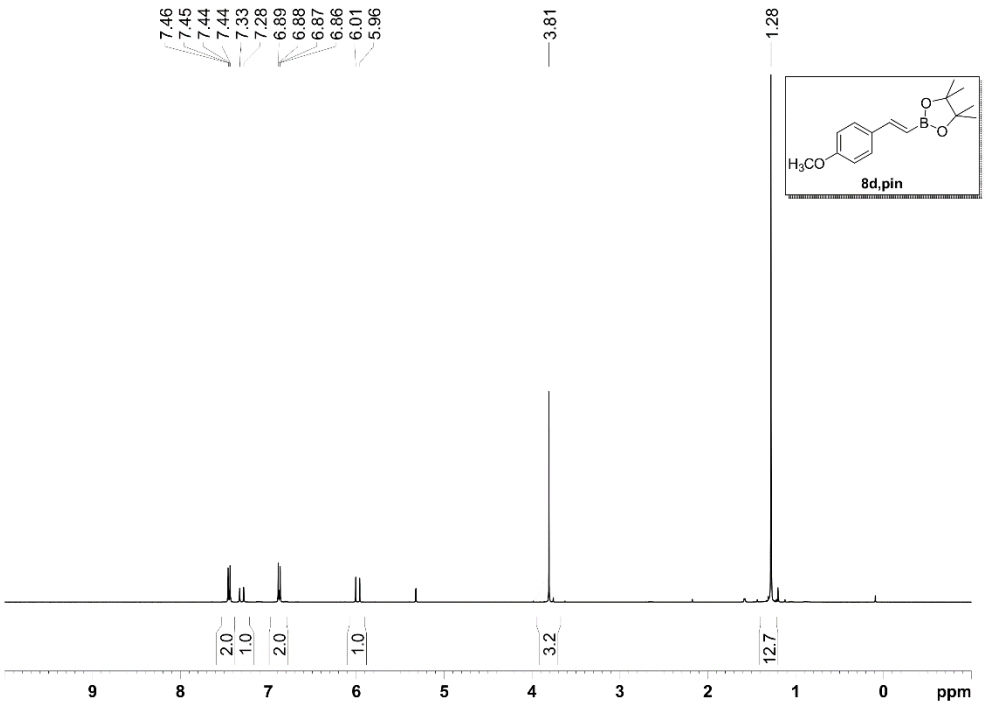

Figure SI 95. ^{1}H NMR (400 MHz, CD_2Cl_2) for product **8d,pin**

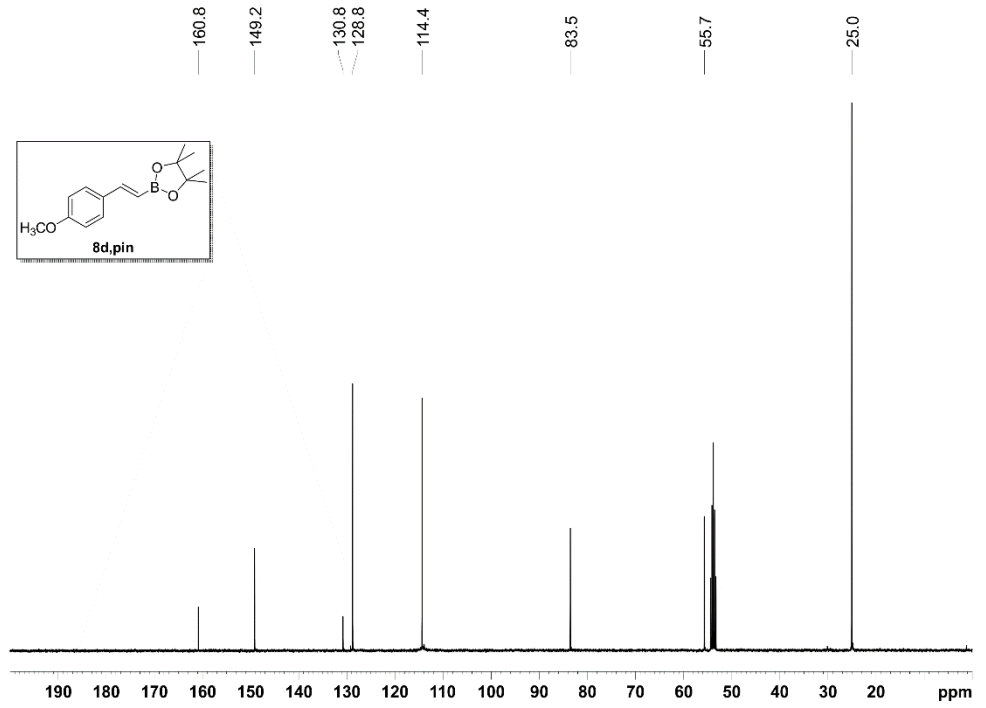

Figure SI 96. $^{13}C\{^{1}H\}$ NMR (100 MHz, CD_2Cl_2) for product **8d,pin**.

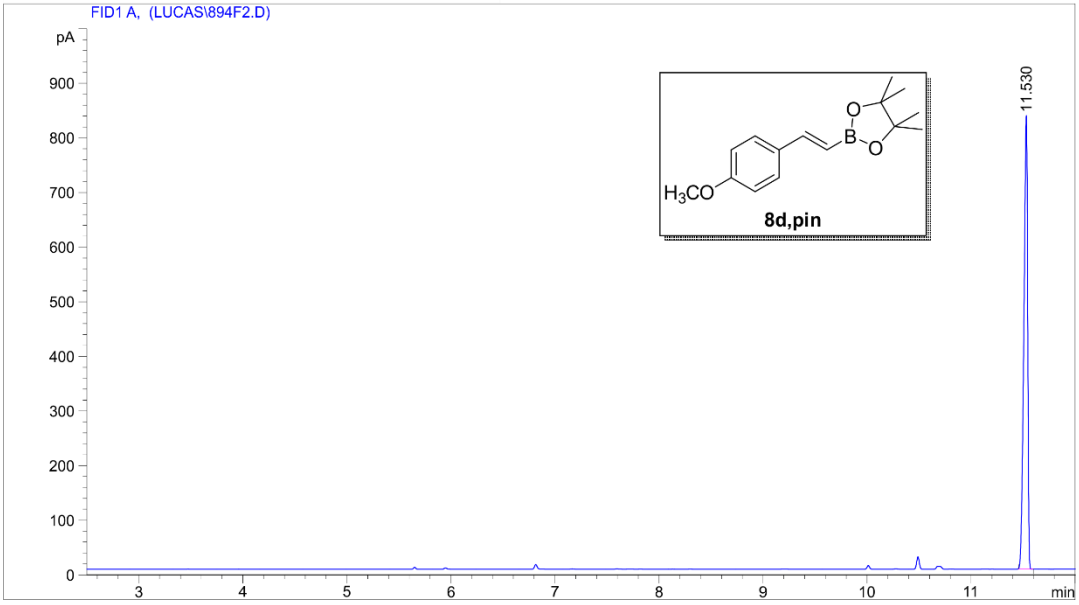

Figure SI 97. GC-FID for product **8d,pin**.

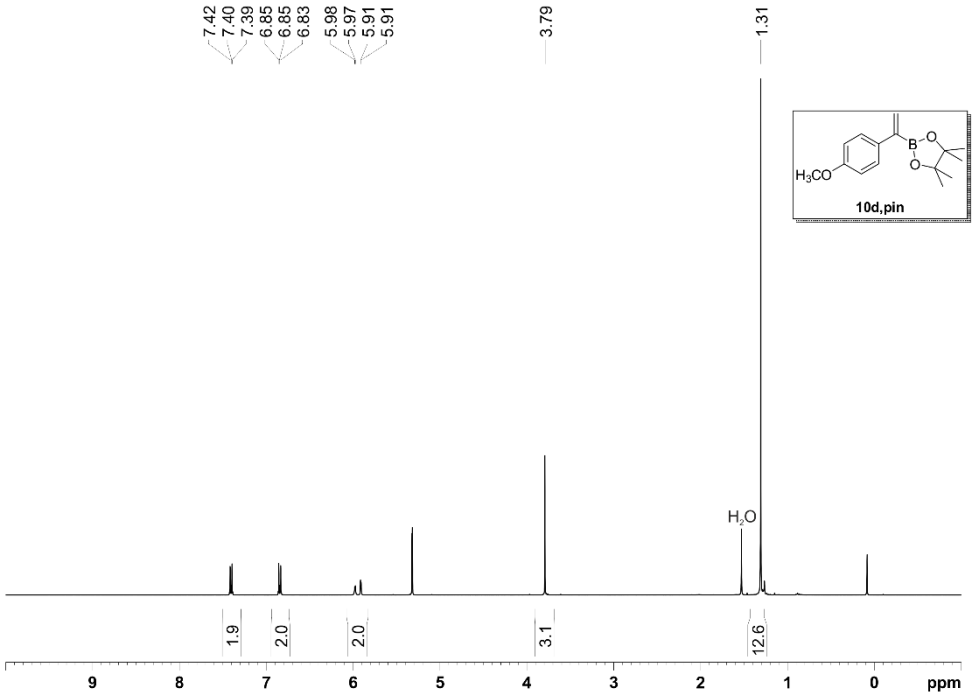

Figure SI 98. ^{1}H NMR (400 MHz, CD_2Cl_2) for product **10d,pin**

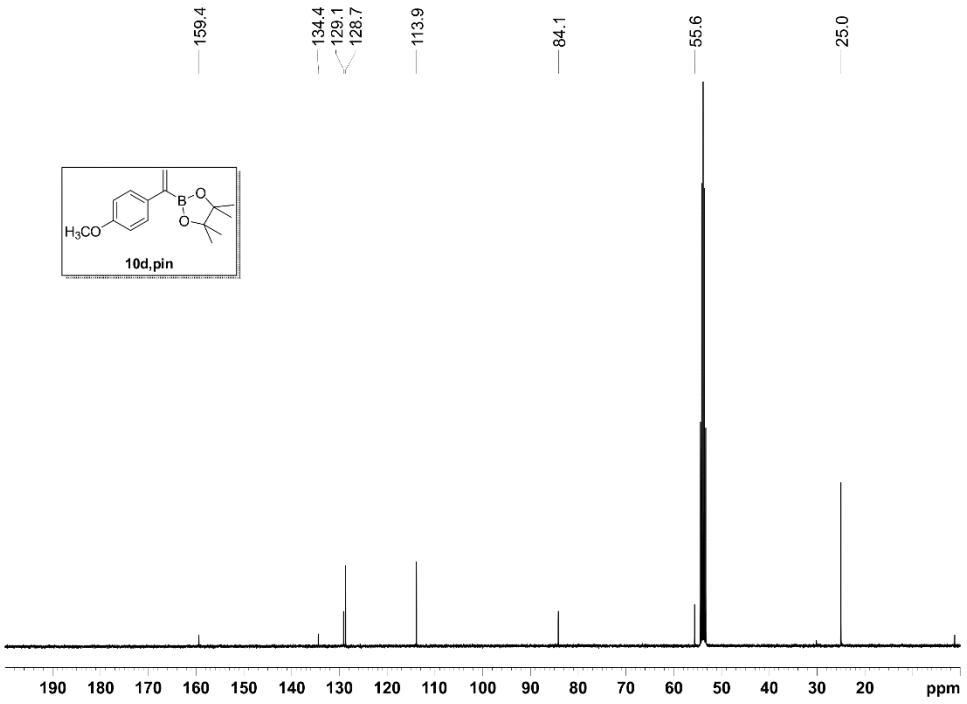

Figure SI 99. $^{13}C\{^{1}H\}$ NMR (100 MHz, CD_2Cl_2) for product **10d,pin**.

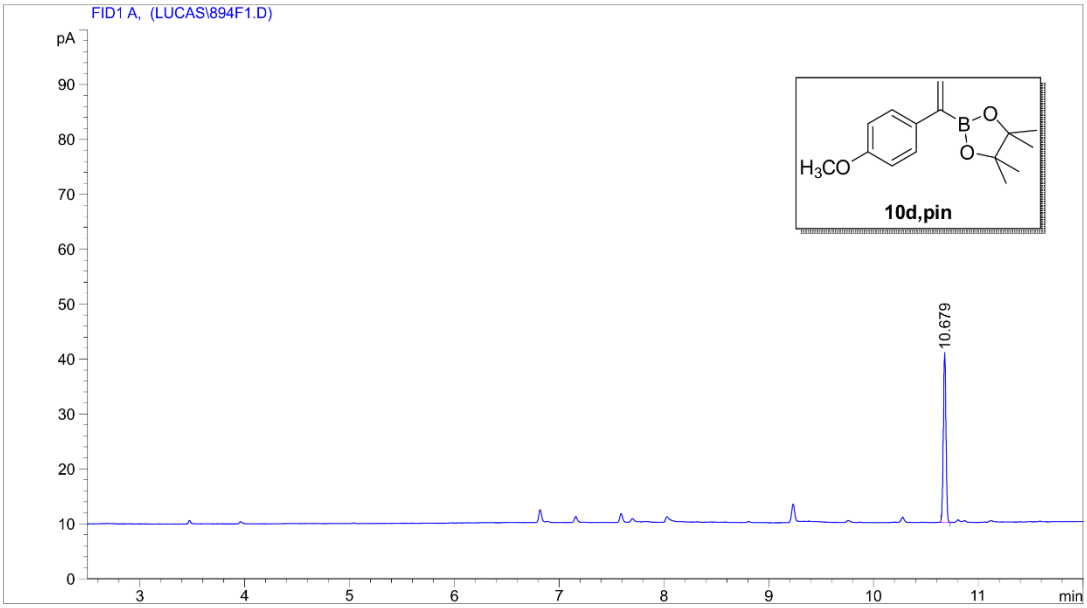

Figure SI 100. GC-FID for product **10d,pin**.